EUROPEAN COMMISSION

Community research

PAMINA
Performance Assessment Methodologies in Application to Guide the Development of the Safety Case

(Contract Number: FP6-036404)

SOFTWARE ARCHITECTURE REPORT
MILESTONE (N°: M2.2.E.3)

[Nagra NAB 09-35]

Author(s):

Stefan Finsterle (*LBNL, USA*)

Peter Robinson (*Quintessa, UK*)

Ulrich Kuhlmann (*TK Consult, Switzerland*)

Jűrg Schneider, Editor (*Nagra, Switzerland*)

Date of issue of this report : **31/03/2009**

Start date of project : **01/10/2006** Duration : 36 Months

Project co-funded by the European Commission under the Euratom Research and Training Programme on Nuclear Energy within the Sixth Framework Programme (2002-2006)		
Dissemination Level		
PU	Public	X
RE	Restricted to a group specified by the partners of the [PAMINA] project	
CO	Confidential, only for partners of the [PAMINA] project	

Foreword

The work presented in this report was developed within the Integrated Project PAMINA: **P**erformance **A**ssessment **M**ethodologies **IN A**pplication to Guide the Development of the Safety Case. This project is part of the Sixth Framework Programme of the European Commission. It brings together 25 organisations from ten European countries and one EC Joint Research Centre in order to improve and harmonise methodologies and tools for demonstrating the safety of deep geological disposal of long-lived radioactive waste for different waste types, repository designs and geological environments. The results will be of interest to national waste management organisations, regulators and lay stakeholders.

The work is organised in four Research and Technology Development Components (RTDCs) and one additional component dealing with knowledge management and dissemination of knowledge:

- In RTDC 1 the aim is to evaluate the state of the art of methodologies and approaches needed for assessing the safety of deep geological disposal, on the basis of comprehensive review of international practice. This work includes the identification of any deficiencies in methods and tools.
- In RTDC 2 the aim is to establish a framework and methodology for the treatment of uncertainty during PA and safety case development. Guidance on, and examples of, good practice will be provided on the communication and treatment of different types of uncertainty, spatial variability, the development of probabilistic safety assessment tools, and techniques for sensitivity and uncertainty analysis.
- In RTDC 3 the aim is to develop methodologies and tools for integrated PA for various geological disposal concepts. This work includes the development of PA scenarios, of the PA approach to gas migration processes, of the PA approach to radionuclide source term modelling, and of safety and performance indicators.
- In RTDC 4 the aim is to conduct several benchmark exercises on specific processes, in which quantitative comparisons are made between approaches that rely on simplifying assumptions and models, and those that rely on complex models that take into account a more complete process conceptualization in space and time.

The work presented in this report was performed in the scope of RTDC 2.

All PAMINA reports can be downloaded from http://www.ip-pamina.eu.

Arbeitsbericht NAB 09-35

PAMINA RTDC-2
Milestone M2.2.E.3
Software Architecture Report

March 2009

Nationale Genossenschaft
für die Lagerung
radioaktiver Abfälle

Hardstrasse 73
CH-5430 Wettingen
Telefon 056-437 11 11

www.nagra.ch

Arbeitsbericht NAB 09-35

PAMINA RTDC-2

Milestone M2.2.E.3

Software Architecture Report

March 2009

KEYWORDS

probabilistic safety analysis, Probabilistische Sicherheitsanalyse, PSA, PSA project, PSA Projekt

Nationale Genossenschaft für die Lagerung radioaktiver Abfälle

Hardstrasse 73
CH-5430 Wettingen
Telefon 056-437 11 11

www.nagra.ch

The bulk of this report (Chapters 2 to 10) was prepared by Stefan Finsterle (LBNL). Appendix 1 was written by Peter Robinson (Quintessa) and Ulrich Kuhlmann (TK Consult). The work described in this report was supported by a working group consisting of (in alphabetical order) Peter Gribi (S+R Consult GmbH, Baden), Georg Kosakowski (PSI), Paul Marschall (Nagra), Gerhard Mayer, Joachim Poppei, Georg Resele (AF-Colenco, Baden), Jürg Schneider (Nagra), Christian Sprecher (Sprecher Consulting GmbH, Wettingen) and Piet Zuidema (Nagra). It was edited by Jürg Schneider.

Table of Contents

List of Tables

List of Figures

1 Objectives and scope of this report

This report describes the software architecture chosen to implement Nagra's probabilistic safety analysis (PSA) concept (Fig. 1). The focus of the present report is on the Integrated Radionuclide Release Code (IRRC, see yellow boxes in Fig. 1), which could be viewed as the "engine" of the entire PSA modelling approach. The key components of the IRRC are (i) the Integrated Flow Code (IFC) and (ii) the Radionuclide Transport Codes (RTC) STMAN-TD, PICNIC-TD and the Gas Model. As indicated by the black arrows in Fig. 1, the IFC, which calculates the time-dependent two-phase flow in the near field and geosphere of a gas-generating nuclear waste repository, passes on its flow results to the RTC, which calculates radionuclide releases from the repository system to the biosphere. Doses are then calculated using Biosphere Dose Conversion Factors (BDCFs, see Nagra 2002b for a definition) for a given biosphere type (not shown in Fig. 1).

A probabilistic driver (GOLDSIM) is used to generate samples ("scenarios" in Fig. 1) for the PSA calculations, indicated by the dark grey box surrounding the yellow IRRC boxes in Fig. 1. To handle alternative, mutually exclusive conceptualisations, a logic tree approach (TREETOOL) is used, indicated by a light grey box surrounding the dark grey GOLDSIM box in Fig. 1. GOLDSIM and TREETOOL are not discussed further in the present report.

The bulk of the report consists of a detailed description of the IFC which was developed specifically for Nagra's PSA project. STMAN-TD (Nagra 2008) and PICNIC-TD (Robinson & Suckling 2009) are variants of pre-existing radionuclide release and transport codes allowing time-dependent flow fields; these are documented separately and are not discussed in any detail in the present report. In the current version of the IRRC, a simplified version of the Gas Model is used which assumes direct transfer of the volatile radionuclides in the gas phase to the biosphere aquifer if continuous gas paths to the biosphere are present (calculated in each realisation by the IFC). The Gas Model is therefore not further discussed in the present report. The network providing the framework for the RTC that was used for a first implementation of the IRRC is described in Appendix 1. The IRRC integrates all safety-relevant features, events and processes identified in the PAMINA report M.2.2.E.2.

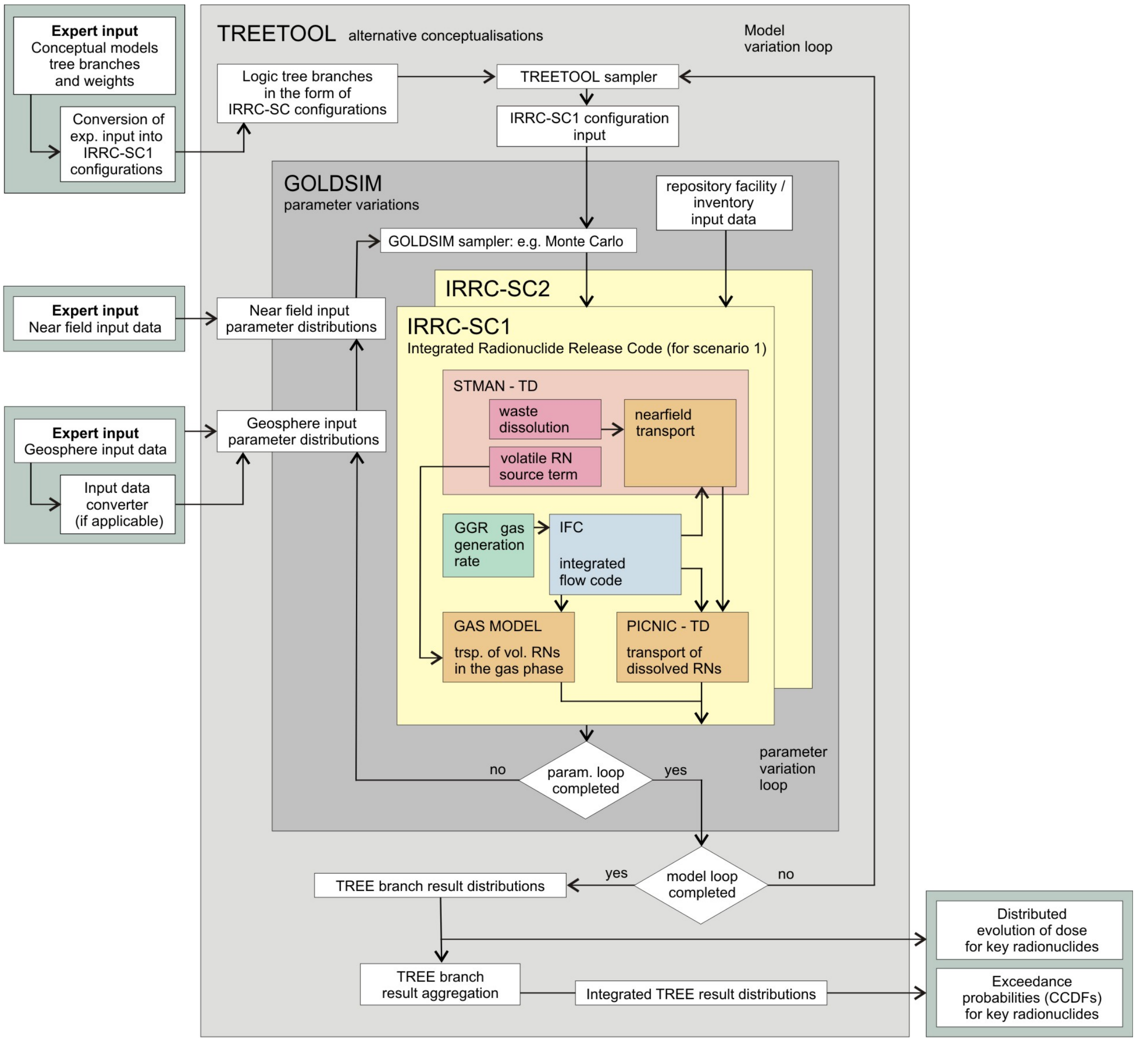

Fig. 1: Software architecture chosen to implement Nagra's probabilistic safety analysis concept.

2 Introduction to the Integrated Flow Code (IFC)

This document describes the development and use of the Integrated Flow Code (IFC), a numerical code and related model to be used for the simulation of time-dependent, two-phase flow in the near field and geosphere of a gas-generating nuclear waste repository system located in an initially fully water-saturated claystone (Opalinus Clay) in Switzerland. The development of the code and model was supported by the Swiss National Cooperative for the Disposal of Radioactive Waste (Nagra), Wettingen, Switzerland.

Gas generation (mainly H_2, but also CH_4 and CO_2) may affect repository performance by (1) compromising the engineered barriers through excessive pressure build-up, (2) displacing potentially contaminated pore water, (3) releasing radioactive gases (e.g., those containing ^{14}C and ^{3}H), (4) changing hydrogeologic properties of the engineered barrier system and the host rock, and (5) altering the groundwater flow field and thus radionuclide migration paths. The IFC aims at providing water and gas flow fields as the basis for the subsequent radionuclide transport simulations, which are performed by the radionuclide transport code (RTC). The IFC, RTC and a waste-dissolution and near-field transport model (STMAN) are part of the Integrated Radionuclide Release Code (IRRC), which integrates all safety-relevant features, events, and processes (FEPs). The IRRC is embedded into a Probabilistic Safety Assessment (PSA) computational tool that (1) evaluates alternative conceptual models, scenarios, and disruptive events, and (2) performs Monte-Carlo sampling to account for parametric uncertainties.

The IFC was developed based on Nagra's PSA concept. Specifically, as many phenomena as possible are to be directly simulated using a (simplified) process model, which is at the core of the IRRC model. Uncertainty evaluation (scenario uncertainty, conceptualization uncertainty, parametric uncertainty) is handled by the outer shell of the PSA model; it is not further discussed in this report. Moreover, justifications for the inclusion or exclusion of FEPs as well as for certain simplifying assumptions are available or can be obtained using detailed process models and other supporting information.

The IFC is both a numerical code and a model of a repository system. The numerical code is a modification of the multiphase, multicomponent simulator TOUGH2 (Pruess et al., 1999), as implemented within the iTOUGH2 (Finsterle, 2007abc) framework. The code modifications are mainly concerned with the implementation of relevant FEPs as outlined in Nagra (FEP-Screening report M.2.2.E.2, 2007a), as well as removal of processes and features that are not needed within the IFC; the modifications are summarized in Appendix 1. In addition, the IFC includes a model, i.e., a simplified representation of the repository system. Specifically, a computational grid was generated, which includes the emplacement tunnels 0for spent fuel, high-level wastes, as well as long-lived intermediate-level wastes. Moreover, the model represents engineered barriers (backfill, seals, plugs, etc.), various tunnels and other underground facilities, and includes a simplified representation of the geological structure, i.e., the host rock (including the excavation disturbed zone (EDZ) around the underground openings), confining units, local aquifers, and a highly-transmissive zone. The IFC model was designed in close collaboration with Nagra.

This report describes all functional requirements of the IFC and how they are implemented in the IFC. The input formats needed to invoke added modeling capabilities are documented. Finally, the IFC model grid is described, and results from a test simulation are presented.

3 Requirements

The intended use of the IFC within a probabilistic performance assessment framework for the Swiss nuclear waste disposal program defines functional, interface, and performance requirements for the software. In general, the code needs to be able to handle features, events, and processes that are considered safety-relevant; these are specified in a list of accepted FEPs (FEP-Screening report M.2.2.E.2). Moreover, the specifics of the Swiss repository system need to be appropriately represented. Integration of the IFC into the PSA concept also requires that the code is computationally efficient and robust, and that it can be integrated with other IRRC components.

The IFC is not intended to be a general-purpose simulation program; it only has to be able to handle a finite number of processes for a specific set of repository layouts, environments, and conditions. The sophistication with which individual processes are represented is limited by their respective treatment in the safety report for a repository in the Opalinus Clay (Nagra, 2002b, NTB 02-05; see also Nagra, 2007b, Order 960.09, p. 2, Bullet 2). The processes may be appropriately abstracted or simplified in accordance with their expected relative impact on overall repository performance. Only post-closure conditions after the thermal pulse will be considered.

The specific functional, interface, and performance requirements for the TOUGH2-based IFC are summarized in the following subsections. The requirements are numbered for later reference. The implementation of each requirement is discussed in Section 4.

3.1 Functional Requirements

The functional requirements define the requested functionality to be implemented in the IFC. They are grouped into requirements related to (1) the representation of the repository system, (2) the hydrogeologic environment, and (3) safety-relevant FEPs as identified in Nagra (FEP-Screening report M.2.2.E.2).

The IFC will be used for probabilistic safety assessment calculations for a repository for spent fuel (SF), vitrified high-level waste (HLW), and long-lived intermediate-level waste (ILW) and a related pilot facility. The repository is sited in Opalinus Clay, as described in Nagra (2002b, NTB 02-05, Section 4.4). For the purposes of the IFC, the individual components of the repository system and their geometries will need to be represented in a simplified, albeit defensible manner, taking advantage of symmetries and reduced model dimensionality, where appropriate.

3.1.1 Functional Requirements Related to Repository Layout

A plan view of the repository layout is shown in Fig. 2; a three-dimensional rendering is shown in Fig. 3. The repository elements to be considered are summarized in Tab. 1.

Tab. 1: Functional Requirements Related to Repository System.

#	Requirement	Comment/Reference
R1	Represent flow conditions within and in the vicinity of waste emplacement tunnels of the main SF/HLW/ILW and pilot facilities.	The main facility consists of an array of 800 m long, parallel emplacement tunnels with a diameter of 2.5 m; the spacing between tunnels is 40 m (Nagra, 2002b, NTB 02-05, Section 4.5.1).
R2	Represent flow through and along the backfill material.	See Fig. 11 and Tab. 9
R3	Represent flow through and along the excavation disturbed zone (EDZ)	EDZ has approximately one order of magnitude increased permeability than undisturbed Opalinus Clay (Nagra, 2002b, NTB 02-05, Section 5.5.1).
R4	Represent operation tunnels, access tunnel (ramp), construction tunnel, shaft, central area, and other backfilled underground structures	See Fig. 2
R5	Represent seals and plugs	See Nagra (Internal Report, 2006, Appendix 15) and Nagra (2002b, NTB 02-05, Sections 4.5.3.4 and 5.5.1).

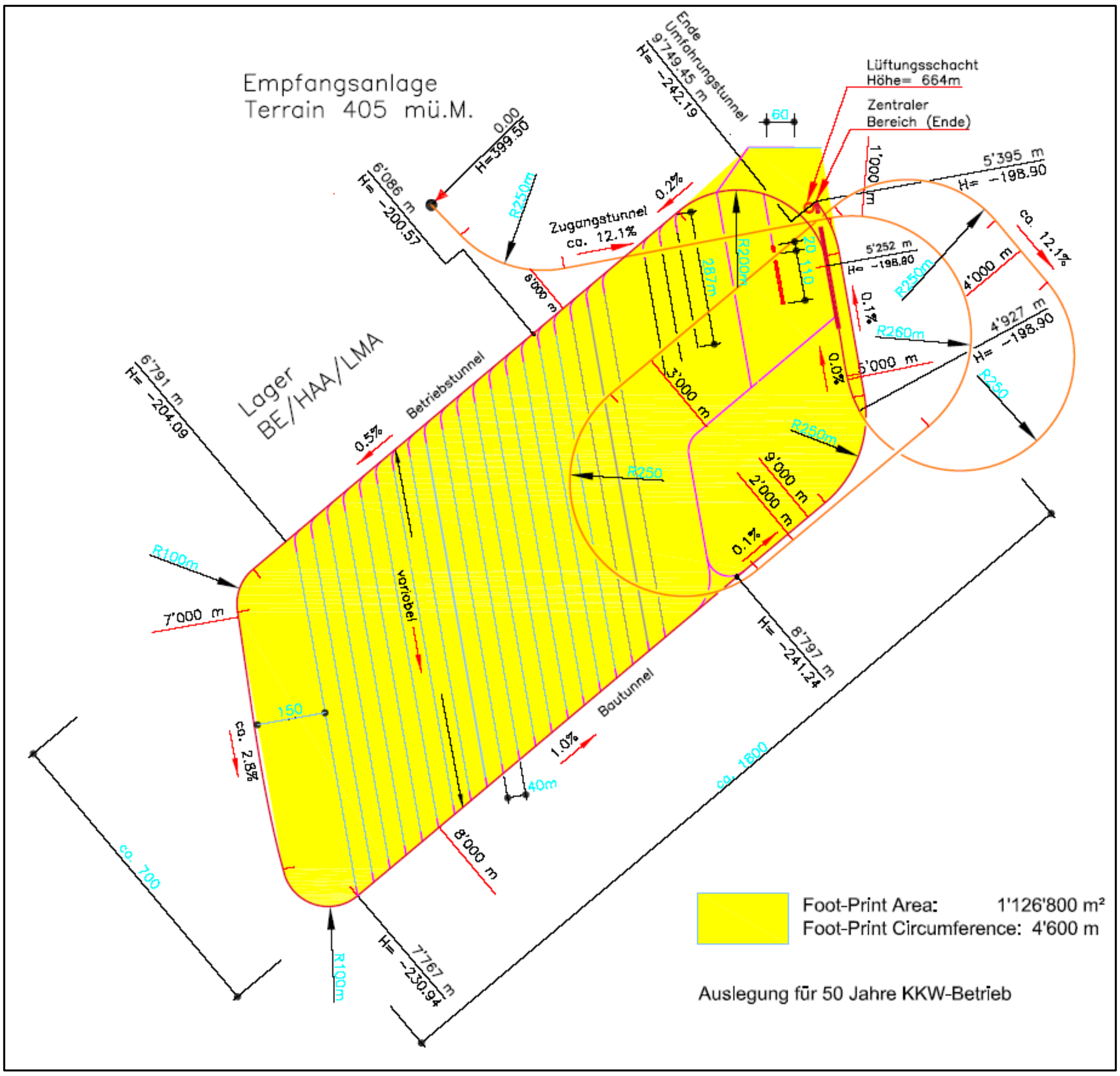

Fig. 2: Plan view of the repository layout for SF/HLW/ILW in Opalinus Clay.

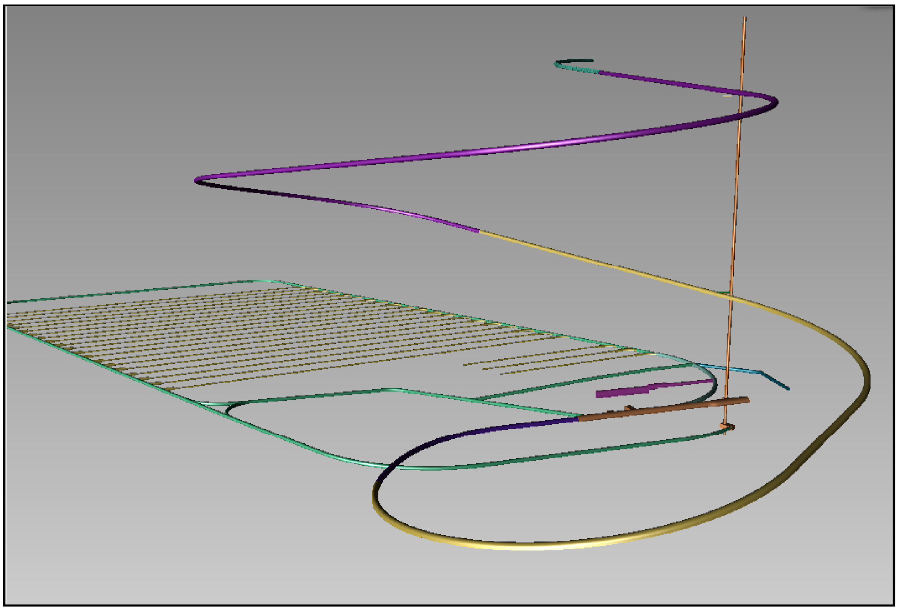

Fig. 3: Three-dimensional view of the repository layout.

3.1.2 Functional Requirements Related to the Hydrogeologic Environment

The IFC development focuses on a model of the Opalinus Clay of the Zürcher Weinland as a potential host formation for a SF/HLW/ILW repository. The geological and hydrogeological environment is described in Nagra (2002b, NTB 02-05, Section 4.2). The Opalinus Clay is considered as a host rock mainly because of its hydrogeologic and geochemical homogeneity, tectonic stability, self-sealing capacity, low permeability, low natural resource potential, geochemical stability and retention capacity, and its favorable engineering properties. Some of these characteristics allow for a simplified treatment of the host rock and its hydrogeologic and geomechanical properties within the IFC. The functional requirements related to the hydrogeological environment are summarized in Tab. 2.

Tab. 2: Functional Requirements Related to the Hydrogeologic Environment.

#	**Requirement**	**Comment/Reference**
R6	Represent relevant hydrogeologic features (stratigraphy and properties) of the repository host rock and confining units.	See Nagra (2002b, NTB 02-05, Tables 4.2-1 and 4.2-2; Figure 4.2-7).
R7	Represent the relevant regional hydrologic conditions.	See Nagra (2002b, NTB 02-05, Section 4.2.5, Figures 4.2-8 and 4.2-10, Table 4.2-3).

3.1.3 Functional Requirements Related to Accepted FEPs

Tab. 3 summarizes the functional requirements that result from the list of safety-relevant phenomena considered in the IFC. The list is a subset of all examined features, events and processes (FEPs). Only accepted FEPs related to environmental processes are considered in the IFC; FEPs related to radionuclide processes, the biosphere, and special issues are not considered. Moreover, FEPs related to short-term, transient effects after repository closure (e.g., resaturation of EDZ and backfill, radiation-related and thermal processes) are currently not considered. The FEP numbering follows that of Nagra (Internal Report, 2006).

Tab. 3: Functional Requirements Related to the Accepted FEPs.

#	Requirement	Comment/Reference
R8	Represent water flow through rock matrix	FEP 1.3.1; discontinuities on a scale less than one meter (referred to as fissures) are considered to be part of the rock matrix
R9	Represent water flow through transmissive discontinuities in host rock	FEP 1.3.2; transmissive discontinuities include fractures and fracture zones; in Opalinus Clay, fractures are hydraulically active only under certain stress conditions.
R10	Represent gas/water flow through EDZ	FEP 1.3.4; consider gas channeling effects in highly heterogeneous EDZ; EDZ properties may be time dependent.
R11	Represent gas/water flow through sealing zones	FEP 1.3.5; includes bentonite seal and sealing-zone EDZ.
R12	Represent gas/water flow through concrete backfill between emplacement tunnel and operation tunnel	FEP 1.3.6; concrete plugs and associated EDZ in ILW facility.
R13	Represent water flow in confining units	FEP 1.3.7; by definition, the model domain is bounded by regional aquifers, which are considered the compliance boundary and are thus excluded from the IFC; however, the upper and lower confining units may contain local aquifers (Nagra, 2002b, NTB 02-05, Figure 7.4-1).
R14	Represent resaturation of cementitious backfill	FEP 1.3.10; considered safety-relevant for ILW facility.
R15	Represent gas generation by anaerobic corrosion of metals, microbial degradation, radiolysis, and decay	FEP 1.3.11; dependence of gas generation rate on water availability is not considered safety-relevant.
R16	Represent water consumption by gas generation	FEP 1.3.13.
R17	Represent gas dissolution/degassing	FEP 1.3.14.
R18	Represent formation of gas phase and gas pressure build-up	FEP 1.3.15.
R19	Represent gas-induced porewater displacement	FEP 1.3.16; see Nagra (2002b, NTB 02-05, Figure 7.4-7)
R20	Represent gas transport by advection and diffusion of dissolved gas	FEP 1.3.17; see Nagra (2004, NTB 04-06, Figure 3.1-1, Illustration 1).
R21	Represent gas transport by two-phase flow	FEP 1.3.18; see Nagra (2004, NTB 04-06, Figure 3.1-1, Illustration 2).

#	Requirement	Comment/Reference
R22	Represent gas transport by dilatant gas pathway formation	FEP 1.3.19; see Nagra (2004, NTB 04-06, Sections 3.1 and 4.2, Figure 3.1-1, Illustration 3).
R23	Represent gas accumulation in confining units	FEP 1.3.21.
R24	Represent rock mechanical evolution of EDZ	FEP 1.4.1; specifically post-closure evolution of EDZ properties.
R25	Represent tunnel convergence	FEP 1.4.3; potentially safety-relevant for ILW facility (Nagra, 2002b, NTB 02-05, Sections 5.3.3.1 and 5.4.3).
R26	Represent increase of hydraulic conductivity by uplift/erosion	FEP 1.4.7; see Nagra (2002b, NTB 02-05, Section 5.2.2.3).
R27	Represent effects of chemical/mineralogical alteration of bentonite	FEP 1.5.2; increase in permeability due to reduction in bentonite swelling pressure.
R28	Represent sealing effect of high-pH plume in host rock	FEP 1.5.4; potential development of skin zone in host rock around ILW facility.
R29	Represent sealing effect of high-pH plume in tunnel backfill	FEP 1.5.11; sealing effect on sand / bentonite backfill of operation tunnels in ILW facility.

3.2 Interface Requirements

The IFC has to be able to exchange input parameters and output variables with other components of the IRRC (see Fig. 1). Moreover, the code needs to be designed such that it can be embedded as a module into a system-level modeling tool such as GoldSim (GoldSim Technology Group, http://www.goldsim.com). These interface requirements are summarized in Tab. 4.

Tab. 4: Interface Requirements.

#	Requirement	Comment/Reference
R30	Provide interfaces for the exchange of parameters and variables with other IRRC modules.	Model calculating gas generation rates, STMAN, and RTC.
R31	Provide interfaces for the integration of IFC into a system-level modeling tool.	E.g., GoldSim (see Nagra, 2007b, Order 960.09, p. 3).

3.3 Performance Requirements

Since the IFC will be called multiple times during a probabilistic analysis using Monte-Carlo simulations, it is essential that the code runs efficiently and in a robust manner for a large set of representative parameter combinations and scenarios. These performance requirements are summarized in Table 5.

Tab. 5: Performance Requirements.

#	Requirement	Comment
R32	Perform a large number of IFC simulations within an acceptable clock time	The acceptable clock time is affected by CPU time and load; the acceptable CPU time depends on the number of processes that can be run in parallel; the manageable model size depends on single-CPU performance.
R33	Perform IFC simulations in a robust manner	Successful completion of individual IFC runs cannot be predicted or guaranteed, requiring the implementation of an acceptable error recovery strategy.

4 Software Design

This section discusses the general design of the IFC and describes how each of the requirements identified in Section 3 is implemented into the numerical code. The model representing the repository system and geosphere (i.e., the IFC model) is described in Section 5.

4.1 General Approach

As mentioned in Section 2 and in accordance with Nagra (2007b, Order 960.09, p. 1), the IFC is developed based on the assumption that most FEPs as well as elements of the repository are to be implemented into the PSA concept using a (simplified) process model. Issues of scenario selection and uncertainty propagation analysis are outside the scope of the IFC.

Since the IFC is intended to be a site-specific prediction model tailored to the design of a SF/HLW/ILW repository located in Opalinus Clay, IFC development is not only concerned with software design, but also with the development of a conceptual model for the repository and tunnel system, and the representation of safety-relevant processes and phenomena. The implementation of the requirements outlined in Section 3 follows an approach that is aimed at (1) providing sufficient flexibility that allows for the potential adaptation of the conceptual model, (2) taking advantage of the well-defined scope of the IFC's intended application, making it computationally efficient, and (3) minimizing software development and testing.

These goals are achieved by basing the IFC on the well-established, general-purpose two-phase flow and transport simulator TOUGH2 (Pruess et al., 1999; http://www-esd.lbl.gov/TOUGH2). The code will be modified to account for FEPs that are specific to the Swiss nuclear waste disposal concept. These modifications are implemented in the inverse modeling code iTOUGH2 (Finsterle, 2007abc; 2004; http://www-esd.lbl.gov/iTOUGH2), which provides a framework for calling the TOUGH2 forward simulator using different parameter sets and for easily extracting certain performance measures. Moreover, iTOUGH2 has the capability to perform Monte Carlo simulations in parallel (Finsterle, 1998), should such an option become desirable. Finally, it has been demonstrated (Zhang et al., 2007) that TOUGH2 (and iTOUGH2) can be linked to the GoldSim system-level modeling tool. Developing the IFC based on iTOUGH2 rather than TOUGH2 may have the disadvantage that the massively-parallel version of TOUGH2 (Wu et al., 2002; Zhang et al., 2003) cannot be utilized. However, should multiple processors be available for PSA calculations, they would most likely be used for the "embarrassingly parallel" task of running multiple Monte Carlo simulations simultaneously. In what follows, we refer to the simulator simply as "TOUGH2", implying that it is the forward model used within the iTOUGH2 framework.

Many of the required processes and phenomena are directly addressed by the capabilities of the standard version of TOUGH2 (see Section 4.2). The site- and repository-specific requirements (specifically R22, R24, R25, R26, R27, R28, and R29) are incorporated by simplified parametric models or by interpolation from look-up tables created by more sophisticate process models. It is beyond the scope of the IFC to develop, examine, or justify these parametric models; references to supporting documentation will be given, if available. Formal testing of the correct implementation of these submodels in iTOUGH2- IFC will be presented in Section 7; however, validation of the submodels (i.e., demonstration of their adequacy for the intended use) may require extensive analyses.

As mentioned above, the IFC consists of (1) a simulation code (i.e., a customized version of a specific iTOUGH2 module), and (2) a site-specific conceptual model of the repository system in the Opalinus Clay. Development of the iTOUGH2-IFC code is discussed in the remainder of this section; the conceptual model development is documented in Section 5.

4.2 Standard TOUGH2 Simulation Capabilities

Table 6 summarizes some of the simulation capabilities that are provided by the standard version of TOUGH2; they are available without the need for code modifications. If invoked by a proper conceptual model, these built-in capabilities address a substantial number of the IFC requirements identified in Section 3. The capabilities are described in detail in Pruess et al. (1999).

The TOUGH2 suite of simulators consists of multiple modules of varying sophistication and complexity (Pruess et al., 1999; Pruess, 2004; Finsterle et al., 2008). While one of the simplest modules will be used for the IFC (e.g., the equation-of-state (EOS) module No. 5 for two-phase flow of water and hydrogen), the more advanced capabilities (which may include density-driven liquid flow, multiple gas species, radionuclide transport, and coupled geomechanical and biogeochemical process simulations) are available for validation studies or to provide input for a suitable abstraction within the IFC.

Tab. 6: Simulation Capabilities of Standard TOUGH2 and iTOUGH2.

#	Capability	Requirement Addressed	Comment
1	Simulation of two-phase (gas and liquid) flow through porous media; handles single- and two-phase conditions, including phase-state changes	R8, R9, R10, R11, R12, R13, R14, R15, R18, R19, R21, R23	Two-phase flow through porous materials is simulated using the extended version of Darcy's law; phase properties (density, viscosity) are calculated internally; phase interference is described by capillary pressure and relative permeability functions.
2	Simulation of two components (water and a non-condensible gas); both components exist in both phases	R17, R18, R20	The two-phase, two-component formulation allows for the simulation of evaporation and dissolution effects, appearance and disappearance of a gas phase, and component diffusion in each of the phases; for the IFC, a single gas component (hydrogen) is chosen.
3	Representation of heterogeneity (zonal or local; above the scale of an individual grid block)	R8, R9, R10, R11, R12, R13	Provided that two-phase flow is appropriately represented by Darcy's law, multiple materials (including matrix, fractures, fracture zones, EDZ, bentonite, concrete, seals, plugs, etc.) can be simulated.
4	Formulations of fractured systems using double-porosity, dual permeability, effective continuum model, Active Fracture Model	R8, R10	Allows for inclusion of fissures, dense fracture networks, or other bi-modal systems; the Active Fracture Model (Liu et al., 1998) may be used to represent gas channeling and gas piping effects. Accounts for pressure-dependent porosity changes.
5	Integral finite difference method with unstructured grids	R1, R2, R3, R4, R5, R6, R7, R9	Enables flexible discretization of complex geometry, and allows for "non-geometric" representation of abstracted repository elements.
6	Capability to handle nonlinearities	R22, R24, R25, R27, R28, R29, R33	Nonlinearities are inherent in all two-phase flow processes; the code's capability to handle these inherent nonlinearities will allow the inclusion of additional nonlinear effects to represent certain FEPs
7	iTOUGH2 framework	R30, R31	Provides convenient interfaces to other modules and programs

4.3 Implementation of Relevant Processes

This subsection describes in more detail those processes that are specific to the IFC, or that required code modifications.

4.3.1 Representation of Resaturation Process

Resaturation of cementitious backfill material into the initially air-filled portions of the ILW facility (R14; FEP 1.3.10) affects the storage volume for gas generated in the repository and thus the related pressure build-up. The effect can be simulated in the IFC using an appropriate discretization of the ILW emplacement tunnels and by specifying a non-zero initial gas saturation. Since the IFC only considers a single gas component (i.e., hydrogen), the initial gas in the IFC needs to be modeled also as hydrogen, rather than air. Resaturation is then simulated using the standard modeling capabilities of TOUGH2. See also the discussion on initial conditions in Sections 4.4 and 10.3.1, and on multi-component gases in Section 10.1.1.

4.3.2 Representation of Gas Generation

Rate of gas generation (R15; FEP 1.3.11) for the SF/HLW/ILW facilities will be provided externally as time-dependent source terms. They are expected to be consistent with the values given in Nagra (2002c, NTB 02-06, Table 4.3-1). Gas generation will cease after about 170,000 years. While waste is emplaced with a 3 m spacing between the 2 m long HLW and 4.6 m long SF canisters, gas generation is modeled as a line source along the emplacement tunnels. If considered relevant, water consumption (R16; FEP 1.3.13) as a result of gas generation could be invoked as a component- or phase-specific sink term that is proportional to the gas generation rate. However, the limitation of gas generation by lack of water is not considered significant (FEP-Screening report M.2.2.E.2); therefore, no water sink terms are specified in the current base-case model.

4.3.3 Representation of Pathway Dilation

The creation of dilatant gas pathways (R22; FEP 1.3.19) is discussed in detail in Nagra (2004, NTB 04-06; Sections 3.1 and 4.2). This microfracturing process is initiated as the gas pressure approaches the minimum principal stress. The threshold pressure for dilatant gas flow is considered a material- and depth-dependent property and is also related to the local stress field. Pressure-dependent pathway dilation leads to increased permeability and reduced capillary strength. Pathway dilation is implemented in the IFC as follows:

- Calculate the depth-dependent threshold pressure p_d [Pa] for dilatant gas flow:

$$p_d(z) = d \cdot (f - z) - e \tag{1}$$

where:

z : elevation [m.a.s.l.]
d : lithostatic pressure gradient [Pa m^{-1}]
e : empirical parameter [Pa]
f : surface elevation [m.a.s.l.]

- Calculate the vertical permeability k_v [m^2] as a function of p_d and pore pressure p:

$$k_v(p,z) = \begin{cases} k_{v,0} & p \le p_d(z) \\ k_{v,0} + b \cdot (p - p_d(z))^a & p > p_d(z) \end{cases} \tag{2}$$

where:

$k_{v,0}$: undisturbed vertical permeability [m^2]
p : absolute pore pressure [Pa]
a : empirical exponent [-]
b : empirical coefficient [m^2 Pa^{-a}]

- Calculate the anisotropy ratio A [-] as a function of k_v:

$$A(k_v) = \frac{k_h}{k_v} = 5^{(k_{v,0}/k_v)^c} \tag{3}$$

where:

c : empirical exponent [-]

- Calculate the horizontal permeability k_h [m^2] as a function of A:

$$k_h(A) = A \cdot k_v$$

- Calculate the capillary-strength parameter $1/\alpha$ [Pa] as a function of kh using Leverett scaling:

$$\frac{1}{\alpha} \sim \frac{1}{\alpha_0}\sqrt{\frac{k_h}{k_{h,0}}} \tag{4}$$

where:

$1/\alpha_0$: undisturbed capillary-strength parameter [Pa]

$k_{v,0}$: undisturbed horizontal permeability [m^2]

- Porosity and the parameters of the characteristic curves (except the capillary-strength parameter) are considered constant.
- Single- and two-phase flow within dilatant pathways will be calculated using the standard TOUGH multi-phase process description.

Different parametric models describing pressure-dependent changes in Opalinus Clay properties can be implemented to evaluate conceptual model uncertainty.

4.3.4 Representation of Mechanical Processes

No geomechanical process simulations are performed within the IFC. However, the impacts of geomechanical processes on hydrogeologic properties are accounted for in an abstracted way by externally provided functions. Potential feedback mechanisms (i.e., coupled hydrologic-mechanical processes) are ignored.

FEP 1.4.1, R24: EDZ Self-Sealing

Self-sealing of the EDZ results in a reduction in permeability, which is implemented as an externally provided, time-dependent permeability-reduction factor $f_{kEDZ}(t)$ applied to all elements representing the EDZ.

$$k_{EDZ} = k_{EDZ,0} \cdot f_{kEDZ}(t) \tag{5}$$

Here, $k_{EDZ,0}$ is the initial permeability of the EDZ; $f_{kEDZ}(t)$ is provided as a look-up table. Corresponding changes in two-phase flow parameters (e.g., increase in capillary strength) are ignored, but could be implemented analogous to Section 4.3.3.

Similarly, the porosity of the EDZ is also reduced as a result of self-sealing. Again, a time-dependent porosity-reduction factor $f_{\phi EDZ}(t)$ is provided as a user-specified look-up table. Since porosity also changes as a function of pore pressure, the effect is implemented in the IFC by calculating a time-dependent rate of porosity change due to self-sealing (rather than a time-dependent porosity itself), which is then added to the porosity change due to pore compressibility $\Delta\phi_c$ to arrive at the new porosity:

$$\Delta\phi_{EDZ} = \phi_{EDZ,0}(f_{\phi EDZ}(t+\Delta t) - f_{\phi EDZ}(t)) \tag{6}$$

$$\phi_{EDZ}(t+\Delta t) = \phi_{EDZ}(t) + \Delta\phi_c + \Delta\phi_{EDZ} \tag{7}$$

Here, $\phi_{EDZ,0}$ is the initial EDZ porosity. Note that a reduction in porosity leads to expulsion of the phase mixture present in the pore space of each element.

FEP.1.4.3, R25: Tunnel Convergence

In the ILW facility, creep of the host rock leads to tunnel convergence, which results in a pore-volume reduction in the repository and potentially in pore-water expulsion. As before, a look-up table provides a time-dependent porosity-reduction factor $f_{\phi LMA}(t)$, which is then used to calculate the porosity change:

$$\Delta\phi_{ILW} = \phi_{LMA,0}(f_{\phi ILW}(t+\Delta t) - f_{\phi ILW}(t)) \tag{8}$$

$$\phi_{ILW}(t+\Delta t) = \phi_{ILW}(t) + \Delta\phi_c + \Delta\phi_{ILW} \tag{9}$$

Corresponding changes in two-phase flow parameters (e.g., increase in capillary strength) could be implemented analogous to Section 4.3.3. The change in bulk volume and repository geometry will be ignored. Note that TOUGH2 provides for the calculation of a pore-pressure-dependent porosity change $\Delta\phi_c$.

Specifying a time-dependent porosity reduction without considering coupled hydro-mechanical effects may lead to unrealistic effects. For example, it is unlikely that tunnel convergence proceeds at a rate that is independent of whether the pore space is gas filled or fully liquid saturated. Prescribing a porosity reduction in a fully water saturated, tight formation may lead to abrupt and excessive pressure increases due to the small water compressibility. To avoid this unrealistic behavior and the associated numerical difficulties, tunnel convergence is limited to elements that contain gas. Despite the significantly higher gas compressibility, pressures in the ILW increase and the gas-water mixture will be expulsed due to tunnel convergence.

FEP 1.4.7, R26: Uplift

Decompaction of the Opalinus Clay due to erosion and uplift leads to an increase in permeability, which is represented by a look-up table of permeability modifiers

$$k_{OPA} = k_{OPA,0} \cdot f_{k,Uplift}(t) \tag{10}$$

Here, $k_{OPA,0}$ is the initial permeability of the Opalinus Clay.

4.3.5 Representation of Chemical Processes

No biogeochemical processes will be performed within the IFC. However, the impact of biogeochemical processes on hydrogeologic properties will be accounted for in an abstracted manner by externally provided functions. Potential feedback mechanisms (i.e., coupled hydrologic-biogeochemical processes) are ignored.

Chemical and mineralogical alterations of bentonite (R27; FEP 1.5.2) may lead to a change in permeability. Moreover, high-pH plumes from cement in the ILW facility may cause changes in the porewater composition and mineralogical alterations in sealing zones and in the host rock (R28, FEP 1.5.4; R29, FEP 1.5.11), most likely resulting in the development of a skin zone. The abstraction of these geochemical effects is described in Kosakowski et al. (2008); their implementation into the IFC is discussed in this subsection.

Permeability reduction due to geochemical sealing occurs in a thin skin zone, in which the pore space is locally clogged. Only flow perpendicular to the skin zone, which develops along the interface between two geochemically active materials, is affected by geochemical sealing processes. A local-scale porosity for this skin zone is calculated as a function of time:

$$\phi(t) = \begin{cases} \phi_0 \exp\left(-l(t/t_c)^m\right) - \left(\phi \exp(-l) - \phi_c\right)\dfrac{t}{t_c} & t \le t_c \\ \phi(t) = \phi_c & t > t_c \end{cases} \tag{11}$$

Parameters l and m are provided by the user for each material interface that leads to geochemical sealing. The clogging time t_c is calculated as a function of liquid saturation:

$$t_c = T_c / S_l \tag{12}$$

where T_c is the user-provided clogging time under fully saturated conditions. The clogging porosity ϕ_c is inversely calculated (using a bisection method) from the minimal clogging permeability (see below).

The skin-zone permeability is calculated from the local-scale porosity using the Kozeny-Carman relationship:

$$k(\phi) = k_0 \left(\frac{\phi(t)}{\phi_0}\right)^3 \left(\frac{1-\phi_0}{1-\phi(t)}\right)^2 \tag{13}$$

The clogging permeability is given as a fraction of the initial permeability:

$$k(\phi_c) = \kappa \cdot k_0 \tag{14}$$

The effective permeability used to calculate flow across an interface between two geochemically active materials is then calculated as the harmonic mean of the unaffected permeability and the time-dependent skin-zone permeability of a user-specified thickness.

4.4 Initial Conditions and Simulation Period

Resaturation, gas generation, the associated flow processes, and other safety-relevant processes are inherently time-dependent. Consequently, the IFC will simulate the transient evolution of the flow field around the repository. However, neither the transient effects during repository construction, operation, and sealing phases are likely to be simulated. Given the expected long lifetime of the waste canisters (Nagra, 2004, NTB 04-06, Table 2.3-1), gas generation is not considered to be significant (with exception of the initial corrosion of construction and tunnel-support materials) during the early period immediately after repository closure. The choice for an appropriate starting time for the IFC simulations (determining initial conditions) will be determined and justified. The corresponding initial conditions for the IFC simulations can either be pre-calculated, or – should they depend on the parameters varied during the Monte Carlo simulation – updated within the IFC.

Gas generation is expected to last for approximately 170,000 years (Nagra 2002c, NTB 02-06, Table 4.3-1). Simulations will be performed for 1 million years.

4.5 Addressing Interface Requirements

Interfaces to the TOUGH2 and iTOUGH2 simulators consist of standard ASCII text files. These text files could be directly used as the interfaces to the upstream and downstream models providing input to or using output from the IFC. In addition, iTOUGH2 provides a convenient interface for varying TOUGH2 input parameters and for selecting TOUGH2 outputs. Finally, experience with linking (i)TOUGH2 to the GoldSim system-level model show that input parameters and output variables of the process simulator can be shared with the system-level simulator.

Appropriate pre- and post-processing routines may need to be developed, depending on the interface requirements of the upstream and downstream models. An interface will be developed that allows for a seamless integration of the code into the PSA framework (R31).

4.6 Replicating Reference Waste Emplacement Tunnel

In response to requirement R32, it is essential to reduce the model size by exploiting inherent symmetries. Specifically, the regular geometry of the array of waste emplacement tunnels exhibits multiple local symmetry planes (i.e., the vertical planes along the tunnel axes, and the vertical midplanes between tunnels; details are discussed in Section 5). This means that the tunnel array can be approximated by a single representative waste emplacement tunnel. However, since there is no global symmetry of the entire repository system and the surrounding host rock, the representative emplacement tunnel submodel has to be multiplied and appropriately connected to the geosphere model. This is accomplished by the following procedure:

1. A global model is generated, consisting of the geosphere and the non-symmetric underground openings.
2. The region of the waste emplacement tunnel array is cut out from the model and left void, drastically reducing the total number of grid blocks.
3. A representative waste emplacement tunnel submodel (RWETS) is generated; it represents half of a single tunnel and the surrounding host formation to the midpoint between neighboring tunnels.
4. The RWETS is connected to the global model; note that it only occupies a small fraction of the void space created in Step 2.
5. The system-state variables calculated at the connection between the RWETS and the global model are extracted and copied to internal, Dirichlet-type boundary elements at the interface between the void and the global model.

iTOUGH2 has been modified to allow replicating primary and secondary variables from parent elements (i.e., each element at the interface between the RWETS and the global model) to one or multiple daughter boundary elements (at the corresponding internal boundary elements between the void space and the global model). Dynamically prescribing the system state as time-dependent Dirichlet-type boundary conditions at these internal boundary elements ensures that gas and liquid that flow from the representative waste emplacement tunnel to the global model are multiplied, entering the global model at the appropriate location.

5 IFC Representation of Repository System

5.1 Model Domain and Dimensionality

The system to be modeled by the IFC consists of the host rock (Opalinus Clay) and all relevant engineered components embedded in it (such as emplacement tunnels, access tunnels, operations tunnels, ventilation tunnels, construction tunnels, observation tunnels, ventilation shafts, test and pilot facilities, plugs and seals; these subsurface structures are backfilled and are surrounded by an EDZ). In addition, the surrounding geosphere needs to be represented, specifically the clay-rich confining units that may contain local aquifers (Wedelsandstein and Sandsteinkeuper aquifers). Regional aquifers (Malm aquifer and Muschelkalk aquifer) are considered to define the compliance boundary, i.e., they do not assume a barrier function (Nagra, 2002b, NTB 02-05, Section 4.2), and flow and transport processes within these aquifers do not need to be simulated within the IFC.

Given the geometry of the system and the expected direction of driving forces, the system to be modeled is inherently three-dimensional. Moreover, the scales to be considered – even if lumping pore- and small-scale features and processes into a continuum representation – span several orders of magnitude, from decimeters (e.g., the thickness of the EDZ) to kilometers (e.g., flow in the local aquifers). Given the constraints on computational efficiency (R32), an accurate, three-dimensional casting of the repository system is not feasible. Consequently, the conceptual model of the repository system for the IFC needs to exploit inherent symmetries, and – if justifiable – compromise on accuracy, fidelity, and transparency for the sake of computational efficiency. The simplifications proposed below appear reasonable, but may need to be formally justified by comparison with detailed process simulations, sensitivity, and impact analyses.

5.2 Representation of Key Model Components

5.2.1 Representation of Far Field

Fig. 4 shows a hydrogeological framework model for a repository in the Opalinus Clay of the Zürcher Weinland. It indicates the following flow regimes (see also Nagra, 2002b, NTB 02-05, Section 4.2):

- Horizontally layered stratigraphy; subvertical, transmissive discontinuities are not shown, but may be present.
- Predominantly vertical flow (and diffusion) in the host rock.
- Predominantly horizontal flow in the local aquifers; potential flow distance to discharge boundaries is large compared to repository footprint.
- Predominantly vertical flow in upper and lower confining units.

While this conceptual model of flow in the far field is predominantly one- or two-dimensional, it is inherently three-dimensional, specifically when considering the gas-release pattern from the engineered system. A three-dimensional model is therefore set up to represent the far field – sensitivity analyses could be performed to evaluate the impact of lower-dimensional models, should computational constraints require the reduction of the number of grid blocks.

Constant pressure boundaries are applied at the top and bottom of the geosphere model, based on measurements from the Benken borehole (Nagra, 2002b, NTB 02-05, Figure 4.2-8) or related information. No-flow boundaries can be applied along the vertical sides, with exception of the layers representing the local aquifers, where a horizontal hydraulic gradient will be imposed based on head measurements. Given the predominantly vertical flow direction within the host rock and the confining layers, the lateral extent of the model (along the direction of the gradient in the local aquifers) can be limited.

Larger, steeply dipping discontinuities (e.g., faults) can be included using discrete elements, accounting for their actual position relative to the repository. Currently, the presence of a single, vertical high-transmissivity zone is accounted for in the mesh design (see Section 5.3.2 for details). Hydrogeologic properties of the geosphere are summarized in Nagra (2004, NTB 04-06, Tables 3.3-1, 3.3-2, and 3.3-3); the properties used in the IFC base-case model are discussed in Section 5.4.

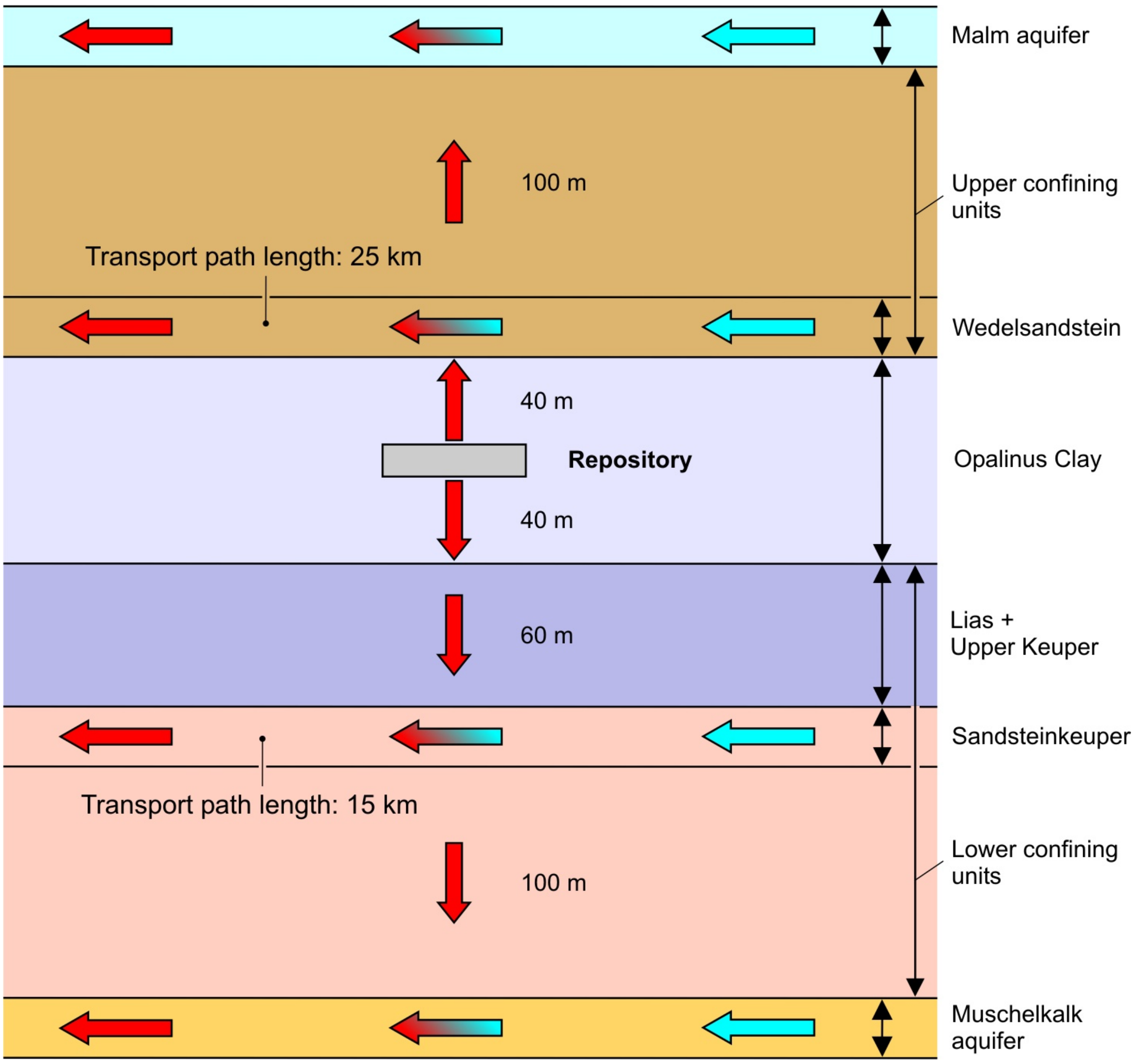

Fig. 4: Hydrogeological framework model of a repository in the Opalinus Clay of the Zürcher Weinland (Nagra, 2002c, NTB 02-06, Figure 3.5-1).

5.2.2 Representation of Waste Emplacement Tunnels

Gas generation by anaerobic corrosion of metals, microbial degradation, radiolysis, and decay originates mainly in the waste emplacement tunnels. The creation of a free gas phase is expected to impact the pressure and flow fields within the backfilled tunnels and the near field, in turn affecting potential radionuclide transport pathways and velocities (to be calculated by the RTC). Moreover, pressure build-up and gas- and liquid-phase transport are affected by the ability of gas to escape the emplacement tunnels, either directly into the surrounding host rock, or along the buffer and backfill materials and EDZ to the operations tunnel and other connected, backfilled cavities. The appropriate representation of the array of emplacement tunnels is therefore a crucial element of the IFC. Different representations are needed for the SF/HLW, pilot, and ILW facilities.

The repository layout is shown in Fig. 2 above. The SF/HLW facility consists of an array of twenty-seven, 800 m long, parallel emplacement tunnels with a diameter of 2.5 m, dipping at an average slope of approximately 4.2 % from the operations tunnel in the north towards the construction tunnel in the south; the spacing between tunnels is 40 m. Operations and construction tunnels have a slope of approximately 0.5 %; the access ramp dips at approximately 12.1 %. A pilot facility (consisting of three emplacement tunnels) is located in the north-eastern corner of the main facility. The ILW facility consists of two short emplacement tunnels, referred to as LMA-1 (110 m) and LMA-2 (60 m). Several seals (R11; FEP 1.3.5) and plugs (R12; FEP 1.3.6) will be installed during closure of the facility. The repository is located at a depth of approximately 600 m below ground surface, in the mid-plane of the 105–115 m thick Opalinus Clay. The repository has a footprint of approximately 1 km^2. Details about the geometry of the emplacement tunnels are summarized in Nagra (Internal report, 2007).

The layout and geometry of the SF/HLW emplacement tunnels and the pilot facility exhibits the following approximate symmetries:

(1) Vertical symmetry plane along axis of emplacement tunnel.

(2) Vertical symmetry plane, halfway between (i.e., 20 m from) and parallel to axes of emplacement tunnels.

These symmetry planes ignore repository edge effects and local heterogeneities. Moreover, it is assumed that the gas conditions in a single emplacement tunnel are not significantly affected by the conditions along the construction and operation tunnels. These conditions are non-uniform as gas accumulates along these tunnels in a cumulative fashion along the prevalent flow direction. The magnitude and behavior of gas flow within the operation, construction, and access tunnels critically determine the validity of this conceptualization. If these fluxes are small and conditions in the tunnels are approximately uniform, only 1/2 of a single emplacement tunnel (i.e., only about 2.5 % of the entire emplacement tunnel array) needs to be represented in the IFC. The connection of the emplacement tunnel to the construction and operation tunnels is described in Section 5.2.3. The end sections of the emplacement tunnels, where no waste will be stored, as well as seals, locks, and turn-out sections will be explicitly included (R5).

Perpendicular to the tunnel axis, discretization will allow for the representation of the canister (as the gas source), the backfilled tunnel, the EDZ, and the host rock. Hydrogeologic properties for the engineered materials and geologic formations are summarized in Section 5.4). According to the calculations presented in Nagra (2004, NTB 04-06, Figure 4.2-5), isobars become essentially horizontal at a distance of about 10 m above and below the tunnel axis. The vertical extent of this zone is also expected to contain the 13 MPa isobar, which corresponds to the threshold pressure for dilatant gas flow (see Section 4.3.3). It seems appropriate to connect the near-field submodel of the waste emplacement drift to the far-field geosphere model (see Section 5.2) at elevations of ±10 m from the elevation of the repository axis.

The ILW emplacement tunnels are implemented explicitly due to a lack of symmetry.

5.2.3 Representation of Other Backfilled Underground Structures

Escape of gas along the backfilled tunnel system (R4) is one of the main gas transport variants described in Nagra (2004, NTB 04-06, Section 4.3, Table 4.3-1). The tunnel system includes the access ramp, construction tunnel, operations tunnel, observation tunnels, detour tunnel, central area, ventilation shaft and other backfilled underground openings. Waste emplacement tunnels are connected to the operations tunnel in the north and construction tunnel in the south. The ILW facility is connected to the tunnel system in the north-eastern corner of the repository, and a construction and ventilation shaft is present in the north-eastern corner of the repository (see Fig. 2). Several seals are in place along the tunnel system. This configuration does not exhibit an obvious symmetry.

To accurately represent this potentially significant gas-release pathway, the tunnel system is represented in full. While the detailed geometry of the tunnel segments is simplified, the connectivity, relative position, and interaction with the geosphere are observed.

The various tunnel cross sections are represented in a simplified manner, reflecting flow-relevant geometrical properties (specifically, cross-sectional area). Each tunnel segment is surrounded by an EDZ (R3 and R11, FEP 1.3.5), and connected to the host rock. Plugs and seals (R5) are represented accordingly, using hydrogeologic properties of the backfill material.

The single, representative waste emplacement tunnel and the near-field host rock surrounding it (see Section 5.2.2) will be connected to the operations and/or construction tunnel at a single location (e.g., that of the central emplacement tunnel). To represent the interaction between the entire SF/HLW facility and the operations and construction tunnels, special elements allowing for time-dependent Dirichlet boundary conditions are attached along the operations and construction tunnels; the pressures and saturations (or hydrogen-mass fraction) specified for these special boundary elements are taken (at each time step) from those elements of the representative emplacement tunnel that are connected to the operations tunnel. Again, this assumes that the conditions in the center emplacement tunnel (connected to the operations tunnel) are representative of all emplacement tunnels. This approach allows for a reasonable representation of the impact of the emplacement tunnels on flow conditions within the tunnel system.

Similarly to the treatment of the emplacement tunnels, potential gas releases from the tunnel system to the host rock and confining layers are enabled by connecting the tunnel system vertically to the far-field model described in Section 5.2. Furthermore, the access ramp is directly connected to the Wedelsandstein aquifer (R23; FEP 1.3.21) to accommodate one of the gas-release scenario described in Nagra (2004, NTB 04-06, Section 4.3).

5.2.4 Equivalent Conceptual Repository Model

The complex repository layout shown in Fig. 2 is simplified to be able to account for approximate symmetries, and to make the model conceptually and computationally tractable. An Equivalent Conceptual Repository Model (ECRM) was developed by Nagra; it is shown in Fig. 5. It preserves essential geometrical aspects of the actual repository layout, specifically tunnel lengths and footprint area. The ECRM is the basis for generating a computational grid, as discussed in Section 5.3.

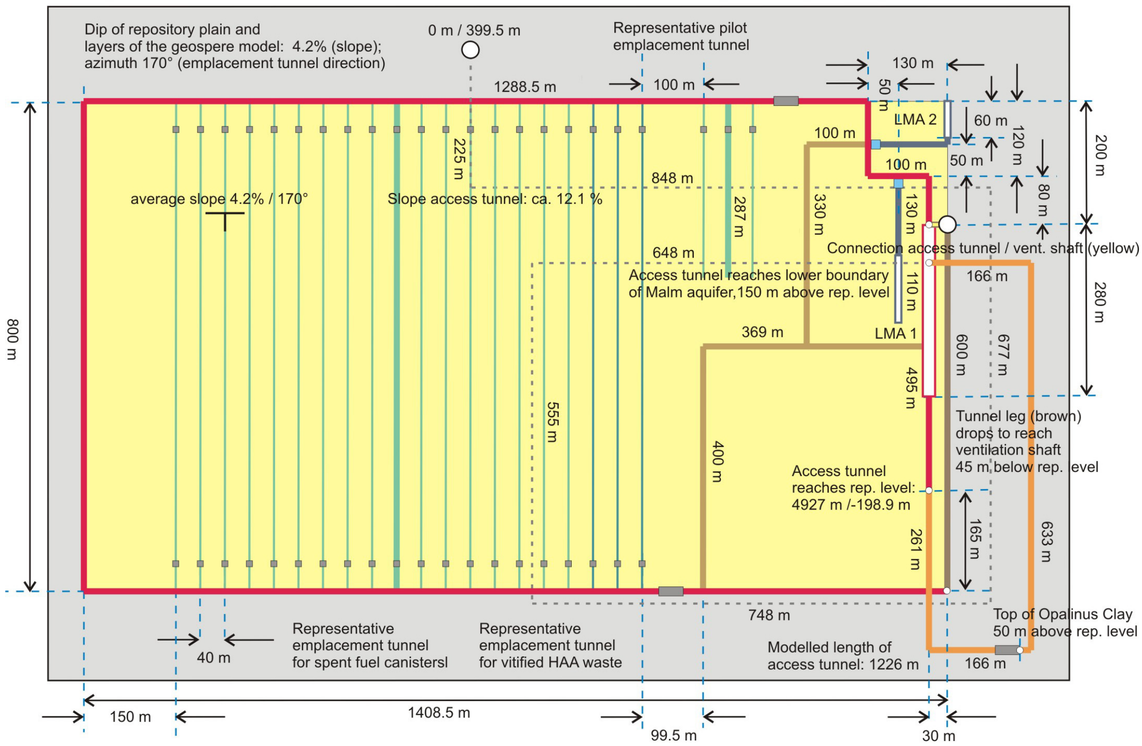

Fig. 5: Equivalent conceptual repository model.

5.3 Mesh Generation

5.3.1 General Approach

A computational mesh for the integral finite differences code iTOUGH2-IFC is generated, properly representing the geometry and properties of all key features of the geologic framework model (see Fig. 4) and the simplified repository system (see Fig. 5). Mesh generation occurs in several steps, where submeshes are generated separately (using a combination of internal mesh generation capabilities of iTOUGH2-IFC, Fortran routines for mesh manipulation, and Unix script files); the resulting submeshes are eventually linked together. The following submeshes are generated:

- Host rock and confining units
- Local aquifers (Wedelsandstein and Sandsteinkeuper aquifers)
- High-transmissivity zone
- Representative emplacement tunnel for SF/HLW facility
- Representative emplacement tunnel for pilot facility
- Emplacement tunnel for long-lived intermediate-level wastes, LMA-1

- Emplacement tunnel for long-lived intermediate-level wastes, LMA-2
- Operations tunnel
- Construction tunnel
- All other backfilled tunnels (i.e., access tunnel, connecting tunnel, detour tunnel, control tunnel, central area, shaft)

The generation of each of these submeshes is described in the following subsections. Fig. 6 shows the submeshes in a three-dimensional depiction; plan views are shown in Fig. 7. Note that the submeshes of the waste emplacement tunnels (shown in red) contain the waste, backfill material, EDZ, and the host rock in the immediate vicinity of the tunnels (see Sections 5.3.3 and 5.3.4 for details); the construction and operations tunnels (shown in green) include the backfilled tunnels, associated EDZ, and the surrounding host rock, which extends in horizontal direction from starter and turn-out tunnels (i.e., the respective connections of the construction and operation tunnels to the waste emplacement tunnels) to the outer (northern and southern) edges of the model (see Section 5.3.5 for details); the remaining underground structures (shown in blue) only represent the backfilled structure and associated EDZ in a simplified manner (see Section 5.3.6 for details).

The mesh has a total of approximately 36,000 grid blocks and 112,000 connections between them. Two equations (one for the component water, one for hydrogen) are set up for each grid block, resulting in a system of nonlinear equations with approximately 72,000 unknowns to be solved at each time step. Approximately 10,000 time steps need to be solved to reach the intended simulation time of 1,000,000 years. Time stepping is automatically adjusted; thus, the number of time steps and total CPU time may considerably depend on the parameter set.

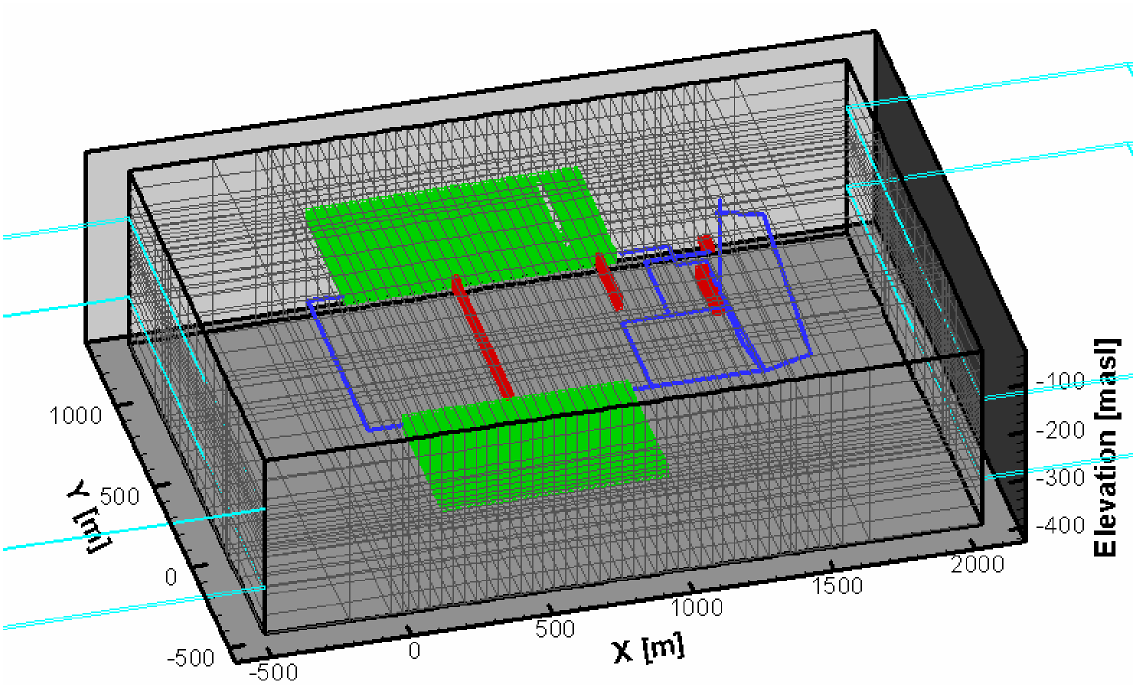

Fig. 6: Three-dimensional view of computational mesh of IFC model; submesh of geosphere (gray), local aquifers (cyan), representative waste emplacement tunnels (red), operations and construction tunnels (green), and other backfilled tunnels (blue).

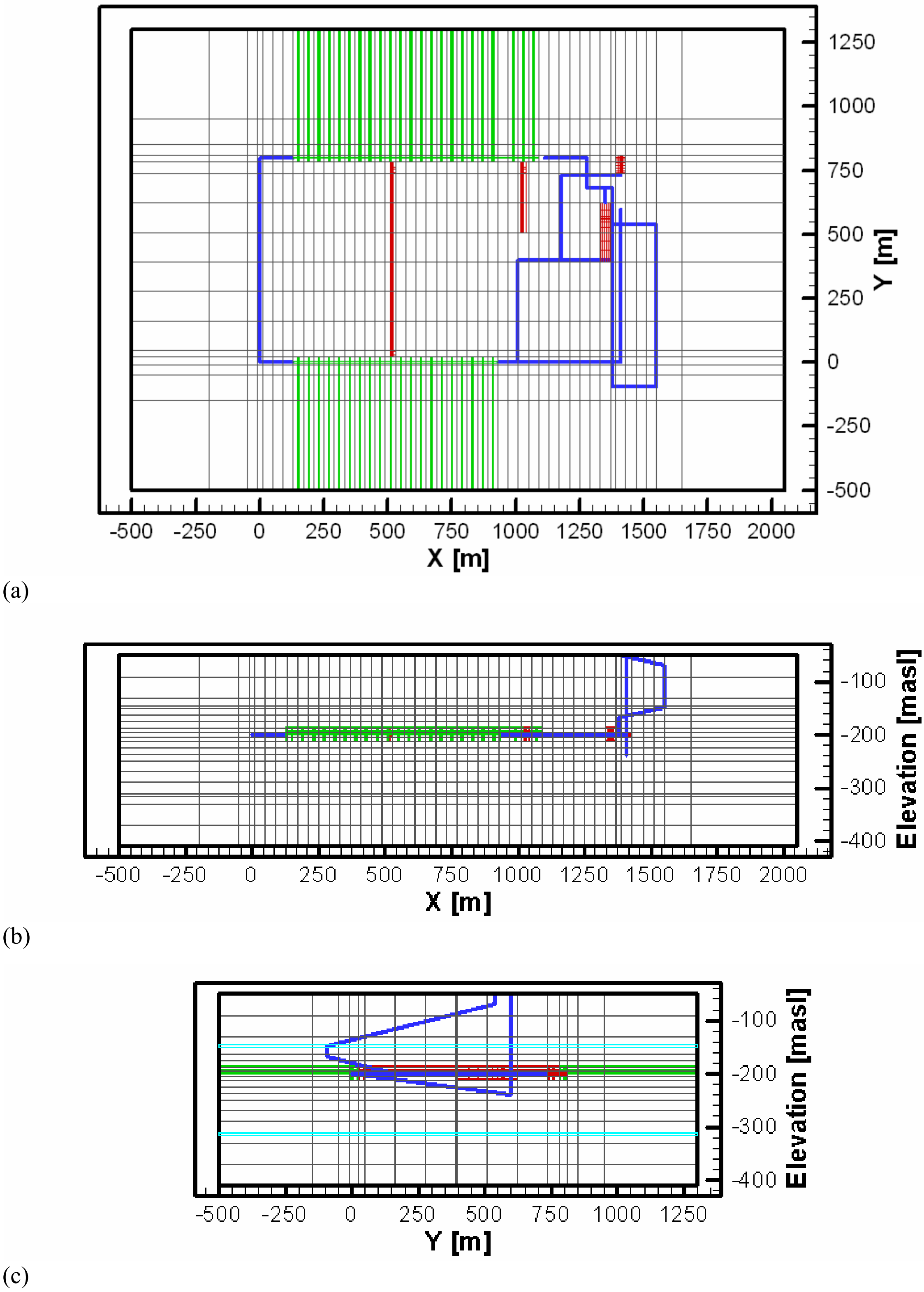

Fig. 7: (a) XY-, (b) XZ-, and (c) YZ-views of computational mesh of IFC model; submesh of geosphere (gray), waste emplacement tunnels (red), operations and construction tunnel submesh (green), and other backfilled tunnels (blue).

5.3.2 Submesh Geosphere

The geosphere mesh comprises the host rock and surrounding confining units and local aquifers. The repository submeshes will be embedded into the geosphere mesh. The basic geosphere mesh is a cube of dimensions 2050 m × 1800 m × 360 m. The horizontal cross section of this cube extends 500 m beyond each side of the repository footprint. The top of the cube is at an elevation of -48.9 m.a.s.l., representing the base of the Malm; the bottom of the geosphere mesh is at an elevation of -408.9 m.a.s.l., representing the top of the Muschelkalk. The repository horizon is at an elevation of -198.9 m.a.s.l. The vertical stratification and discretization is shown in Fig. 7b and c and summarized in Table 7.

Tab. 7: Vertical stratification of geosphere model.

Elevation [m.a.s.l.]	Thickness [m]	Material name	Stratigraphic unit	Element name
-48.9	-	bMALM	Malm	T-g 1
-48.9 -143.9	95.0	DOGGE	Dogger	A2... A4...
-143.9 -148.9	5.0	WEDEL	Wedelsandstein (local aquifer)	A5...
-148.9 -248.9	100.0	OPALI	Opalinus Clay	A6... AE...
-248.9 -308.9	60.0	LIAS	Lias and Upper Keuper	AF... AH...
-308.9 -313.9	5.0	SANDS	Sandsteinkeuper (local aquifer)	AI...
-313.9 -408.9	95.0	KEUPE	Lower confining unit	AJ... AL...
-408.9	-	bMUSC	Muschelkalk	B-g 1

At the left (approximately south-west) and right (approximately north-east) sides of the model at elevations of -146.4 and -311.4 m.a.s.l., four one-dimensional, horizontal submeshes are attached to represent the Wedelsandstein and Sandsteinkeuper These two local aquifers extend 25 km and 15 km downstream to their respective compliance boundaries. The length of the upstream branches of the local aquifers is 10 km.

Provisions are made to introduce a vertical, high-transmissivity zone through the center of the repository in east-western direction at Y = 392.5 m. The vertical extent of the 1-m thick zone (discretization too small to be visible in Fig. 7) can be adjusted by providing appropriate fault properties within the zone for each stratigraphic layer as listed in Tab. 7. (See also discussion of Tab. 17 in Section 5.4).

After generation of the geosphere base mesh, all elements within the repository footprint at the elevation of the repository horizon are removed to make room for the representative waste emplacement tunnel meshes (for spent fuel and high level waste, for the pilot facility, and for the two long-lived intermediate level waste facilities). Averaging planes and Dirichlet boundary elements are attached to the internal faces of the cut-out regions. The averaging planes are used to connect the representative waste emplacement tunnels to the geosphere model at their representative locations; the internal Dirichlet boundary elements are used to provide the replicated state variables where virtual tunnels are located.

5.3.3 Submesh Representative Emplacement Tunnels

A single waste emplacement tunnel is discretized to represent the twenty tunnels for the disposal of spent fuel and high-level waste. The submesh of the representative emplacement tunnel is embedded into the geosphere mesh and connected to the operations and construction tunnel submeshes (see Section 5.3.5) at a representative location (i.e., the central tunnel at X = 510 m, see Fig. 7a). The conditions calculated at the submodel boundaries are then replicated to all interfaces between virtual emplacement tunnels and the surrounding submeshes.

The domain of the representative emplacement tunnel submodel extends in X-direction from the center of the tunnel to the midpoint between two tunnels (i.e., a length of 20.0 m); in Y direction from the starter tunnel near the construction tunnel (at Y = 22.0 m) to the lock near the operations tunnel (at Y = 783.0 m) – the starter and turn-off tunnels are not part of the emplacement tunnel submesh; they belong to the construction and operations tunnel submeshes, respectively. Vertically, the submesh is 26.0 m thick, centered at the elevation of the tunnel axis (Z = -198.9 m.a.s.l.).

The model domain is discretized such that the different elements of the emplacement tunnels are approximately represented using a Cartesian grid. These elements include:

- Waste
- Backfilled emplacement drift
- Lock
- Abutment
- Seal
- EDZ
- Opalinus Clay

A three-dimensional view of the mesh is shown in Fig. 8.

The two YZ-planes that intersect the tunnel axis and the mid-plane between emplacement tunnels are symmetry planes and thus no-flow boundaries. The XZ-planes at end faces of the tunnel are connected to three averaging planes at each side (the construction and operations tunnel sides). The three averaging planes average the conditions in the backfilled tunnel, the surrounding EDZ, and the host rock.

Starting with the XZ averaging planes near the construction tunnel, individual tunnel sections are discretized. The horizontal planes at the top and bottom of the submodel are averaged to match the discretization of the geosphere model.

The discretization in Z-direction approximately captures the varying geometries of the tunnel cross sections and their respective EDZs, specifically the higher lock on the operations tunnel side of the model.

The discretization of the representative tunnel of the pilot facility is identical to that of the northern section (Y > 508.0 m) of the representative emplacement tunnel for spent fuel and high-level waste, with the exception that all elements start with the letter "p".

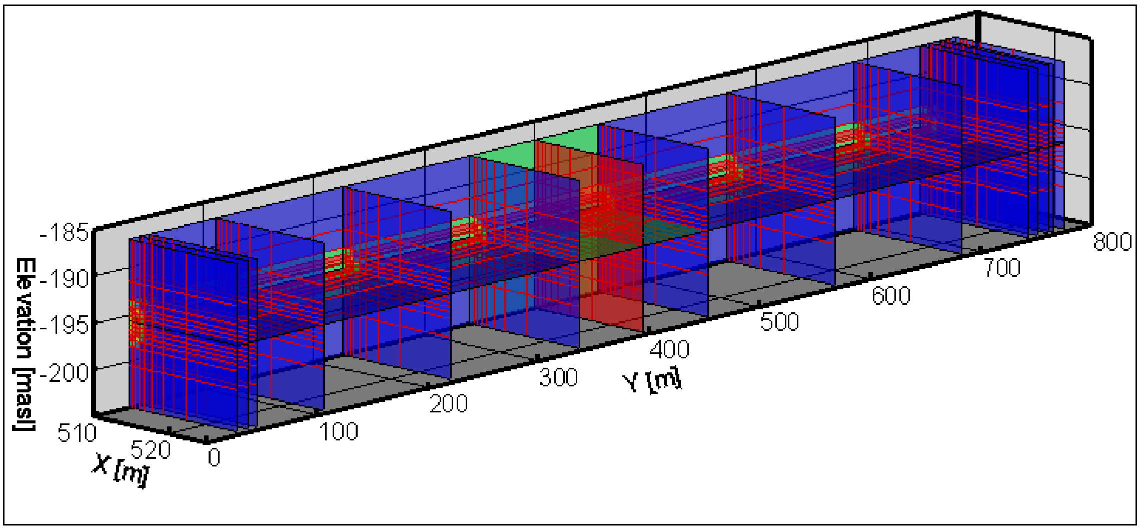

Fig. 8: Three-dimensional view of representative waste emplacement tunnel model.

5.3.4 Submesh Intermediate-Level Waste Facility

Two submeshes representing the two intermediate-level waste facilities are created and inserted into the geosphere model as local grid refinements. Fig. 9 shows the discretization of the first facility. Multiple averaging elements are attached at the six sides of the model to facilitate the connection to the coarser geosphere model.

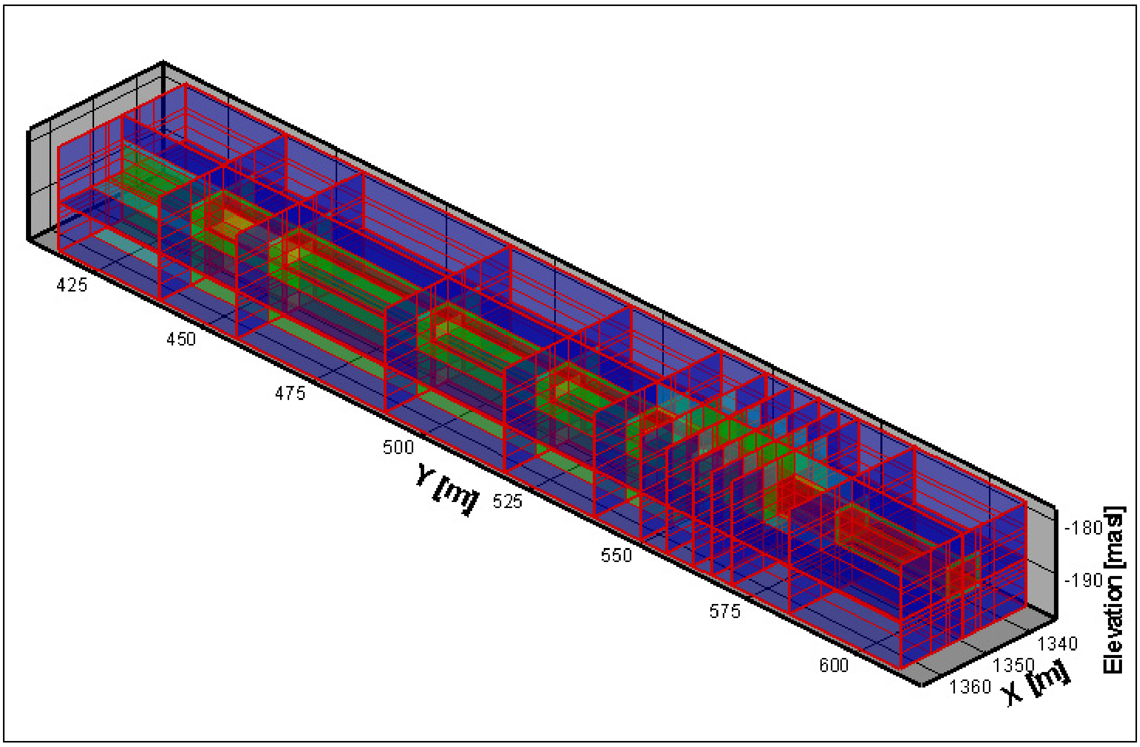

Fig. 9: Three-dimensional view of intermediate-level waste facility.

5.3.5 Submesh Operations and Construction Tunnels

Submeshes with relatively high resolution are constructed for the operations and construction tunnels to be able to provide the connections (turn-out and starter tunnels) to the 17 waste emplacement tunnels for spent fuel, the three tunnels for high-level wastes, and the three tunnels of the pilot facility. Moreover, EDZs of the various openings with different diameter have to be accommodated. A three-dimensional view of a section of the operations tunnel mesh in the vicinity of the representative waste emplacement tunnel is shown in Fig. 10. Recall that the single representative waste emplacement tunnel mesh is fully connected to the operations tunnel mesh, whereas the (19) virtual emplacement tunnels are connected through internal Dirichlet boundary elements attached to the operations tunnel mesh; the system state calculated at the connection between the representative emplacement tunnel and the operations tunnel is prescribed at these internal boundary elements to achieve the desired replication effect.

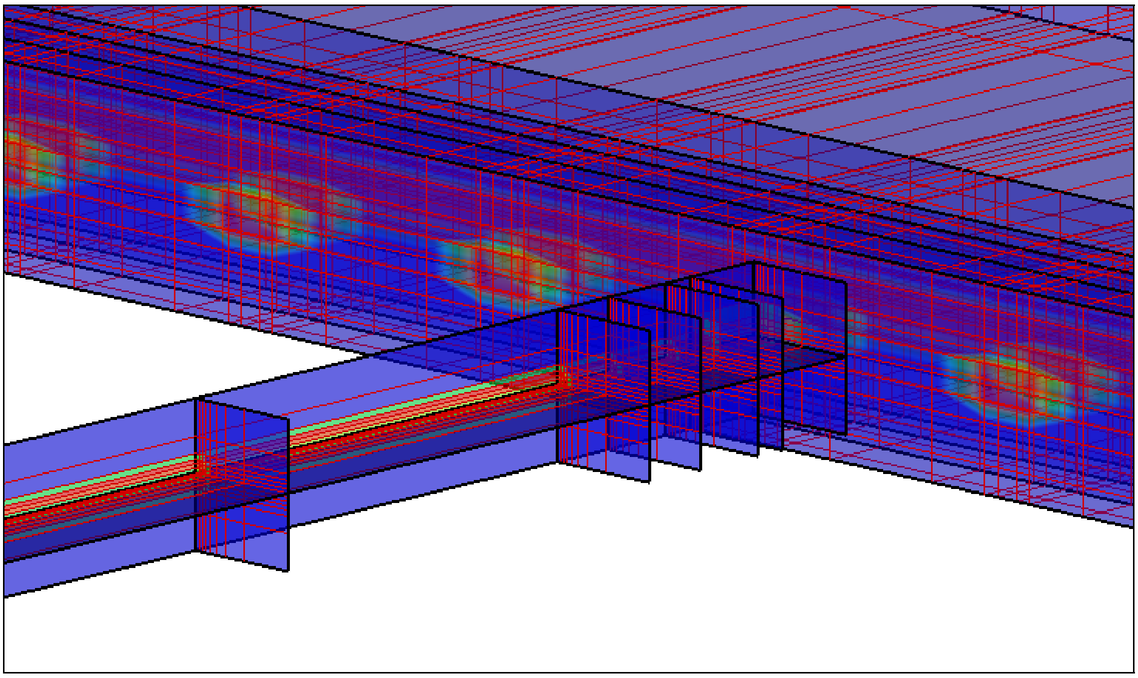

Fig. 10: Three-dimensional view of connection between representative waste emplacement tunnel and operations tunnel.

5.3.6 Submesh Backfilled Underground Structures

With the exception of the waste emplacement tunnels as well as the operations and construction tunnels, all the other backfilled underground structures (i.e., access tunnel, central area, connection tunnel between operations and construction tunnel, the shaft, connection tunnel between construction tunnel and shaft, the detour and control tunnels, and other minor tunnel sections; see blue lines in Fig. 6 and Fig. 7) are discretized in the following, simplified manner. The backfilled tunnel and surrounding EDZ are represented by two concentric, cylindrical elements that are inserted into each quadrilateral elements of the geosphere model that is intersected by the respective tunnel segment. While this simplified approach allows for buoyancy-driven gas flow along inclined tunnels and their EDZs, buoyancy effects within the tunnel cross section are ignored.

5.4 Hydrogeologic Properties

Hydrogeologic properties need to be specified for the various natural and man-made materials in the IFC model. While many of these parameters are uncertain and thus varied as part of a probabilistic assessment of the repository performance, a base-case parameter set is given here as a reference. The hydrogeologic parameter sets summarized in Tab. 8 throughTab. 16 can be used for testing and initial sensitivity analyses. The source of each value is indicated, if available. Assumed values are considered reasonable.

Tab. 8: Material Properties, EDZs.

Symbol	Description	Value	Units	Comment
k	Permeability $EDZ_{SF/HLW/Pilot}$ EDZ_{LMA} $EDZ_{seal/plug}$ $EDZ_{all\ tunnels}^{*}$ EDZ_{shaft}	 1×10^{-19} 1×10^{-19} 5×10^{-20} 1×10^{-19} 1×10^{-19}	m^2	
ϕ	Porosity	0.22	-	
c_ϕ	Pore compressibility	2.3×10^{-11}	1/Pa	Derived from porosity and specific storage coefficient: $c_\varphi = S_s \frac{1}{\rho g \varphi} - c_w$
$1/\alpha$	Gas-entry value	3.0	MPa	
n	Pore-size distribution index	1.67	-	
S_{lr}	Residual liquid saturation	0.0	-	
S_{gr}	Residual gas saturation	0.0	-	

* "all tunnels" includes: operations tunnel, construction tunnel, access tunnel, detour tunnel, connection tunnel, control tunnel, central area

Tab. 9: Material Properties, Backfill and Sealing Materials.

Symbol	Description	Value	Units	Comment
k	*Permeability* Crushed OPA* Gravel& S/B 70/30% Comp. Bentonite# Mortar@	 1×10^{-12} 1×10^{-10} 1×10^{-18} 1×10^{-19} 1×10^{-15}	m^2	
ϕ	*Porosity* Crushed OPA Gravel S/B 70/30 Comp. Bentonite Mortar	 0.22 0.30 0.30 0.40 0.25	-	
c_ϕ	*Pore compressibility* Crushed OPA Gravel S/B 70/30 Comp. Bentonite Mortar	 0.00 0.00 0.00 0.00 0.00	1/Pa	Derived from porosity and specific storage coefficient: $c_\varphi = S_s \dfrac{1}{\rho g \varphi} - c_w$ results in negative pore compressibility → set to zero
$1/\alpha$	*Gas-entry value* Crushed OPA Gravel S/B 70/30 Comp. Bentonite Mortar	 0.001 0.001 1.00 18.00 0.004	MPa	
n	Pore-size distribution index	2.00	-	
S_{lr}	Residual liquid saturation	0.25	-	
S_{gr}	Residual gas saturation	0.01	-	

Application areas of each backfill material are shown in Fig. 11.

* Crushed Opalinus Clay; used in access tunnel section above Opalinus Clay

& Gravel; used in abutment and shaft above Opalinus Clay

% S/B 70/30: Sand/Bentonite-70/30; used in all underground structures in Opalinus Clay, except waste emplacement tunnels, shaft, and seals

\# Compacted Bentonite; used in SF and HLW emplacement tunnels, seals, and shaft within Opalinus Clay

@ Mortar; used in ILW facilities

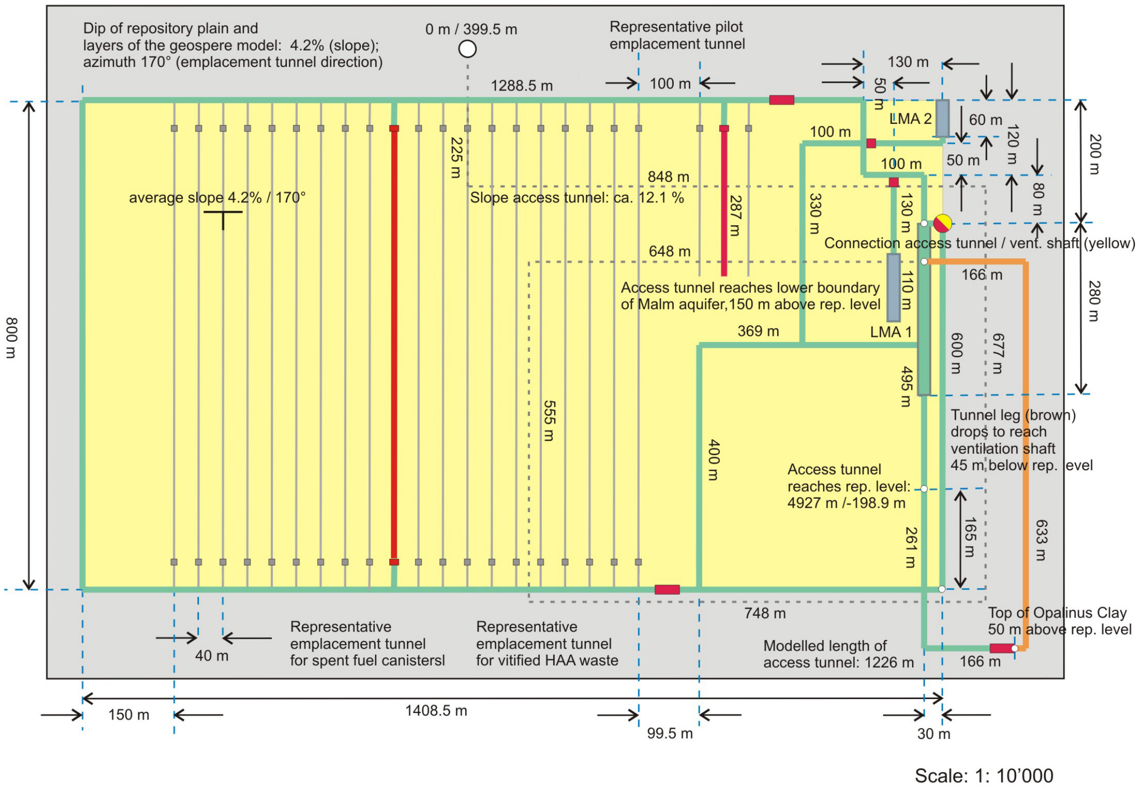

Compacted Bentonite: (s. NTB 02-05, Fig. 4.5-7). Initially consisting of supporting bentonite blocks and bentonite pellet backfill. Blocks and pellets are expected to assume the same form and material properties after resaturation. Note: All sealing zones are filled with compacted Bentonite.

Sand / Bentonite 70/30 : (70% Sand / 30% Bentonite, s. NTB 06-07, Section 9.3.2). This backfill is used for all cavities within the Opalinus Clay, with the exception of the emplacement tunnels (HAA and LMA), and the ventilation shaft.

Mortar: Assumed to be representative for all the contents of the LMA emplacement tunnels (-caverns), i.e. waste drums, waste containers and backfill.

Crushed Opalinus Clay: Material used in the Access Tunnel section *above* the Opalinus Clay.

Compacted Bentonite / Gravel: (s. NTB 02-02, Fig. 8.6). Compacted Bentonite is used to backfill / seal the ventilation shaft in the Opalinus Clay section. The section above will be filled with gravel.

Fig. 11: Equivalent conceptual repository model with application of backfill materials.

Tab. 10: Material Properties, Opalinus Clay.

Symbol	Description	Value	Units	Comment
k	Permeability	1×10^{-20} 2×10^{-21}	m^2	
ϕ	Porosity	0.12	-	
c_ϕ	Pore compressibility	8.05×10^{-9}	1/Pa	Derived from porosity and specific storage coefficient (10^{-5}) from NTB 02-03, Table 9.4-2 $c_\varphi = S_s \frac{1}{\rho g \varphi} - c_w$
$1/\alpha$	Gas-entry value	1.80	MPa	
n	Pore-size distribution index	1.67	-	
S_{lr}	Residual liquid saturation	0.00	-	
S_{gr}	Residual gas saturation	0.003	-	

Tab. 11: Material Properties, Steeply Dipping Discontinuity.

Symbol	Description	Value	Units	Comment
k	Transmissivity	1×10^{-10}	m^2/s	NTB 02-03, Table 9.4-4c
ϕ	Porosity	0.10	-	
c_ϕ	Pore compressibility	1×10^{-8}	1/Pa	
$1/\alpha$	Gas-entry value	0.10	MPa	
n	Pore-size distribution index	2.00	-	
S_{lr}	Residual liquid saturation	0.20	-	
S_{gr}	Residual gas saturation	0.01	-	

Tab. 12: Material Properties, Dogger.

Symbol	Description	Value	Units	Comment
k	Permeability	1×10^{-19}	m^2	
ϕ	Porosity	0.20	-	
c_ϕ	Pore compressibility	1×10^{-8}	1/Pa	
$1/\alpha$	Gas-entry value	10.00	MPa	
n	Pore-size distribution index	2.00	-	
S_{lr}	Residual liquid saturation	0.20	-	
S_{gr}	Residual gas saturation	0.01	-	

Tab. 13: Material Properties, Lias and Upper Keuper.

Symbol	Description	Value	Units	Comment
k	Permeability	5×10^{-21}	m^2	NTB 02-03, Table 9.4-4a
ϕ	Porosity	0.10	-	
c_ϕ	Pore compressibility	2.6×10^{-9}	1/Pa	Derived from porosity and specific storage coefficient (3×10^{-6}) $$c_\varphi = S_s \frac{1}{\rho g \varphi} - c_w$$
$1/\alpha$	Gas-entry value	1.00	MPa	
n	Pore-size distribution index	2.00	-	
S_{lr}	Residual liquid saturation	0.25	-	
S_{gr}	Residual gas saturation	0.01	-	

Tab. 14: Material Properties, Lower Keuper.

Symbol	Description	Value	Units	Comment
k	Permeability	5×10^{-21}	m^2	
ϕ	Porosity	0.10	-	
c_ϕ	Pore compressibility	1.0×10^{-9}	1/Pa	
$1/\alpha$	Gas-entry value	1.00	MPa	
n	Pore-size distribution index	2.00	-	
S_{lr}	Residual liquid saturation	0.25	-	
S_{gr}	Residual gas saturation	0.01	-	

Tab. 15: Material Properties, Wedelsandstein Aquifer.

Symbol	Description	Value	Units	Comment
k	Permeability	5×10^{-17}	m^2	NTB 02-03, Table 9.4-4a
ϕ	Porosity	0.10	-	
c_ϕ	Pore compressibility	1×10^{-8}	1/Pa	
$1/\alpha$	Gas-entry value	0.20	MPa	NTB 04-06, Table 3.3-3
n	Pore-size distribution index	2.00	-	
S_{lr}	Residual liquid saturation	0. 90	-	assumed to obtain gas accessible porosity of 0.001 given in NTB 04-06, Table 3.3-3
S_{gr}	Residual gas saturation	0.01	-	

Tab. 16: Material Properties, Sandsteinkeuper Aquifer.

Symbol	Description	Value	Units	Comment
k	Permeability	2×10^{-15}	m^2	NTB 02-03, Table 9.4-4a
ϕ	Porosity	0.05	-	NTB 02-03, Table 9.4-4a
c_ϕ	Pore compressibility	1×10^{-8}	1/Pa	
$1/\alpha$	Gas-entry value	0.10	MPa	
n	Pore-size distribution index	2.00	-	
S_{lr}	Residual liquid saturation	0. 90	-	assumed to obtain gas accessible porosity of 0.001 given in NTB 04-06, Table 3.3-3
S_{gr}	Residual gas saturation	0.01	-	

Table 17 contains a list of all five-character material names used in the ROCKS block of the iTOUGH2-IFC model. Material names starting with a "b" are boundary elements. Material names starting with a "F" followed by the material name in lower-case characters are elements within the fault zone of that material; to introduce the steeply dipping continuity, assign fault properties (see Tab. 11 or material "FAULT") to all these materials; otherwise, the properties should be identical to those of the corresponding stratigraphic layer. Material names starting with "EDZ" refer to the excavation-disturbed zones around specific tunnel segments. Material names starting with "WA" represent the gas-generating waste. Material names starting with "SEAL" refer seals and plugs. Material names starting with "ET" refer to backfilled waste emplacement tunnels. Material names starting with "T" refer to various backfilled tunnel segments.

Tab. 17: Material Names and Description.

Name	Material
OPALI	Opalinus Clay
Fopal	Potential fault zone in Opalinus Clay
bOPAL	Opalinus Clay boundary element
FAULT	Generic fault (not used; copy to all Fxxxx materials if needed)
bFAUL	Fault boundary elements
bMALM	Malm (upper boundary)
DOGGE	Dogger
Fdogg	Potential fault in Dogger
WEDEL	Wedelsandstein aquifer
Fwede	Potential fault in Wedelsandstein aquifer
bWEDE	Wedelsandstein aquifer boundary elements
LIAS	Lias and Keuper
Flias	Potential fault in Lias and Keuper
SANDS	Sandsteinkeuper aquifer
Fsand	Potential fault in Sandsteinkeuper aquifer
bSAND	Sandsteinkeuper aquifer boundary elements
KEUPE	Lower Keuper
Fkeup	Potential fault in Lower Keuper
bMUSC	Muschelkalk aquifer (lower boundary)
EDZsf	EDZ around waste emplacement tunnels (spent fuel and high-level waste)
EDZpi	EDZ around pilot facility
EDZco	EDZ around construction tunnel
EDZop	EDZ around operations tunnel
EDZac	EDZ around access tunnel
EDZvt	EDZ around connection tunnel between operations and construction tunnels
EDZca	EDZ around central area
EDZkt	EDZ around control tunnel
EDZdt	EDZ around detour tunnel
EDZsh	EDZ around shaft
EDZl1	EDZ around intermediate-level waste facility 1
EDZl2	EDZ around intermediate-level waste facility 2
EDZse	EDZ around seals
bEDZs	Internal boundary elements for EDZ around waste emplacement tunnels for spent fuel and high-level waste
bEDZp	Internal boundary elements for EDZ around pilot facility
WAsf	Waste (spent fuel and high-level waste)

Name	Material
WApil	Waste in pilot facility
WAlm1	Waste in intermediate-level waste facility 1
WAlm2	Waste in intermediate-level waste facility 2
SEAL	Seal emplacement tunnels (compacted bentonite)
SEALa	Seal access tunnels (compacted bentonite)
SEALs	Seal shaft (compacted bentonite)
ABUTM	Abutment (gravel)
ETsf	Emplacement tunnel for spent fuel and high-level waste (backfill: compacted bentonite)
ETpil	Pilot facility (compacted bentonite)
ETlm1	Emplacement tunnel of intermediate-level waste facility 1 (backfill: mortar)
ETlm2	Emplacement tunnel of intermediate-level waste facility 2 (backfill: mortar)
TURNO	Turn-out from spent fuel, high-level waste, and pilot facility into operations tunnel (backfill: S/B 70/30)
bTURN	Internal boundary elements connecting to turn-outs from spent fuel, high-level waste, and pilot facilities into operations tunnel
START	Starter tunnel off the construction tunnel to spent fuel, high-level waste, and pilot facilities (backfill: S/B 70/30)
bSTAR	Internal boundary elements connecting to starter tunnels off the construction tunnel to spent fuel, high-level waste, and pilot facilities
LOCK	Lock (backfill: S/B 70/30)
Tshaf	Shaft above Opalinus Clary Shaft (backfill: gravel)
TacCO	Access tunnel above Opalinus Clay (backfill: crushed Opalinus Clay)
Tacce	Access tunnel (backfill: S/B 70/30)
Tconn	Connection tunnel between operations and construction tunnels (backfill: S/B 70/30)
Tcons	Construction tunnel (backfill: S/B 70/30)
Tcont	Control tunnel (backfill: S/B 70/30)
Tdeto	Detour tunnel (backfill: S/B 70/30)
Toper	Operations tunnel (backfill: S/B 70/30)
Tcent	Central area (backfill: S/B 70/30)
Tlma1	Connection to intermediate-level facility 1 (backfill: S/B 70/30)
Tlma2	Connection to intermediate-level facility 2 (backfill: S/B 70/30)

5.5 Parameters of Geomechanical and Geochemical FEPs

Table 18 shows the base-case parameter set for the geomechanical and geochemical FEPs discussed in Sections 4.3.3 through 4.3.5.

Tab. 18: Parametric Models for Special FEPs and Related Coefficients.

FEP	**Description**	**Parametric Model/ Coefficients/ Reference/Comment**
1.3.19	*Pathway dilation:* Parametric model describing change in absolute permeability as a function of gas pressure and coefficients	$k_v(p,z) = \begin{cases} k_{v,0} & p \le p_d(z) \\ k_{v,0} + b(p - p_d(z))^a & p > p_d(z) \end{cases}$ $k_h(k_v) = k_v / A(p)$ $A(p,z) = \begin{cases} 5 & p \le p_d(z) \\ 5^{(k_{v,0}/k_v(p,z))^c} & p > p_d(z) \end{cases}$ $p_d(z) = d \cdot (f - z) - e$ Coefficients: a = 3.0 (1 ≤ a ≤ 8) b = $1{\times}10^{-21}$ m^2 Pa^{-a} c = 0.25 (0 < c < 1) d = $2.5{\times}10^4$ Pa/m e = $2.0{\times}10^6$ Pa f = 399.5 m.a.s.l. Apply to Opalinus Clay only
	Parametric model describing change in porosity as a function of permeability or gas pressure	No change
	Parametric model describing change in gas-entry value as a function of permeability, porosity, or gas pressure	Leverett scaling for capillary strength $\frac{\alpha(p,z)}{\alpha_0} \sim \sqrt{\frac{k(p,z)}{k_0}}$
1.4.1	*Self-sealing of EDZ:* Parametric model describing change in absolute permeability of EDZ as a function of time	$k_{EDZ} = k_{EDZ,0} f_{EDZ,k}(t)$ $f_{EDZ,k}(t)$ provided as look-up table or coefficients of a polynomial, separate for individual EDZs
	Parametric model describing change in porosity as a function of permeability or time	$\phi_{EDZ} = \phi_{EDZ,0} f_{EDZ,\phi}(t)$ $f_{EDZ,\phi}(t)$ provided as look-up table or coefficients of a polynomial, separate for individual EDZs
	Parametric model describing change in gas-entry value as a function of permeability, porosity, or time	no change

FEP	**Description**	**Parametric Model/ Coefficients/ Reference/Comment**
1.4.3	*Tunnel convergence:* Parametric model of L/ILW porosity as a function of time and pressure	$\phi_{BF} = \phi_{BF,0} f_{\phi BF}(t)$ $f_{\phi BF}(t)$ provided as look-up table or coefficients of a polynomial, applied to porosity of backfill material in intermediate-level waste facility $\phi_{BF,0} = 0.25$
1.4.7	*Uplift:* Parametric model of material-dependent absolute permeability as a function of time (and depth)	Option A: $k_{OPA} = k_{OPA,0} f_{k,Uplift}(t)$ $f_{k,Uplift}(t)$ provided as look-up table or coefficients of a polynomial; applied to Opalinus Clay only Option B: Same as FEP 1.3.19, with a time- (and depth-) dependent threshold pressure p_d provided by a look-up table of surface elevations.
1.5.2, 1.5.4, 1.5.11	*Chemical alteration effects*: Abstraction methodology and corresponding parametric model of changes in material properties of bentonite and skin zone.	Block-scale porosity remains unchanged *Minimal local-scale porosity:* $\phi(t) = \phi_0 \exp\left(l - (t/t_c)^m\right) - \left(\phi \exp(-l) - \phi_c\right)\frac{t}{t_c} \quad t$ $\phi(t) = \phi_c \quad t > t_c$ $t_c = T_c / S_l$ *Porosity-permeability relationship:* $\frac{k(\phi)}{k_0} = \left(\frac{\phi(t)}{\phi_0}\right)^3 \left(\frac{1-\phi_0}{1-\phi(t)}\right)^2$ *Coefficients*: Sealing layer thickness: 1 mm Cement-OPA $l = 1.0$ $m = 0.4$ $T_c = 100$ years $\quad (40 \le T_c \le 750)$ $\phi_c \leftarrow k(\phi_c) = \kappa \cdot k_0$ $\kappa = 0.01$ Cement-tunnel backfill $l = 1.0$ $m = 0.45$ $T_c = 200$ years $\quad (100 \le T_c \le 2000)$ $\phi_c \leftarrow k(\phi_c) = \kappa \cdot k_0$ $\kappa = 0.01$

5.6 Initial and Boundary Conditions

The calculated pressure and flow fields are determined by (among other factors) the conditions applied at the model boundaries. Constant pressures are prescribed at the top and bottom of the model (inducing vertical upflow), and on the eastern and western end points of the two local aquifers (Wedelsandstein and Sandsteinkeuper), providing a regional, horizontal flow field within these aquifers. No-flow conditions are prescribed elsewhere; details can be found in Tab. 19.

Gas production in the waste emplacement tunnels are prescribed as time-dependent mass generation rates per tunnel length (for spent fuel and high-level waste) or volume of waste (for intermediate-level waste). The values are given in Tab. 20 and Tab. 21. The gas generation rates shown in Tab. 21 were derived from Nagra (2002c, NTB 02-06, Table 4.3-1), assuming a hydrogen density under standard conditions of 0.089 kg m^{-3}, and a total waste volume in both intermediate-level waste facilities of 6000 m^3. The waste volume is that of the IFC model grid, which was constructed based on the drawings of Nagra (Internal Report, 2006).

The entire model domain is assumed to be initially fully liquid saturated. The initial pressure distribution (i.e., prior to gas generation) is calculated by running the model to steady state using the Dirichlet boundary condition discussed above and summarized in Tab. 19. To improve computational efficiency, the steady-state simulation performed to obtain initial conditions is conducted in two steps, where the first step uses homogeneous material properties throughout the model domain.

Should the boundary pressures be considered uncertain and varied during a PSA calculation, the pre-gas-generation steady-state run has to be included in the simulation.

Tab. 19: Boundary Conditions in Aquifers.

	Description	Value	Units	Reference/Comment
P_{top}	Absolute pressure at top of IFC model (i.e., base Malm aquifer, 150 m above repository horizon)	4.50	MPa	Assuming hydrostatic pressure distribution with ρ_w = 1000 kg m^{-3}, and g = 9.81 m^2 s^{-1}. Surface elevation (399.5 m.a.s.l.) and base Malm aquifer (-48.9 m.a.s.l.)
P_{bot}	Absolute pressure at bottom of IFC model (i.e., top of Muschelkalk aquifer, 210 m below repository horizon)	8.03	MPa	Assuming hydrostatic pressure distribution with ρ_w = 1000 kg m^{-3}, and g = 9.81 m^2 s^{-1}. Surface elevation (399.5 m.a.s.l.) and top Muschelkalk aquifer (-408.9 m.a.s.l.)
i_{Wedel}	Hydraulic gradient in Wedelsandstein aquifer	0.001	m/m	Absolute pressure at center of Wedelsand-stein aquifer: 4.82 MPa, i.e., -62 m head difference, NTB 02-03, Figure 4.61; Surface elevation (399.5 m.a.s.l.) and base Malm aquifer (-146.4 m.a.s.l.)
$p_{,Wedel,u}$	Upstream pressure Wedelsandstein	4.9331	MPa	11.275 km upstream of model center with gradient i_{Wedel}
$p_{,Wedel,d}$	Downstream pressure Wedelsandstein	4.5648	MPa	26.275 km downstream of model center with gradient i_{Wedel}
i_{Sand}	Hydraulic gradient in Sandsteinkeuper aquifer	0.005	m/m	NTB 02-03, Tab. 9.4.4a Absolute pressure at center of Sandstein-keuper aquifer: 7.70 MPa, i.e., +61 m head difference, NTB 02-03, Figure 4.61 Surface elevation (399.5 m.a.s.l.) and base Malm aquifer (-311.9 m.a.s.l.)
$p_{Sand,u}$	Upstream pressure Sandsteinkeuper	8.2499	MPa	11.275 km upstream of model center with gradient i_{Sand}
$p_{,Sand,d}$	Downstream pressure Sandsteinkeuper	6.8986	MPa	16.275 km downstream of model center with gradient i_{Sand}

Tab. 20: Neumann Boundary Conditions (Gas Generation Rates).

	Description	Value	Units	Reference/Comment
$q_{SF,HLW}$	Gas generation rates (kg/s per meter of SF or HLW emplacement tunnel) as a function of time	4.88×10^{-11} for $0 < t <$ 200,000 years	kg s^{-1} m^{-1}	NTB 02-06, Tab. 4.3-1
q_P	Gas generation rates (kg/s per meter of pilot facility tunnel) as a function of time	4.88×10^{-11} for $0 < t <$ 200,000 years	kg s^{-1} m^{-1}	NTB 02-06, Tab. 4.3-1
q_{LMA1}	Table of gas generation rates (kg/s per m^3 of LMA 1 waste) as a function of time	see Tab. 21	kg s^{-1} m^{-3}	Derived from NTB 02-06, Tab. 4.3-1
q_{LMA2}	Table of gas generation rates (kg/s per m^3 of LMA 2 waste) as a function of time	see Tab. 21	kg s^{-1} m^{-3}	Derived from NTB 02-06, Tab. 4.3-1

Tab. 21: Time-Dependent Gas Generation Rate for LMA1 and LMA2 in Kilograms per Second and Cubic-Meter of Waste.

Time [years]	Gas Generation Rate [kg s^{-1} m^{-3}]
0	3.27×10^{-10}
3	3.18×10^{-10}
10	5.21×10^{-11}
30	5.21×10^{-11}
100	4.65×10^{-11}
300	3.74×10^{-11}
1000	2.13×10^{-11}
3000	9.48×10^{-12}
10000	4.74×10^{-12}
30000	2.40×10^{-12}
100000	9.48×10^{-13}
170000	0.0
1000000	0.0

5.7 Parameters Potentially Varied in PSA Calculations

As part of a probabilistic performance assessment calculation, many of the input parameters are varied to examine the impact of parameter uncertainty on model predictions. This impact may be evaluated either through a sensitivity analysis or Monte Carlo sampling during probabilistic safety assessment simulations. Unique designations for each *potentially* varied parameter are given in Tab. 22. These parameters include a set of hydrogeologic properties for each material listed in Tab. 17, parameters of the geomechanical and geochemical FEPs (see Tab. 18), as well as certain boundary conditions (see Tab. 19 through Tab. 21.

Potential statistical correlations among the uncertain parameters must be generated by the sampling procedure.

Aspects of the conceptual model may also be changed during a PSA analysis. Some of these conceptual choices are invoked by setting appropriate flags in the iTOUGH2-IFC input file; however, they are not listed here, because these flags are not numerical values sampled from a probability distribution function.

Tab. 22: Parameters Potentially Varied in Sensitivity Analyses or PSA Calculations.

#	Parameter Designation	Description		Base-Case Value	Units	V/F/S @
		Dogger				
1	DOGGE_POR	porosity	Φ	0.2	-	V
2	DOGGE_PERX	absolute permeability in x	k_x	1.00E-19	m^2	V
3	DOGGE_PERY	absolute permeability in y	k_y	1.00E-19	m^2	V
4	DOGGE_PERZ	absolute permeability in z	k_z	1.00E-19	m^2	V
5	DOGGE_COM	pore compressibility	c_Φ	1.00E-08	1/Pa	V
6	DOGGE_TORTX	tortuosity factor for binary diffusion	τ	0.00E+00	-	V
7	DOGGE_GK	Klinkenberg parameter b	b	0.00E+00	1/Pa	S
8	DOGGE_RP_Slrk	residual liquid saturation for relative permeability functions	S_{lrk}	2.00E-01	-	S
9	DOGGE_RP_Sgr	residual gas saturation	S_{gr}	1.00E-02	-	S
10	DOGGE_CP_Slrc	residual liquid saturation for capillary pressure function	S_{lrc}	2.00E-01	-	S
11	DOGGE_CP_n	van Genuchten parameter	n	2.00E+00	-	S
12	DOGGE_CP_1/a	van Genuchten parameter	$1/\alpha$	1.00E+07	Pa	S
13	DOGGE_CP_g	van Genuchten active fracture model parameter	γ	0.00E+00	-	S
		Wedelsandstein				
14	WEDEL_POR	porosity	Φ	0.1	-	V
15	WEDEL_PERX	absolute permeability in x	k_x	5.00E-17	m^2	V
16	WEDEL_PERY	absolute permeability in y	k_y	5.00E-17	m^2	V
17	WEDEL_PERZ	absolute permeability in z	k_z	5.00E-17	m^2	V
18	WEDEL_COM	pore compressibility	c_Φ	1.00E-08	1/Pa	V
19	WEDEL_TORTX	tortuosity factor for binary diffusion	τ	0.00E+00	-	V
20	WEDEL_GK	Klinkenberg parameter b	b	0.00E+00	1/Pa	S
21	WEDEL_RP_Slrk	residual liquid saturation for relative permeability functions	S_{lrk}	9.00E-01	-	S
22	WEDEL_RP_Sgr	residual gas saturation	S_{gr}	1.00E-02	-	S
23	WEDEL_CP_Slrc	residual liquid saturation for capillary pressure function	S_{lrc}	9.00E-01	-	S
24	WEDEL_CP_n	van Genuchten parameter	n	2.00E+00	-	S
25	WEDEL_CP_1/a	van Genuchten parameter	$1/\alpha$	2.00E+05	Pa	S

@ Indicates whether parameter is variable and can be sampled in a PSA calculation (V), is fixed (F, shaded red), or can be varied in a sensitivity analysis prior to the PSA calculation to determine whether it is fixed or variable (S; shaded yellow).

#	Parameter Designation	Description		Base-Case Value	Units	V/F/S @
26	WEDEL_CP_g	van Genuchten active fracture model parameter	γ	0.00E+00	-	S
		Opalinus Clay				
27	OPALI_POR	porosity	Φ	0.12	-	V
28	OPALI_PERX	absolute permeability in x	k_x	1.00E-20	m^2	V
29	OPALI_PERY	absolute permeability in y	k_y	1.00E-20	m^2	V
30	OPALI_PERZ	absolute permeability in z	k_z	2.00E-21	m^2	V
31	OPALI_COM	pore compressibility	c_Φ	8.05E-09	1/Pa	V
32	OPALI_TORTX	tortuosity factor for binary diffusion	τ	0.00E+00	-	V
33	OPALI_GK	Klinkenberg parameter b	b	0.00E+00	1/Pa	V
34	OPALI_RP_Slrk	residual liquid saturation for relative permeability functions	S_{lrk}	0.00E-00	-	V
35	OPALI_RP_Sgr	residual gas saturation	S_{gr}	3.00E-03	-	V
36	OPALI_CP_Slrc	residual liquid saturation for capillary pressure function	S_{lrc}	0.00E-00	-	V
37	OPALI_CP_n	van Genuchten parameter	n	1.67E+00	-	V
38	OPALI_CP_1/a	van Genuchten parameter	$1/\alpha$	1.80E+06	Pa	V
39	OPALI_CP_g	van Genuchten active fracture model parameter	γ	0.00E+00	-	V
		Lias + Upper Keuper				
40	LIAS_POR	porosity	Φ	0.1	-	V
41	LIAS_PERX	absolute permeability in x	k_x	5.00E-21	m^2	V
42	LIAS_PERY	absolute permeability in y	k_y	5.00E-21	m^2	V
43	LIAS_PERZ	absolute permeability in z	k_z	5.00E-21	m^2	V
44	LIAS_COM	pore compressibility	c_Φ	2.62E-09	1/Pa	V
45	LIAS_TORTX	tortuosity factor for binary diffusion	τ	0.00E+00	-	V
46	LIAS_GK	Klinkenberg parameter b	b	0.00E+00	1/Pa	S
47	LIAS_RP_Slrk	residual liquid saturation for relative permeability functions	S_{lrk}	2.50E-01	-	S
48	LIAS_RP_Sgr	residual gas saturation	S_{gr}	1.00E-02	-	S
49	LIAS_CP_Slrc	residual liquid saturation for capillary pressure function	S_{lrc}	2.50E-01	-	S
50	LIAS_CP_n	van Genuchten parameter	n	2.00E+00	-	S
51	LIAS_CP_1/a	van Genuchten parameter	$1/\alpha$	1.00E+06	Pa	S
52	LIAS_CP_g	van Genuchten active fracture model parameter	γ	0.00E+00	-	S
		Lower Keuper				
53	KEUPE_POR	porosity	Φ	0.1	-	V
54	KEUPE_PERX	absolute permeability in x	k_x	5.00E-21	m^2	V
55	KEUPE_PERY	absolute permeability in y	k_y	5.00E-21	m^2	V
56	KEUPE_PERZ	absolute permeability in z	k_z	5.00E-21	m^2	V
57	KEUPE_COM	pore compressibility	c_Φ	1.00E-09	1/Pa	V
58	KEUPE_TORTX	tortuosity factor for binary diffusion	τ	0.00E+00	-	V
59	KEUPE_GK	Klinkenberg parameter b	b	0.00E+00	1/Pa	S

#	Parameter Designation	Description		Base-Case Value	Units	V/F/S @
60	KEUPE_RP_Slrk	residual liquid saturation for relative permeability functions	S_{lrk}	2.50E-01	-	S
61	KEUPE_RP_Sgr	residual gas saturation	S_{gr}	1.00E-02	-	S
62	KEUPE_CP_Slrc	residual liquid saturation for capillary pressure function	S_{lrc}	2.50E-01	-	S
63	KEUPE_CP_n	van Genuchten parameter	n	2.00E+00	-	S
64	KEUPE_CP_1/a	van Genuchten parameter	$1/\alpha$	1.00E+06	Pa	S
65	KEUPE_CP_g	van Genuchten active fracture model parameter	γ	0.00E+00	-	S
		Sandsteinkeuper				
66	SANDS_POR	porosity	Φ	0.05	-	V
67	SANDS_PERX	absolute permeability in x	k_x	2.00E-15	m^2	V
68	SANDS_PERY	absolute permeability in y	k_y	2.00E-15	m^2	V
69	SANDS_PERZ	absolute permeability in z	k_z	2.00E-15	m^2	V
70	SANDS_COM	pore compressibility	c_Φ	1.00E-08	1/Pa	V
71	SANDS_TORTX	tortuosity factor for binary diffusion	τ	0.00E+00	-	V
72	SANDS_GK	Klinkenberg parameter	b	0.00E+00	1/Pa	S
73	SANDS_RP_Slrk	residual liquid saturation for relative permeability functions	S_{lrk}	9.00E-01	-	S
74	SANDS_RP_Sgr	residual gas saturation	S_{gr}	1.00E-02	-	S
75	SANDS_CP_Slrc	residual liquid saturation for capillary pressure function	S_{lrc}	9.00E-01	-	S
76	SANDS_CP_n	van Genuchten parameter	n	2.00E+00	-	S
77	SANDS_CP_1/a	van Genuchten parameter	$1/\alpha$	1.00E+05	Pa	S
78	SANDS_CP_g	van Genuchten active fracture model parameter	γ	0.00E+00	-	S
		EDZ other tunnels				
79	EDZac_POR	porosity	Φ	0.22	-	V
80	EDZac_PER	absolute permeability (isotropic)	k	1.00E-19	m^2	V
		EDZ waste emplacement tunnels				
81	EDZsf_POR	porosity	Φ	0.22	-	V
82	EDZsf_PER	absolute permeability (isotropic)	k	1.00E-19	m^2	V
		EDZ shaft				
83	EDZsh_POR	porosity	Φ	0.22	-	V
84	EDZsh_PER	absolute permeability (isotropic)	k	1.00E-19	m^2	V
		EDZ parameters (all structures)				
85	EDZ_COM	pore compressibility	c_Φ	2.33E-11	1/Pa	V
86	EDZ_TORTX	tortuosity factor for binary diffusion	τ	0.00E+00	-	V
87	EDZ_GK	Klinkenberg parameter	b	0.00E+00	1/Pa	V
88	EDZ_RP_Slrk	residual liquid saturation for relative permeability functions	S_{lrk}	0.00E+00	-	V
89	EDZ_RP_Sgr	residual gas saturation	S_{gr}	0.00E+00	-	V
90	EDZ_CP_Slrc	residual liquid saturation for capillary pressure function	S_{lrc}	0.00E+00	-	V

#	Parameter Designation	Description		Base-Case Value	Units	V/F/S @
91	EDZ_CP_n	van Genuchten parameter	n	1.67E+00	-	V
92	EDZ_CP_1/a	van Genuchten parameter	$1/\alpha$	3.00E+06	Pa	V
93	EDZ_CP_g	van Genuchten active fracture model parameter	γ	0.00E+00	-	V
		Backfill, gravel (ABUTM, Tshaf)				
94	GRAVEL_POR	porosity	Φ	0.3	-	S
95	GRAVEL_PERX	absolute permeability in x	k_x	1.00E-12[&]	m^2	S
96	GRAVEL_PERY	absolute permeability in y	k_y	1.00E-12	m^2	S
97	GRAVEL_PERZ	absolute permeability in z	k_z	1.00E-12	m^2	S
98	GRAVEL_COM	pore compressibility	c_Φ	0.00E+00	1/Pa	S
99	GRAVEL_TORTX	tortuosity factor for binary diffusion	τ	0.00E+00	-	S
100	GRAVEL_GK	Klinkenberg parameter	b	0.00E+00	1/Pa	S
101	GRAVEL_RP_Slrk	residual liquid saturation for relative permeability functions	S_{lrk}	2.50E-01	-	S
102	GRAVEL_RP_Sgr	residual gas saturation	S_{gr}	1.00E-02	-	S
103	GRAVEL_CP_Slrc	residual liquid saturation for capillary pressure function	S_{lrc}	2.50E-01	-	S
104	GRAVEL_CP_n	van Genuchten parameter	n	2.00E+00	-	S
105	GRAVEL_CP_1/a	van Genuchten parameter	$1/\alpha$	1.00E+03	Pa	S
106	GRAVEL_CP_g	van Genuchten active fracture model parameter	γ	0.00E+00	-	S
		Backfill, mortar (ETlm1, ETlm2)				
107	MORTA_POR	porosity	Φ	0.25	-	V
108	MORTA_PERX	absolute permeability in x	k_x	1.00E-15	m^2	V
109	MORTA_PERY	absolute permeability in y	k_y	1.00E-15	m^2	V
110	MORTA_PERZ	absolute permeability in z	k_z	1.00E-15	m^2	V
111	MORTA_COM	pore compressibility	c_Φ	0.00E+00	1/Pa	V
112	MORTA_TORTX	tortuosity factor for binary diffusion	τ	0.00E+00	-	V
113	MORTA_GK	Klinkenberg parameter	b	0.00E+00	1/Pa	V
114	MORTA_RP_Slrk	residual liquid saturation for relative permeability functions	S_{lrk}	2.50E-01	-	V
115	MORTA_RP_Sgr	residual gas saturation	S_{gr}	1.00E-02	-	V
116	MORTA_CP_Slrc	residual liquid saturation for capillary pressure function	S_{lrc}	2.50E-01	-	V
117	MORTA_CP_n	van Genuchten parameter	n	2.00E+00	-	V
118	MORTA_CP_1/a	van Genuchten parameter	$1/\alpha$	4.00E+03	Pa	V
119	MORTA_CP_g	van Genuchten active fracture model parameter	γ	0.00E+00	-	V
		Backfill, compacted bentonite (ETsf, ETpil, SEALa, SEALs)				
120	CBENT_POR	Porosity	Φ	0.4	-	V

[&] Permeabilities for gravel reduced compared to the values given in Table 9 to avoid numerical difficulties arising from extreme permeability contrasts to surrounding materials; impact to be evaluated in sensitivity analysis.

#	Parameter Designation	Description		Base-Case Value	Units	V/F/S @
121	CBENT_PER	absolute permeability (isotropic)	k_x	1.00E-19	m^2	V
122	CBENT_COM	pore compressibility	c_Φ	0.00E+00	1/Pa	V
123	CBENT_TORTX	tortuosity factor for binary diffusion	τ	0.00E+00	-	V
124	CBENT_GK	Klinkenberg parameter	b	0.00E+00	1/Pa	V
125	CBENT_RP_Slrk	residual liquid saturation for relative permeability functions	S_{lrk}	2.50E-01	-	V
126	CBENT_RP_Sgr	residual gas saturation	S_{gr}	1.00E-02	-	V
127	CBENT_CP_Slrc	residual liquid saturation for capillary pressure function	S_{lrc}	2.50E-01	-	V
128	CBENT_CP_n	van Genuchten parameter	n	2.00E+00	-	V
129	CBENT_CP_1/a	van Genuchten parameter	$1/\alpha$	1.80E+07	Pa	V
130	CBENT_CP_g	van Genuchten active fracture model parameter	γ	0.00E+00	-	V
Backfill, S/B 70/30 (Tacce, Tconn, Tcons, Tdeto, Toper, Tcent, TURNO, START, LOCK)						
131	S/B73_POR	Porosity	Φ	0.3	-	V
132	S/B73_PER	absolute permeability (isotropic)	k_x	1.00E-18	m^2	V
133	S/B73_COM	pore compressibility	c_Φ	0.00E+00	1/Pa	V
134	S/B73_TORTX	tortuosity factor for binary diffusion	τ	0.00E+00	-	V
135	S/B73_GK	Klinkenberg parameter	b	0.00E+00	1/Pa	V
136	S/B73_RP_Slrk	residual liquid saturation for relative permeability functions	S_{lrk}	2.50E-01	-	V
137	S/B73_RP_Sgr	residual gas saturation	S_{gr}	1.00E-02	-	V
138	S/B73_CP_Slrc	residual liquid saturation for capillary pressure function	S_{lrc}	2.50E-01	-	V
139	S/B73_CP_n	van Genuchten parameter	n	2.00E+00	-	V
140	S/B73_CP_1/a	van Genuchten parameter	$1/\alpha$	1.00E+06	Pa	V
141	S/B73_CP_g	van Genuchten active fracture model parameter	γ	0.00E+00	-	V
Backfill, crushed Opalinus Clay (TacCO)						
142	CROPA_POR	Porosity	Φ	0.22	-	V
143	CROPA_PER	absolute permeability (isotropic)	k_x	1.00E-12	m^2	V
144	CROPA_COM	pore compressibility	c_Φ	0.00E+00	1/Pa	V
145	CROPA_TORTX	tortuosity factor for binary diffusion	τ	0.00E+00	-	V
146	CROPA_GK	Klinkenberg parameter	b	0.00E+00	1/Pa	V
147	CROPA_RP_Slrk	residual liquid saturation for relative permeability functions	S_{lrk}	2.50E-01	-	V
148	CROPA_RP_Sgr	residual gas saturation	S_{gr}	1.00E-02	-	V
149	CROPA_CP_Slrc	residual liquid saturation for capillary pressure function	S_{lrc}	2.50E-01	-	V
150	CROPA_CP_n	van Genuchten parameter	n	2.00E+00	-	V
151	CROPA_CP_1/a	van Genuchten parameter	$1/\alpha$	1.00E+03	Pa	V
152	CROPA_CP_g	van Genuchten active fracture model parameter	γ	0.00E+00	-	V

#	Parameter Designation	Description		Base-Case Value	Units	V/F/S @
		Intermediate-level waste (Walm1, Walm2)				
153	WAlma_POR	porosity	Φ	0.25	-	V
154	WAlma_PER	absolute permeability (isotropic)	k_x	1.00E-15	m^2	V
155	WAlma_COM	pore compressibility	c_Φ	0.00E+00	1/Pa	V
156	WAlma_TORTX	tortuosity factor for binary diffusion	τ	0.00E+00	-	V
157	WAlma_GK	Klinkenberg parameter	b	0.00E+00	1/Pa	V
158	WAlma_RP_Slrk	residual liquid saturation for relative permeability functions	S_{lrk}	2.50E-01	-	V
159	WAlma_RP_Sgr	residual gas saturation	S_{gr}	1.00E-02	-	V
160	WAlma_CP_Slrc	residual liquid saturation for capillary pressure function	S_{lrc}	2.50E-01	-	V
161	WAlma_CP_n	van Genuchten parameter	n	2.00E+00	-	V
162	WAlma_CP_1/a	van Genuchten parameter	$1/\alpha$	4.00E+03	Pa	V
163	WAlma_CP_g	van Genuchten active fracture model parameter	γ	0.00E+00	-	V
		SF/HLW/PIL waste (WAsf, WApil)				
164	WAhlw_POR	porosity	Φ	0.001	-	V
165	WAhlw_PER	absolute permeability (isotropic)	k	1.00E-20	m^2	V
166	WAhlw_COM	pore compressibility	c_Φ	0.00E+00	1/Pa	F
167	WAhlw_TORTX	tortuosity factor for binary diffusion	τ	0.00E+00	-	F
168	WAhlw_GK	Klinkenberg parameter	b	0.00E+00	1/Pa	F
169	WAhlw_RP_Slrk	residual liquid saturation for relative permeability functions	S_{lrk}	2.50E-01	-	F
170	WAhlw_RP_Sgr	residual gas saturation	S_{gr}	0.00E+00	-	F
171	WAhlw_CP_Slrc	residual liquid saturation for capillary pressure function	S_{lrc}	2.50E-01	-	F
172	WAhlw_CP_n	van Genuchten parameter	n	2.00E+00	-	F
173	WAhlw_CP_1/a	van Genuchten parameter	$1/\alpha$	4.00E+03	Pa	F
174	WAhlw_CP_g	van Genuchten active fracture model parameter	γ	0.00E+00	-	F
		Pathway Dilation				
175	OPALI_PD_a	Pathway dilation model: Exponent in Eq. (2)	a	3		V
176	OPALI_PD_c	Pathway dilation model: Exponent in Eq. (3)	c	0.25	-	V
177	OPALI_PD_b	Pathway dilation model: Coefficient in Eq. (2)	b	1.00E-21	$m^{2/}Pa$	V
178	OPALI_PD_d	Pathway dilation model: Lithostatic pressure gradient in Eq. (1)	d	2.50E+04	Pa/m	V
179	OPALI_PD_e	Pathway dilation model: Empirical parameter in Eq. (1)	e	2.00E+06	Pa	V
180	OPALI_PD_f	Pathway dilation model: Surface elevation in Eq. (1)	f	399.5	masl	V

#	Parameter Designation	Description		Base-Case Value	Units	V/F/S @
EDZ Self Sealing – LMA caverns (EDZl1, EDZl2)						
181	EDZlma_SS_K_i	Permeability modification factor due to self-sealing at time index i	$f_{K,EDZ,i}$		-	V
		i=1: t = 0 s		1		
		i=2: t = 1.57788E10 s		0.01		
182	EDZlma_SS_P_i	porosity modification factor due to self-sealing at time index i	$f_{\Phi,EDZ,i}$		-	V
		i=1: t = 0 s		1		
		i=2: t = 1.57788E10 s		0.1		
EDZ Self Sealing – other tunnels (EDZce, EDZco, EDZdt, EDZkt, EDZop, EDZpi, EDZse, EDZsf, EDZsh, EDZvt)						
183	EDZtun_SS_K_i	Permeability modification factor due to self-sealing at time index i	$f_{K,EDZ,i}$		-	V
		i=1: t = 0 s		1		
		i=2: t = 1.57788E10 s		0.01		
184	EDZtun_SS_P_i	porosity modification factor due to self-sealing at time index i	$f_{\Phi,EDZ,i}$		-	V
		i=1: t = 0 s		1		
		i=2: t = 1.57788E10 s		0.1		
Tunnel Convergence – intermediate-level waste facility						
185	ETlma_TC_P_i	porosity modification factor due to tunnel convergence of LMA backfill material at time index i	$f_{\Phi,BF,i}$		-	V
		i=1: t = 0 s		1		
		i=2: t = 1.57788E10 s		0.8		
Uplift						
186	OPALI_UL_K_i	Permeability modification factor due to uplift at time index i	$t_{K,Uplift,i}$		s	V
		i=1: t = 0 s		1		
		i=2: t = 3.15576E13s		100		
Geochemical Sealing interface: mortar / gravel ↔ EDZ						
187	GRAVEL_EDZ_GS_t	Clogging time (Eq. 13)	T_c	3155760000	s	V
188	GRAVEL_EDZ_GS_l	Geochemical sealing model (Eq. 12)	l	1	-	V
189	GRAVEL_EDZ_GS_m	Geochemical sealing model (Eq. 12)	m	0.4	-	V
190	GRAVEL_EDZ_GS_k	Geochemical sealing model (Eq. 12)	κ	0.01	-	V
191	GRAVEL_EDZ_GS_d	Thickness of sealing layer	d	0.001	m	V
Geochemical Sealing interface: mortar ↔ Sand/Bentonite						
192	MORTA_S/B_GS_t	Clogging time (Eq. 13)	T_c	631152000 0	s	V
193	MORTA_S/B_GS_l	Geochemical sealing model (Eq. 12)	l	1	-	V
194	MORTA_S/B_GS_m	Geochemical sealing model (Eq. 12)	m	0.45	-	V
195	MORTA_S/B_GS_k	Geochemical sealing model (Eq. 12)	κ	0.01	-	V
196	MORTA_S/B_GS_d	Thickness of sealing layer	d	0.001	m	V
Gas Generation Rates - intermediate-level waste						
197	WAlma_Q_i	Gas generation rate at time index i	q_i		kg/s/m^3	V

#	Parameter Designation	Description		Base-Case Value	Units	V/F/S @
		i = 1: t = 0.0 s		0		
		i = 2: t = 1.0 s		5.56E-08		
		i = 3: t = 31557600.0 s		5.56E-08		
		i = 4: t = 94672800.0 s		5.40E-08		
		i = 5: t = 315576000.0 s		8.86E-09		
		i = 6: t = 946728000.0 s		8.86E-09		
		i = 7: t = 3155760000.0 s		7.90E-09		
		i = 8: t = 9467280000.0 s		6.37E-09		
		i = 9: t = 31557600000.0 s		3.63E-09		
		i = 10: t = 94672800000.0 s		1.61E-09		
		i = 11: t = 3.15576E+11 s		8.06E-10		
		i = 12: t = 9.46728E+11 s		4.03E-10		
		i = 13: t = 3.15576E+12 s		1.61E-10		
		i = 14: t = 5.36479E+12 s		0		
Gas Generation Rates - spent fuel, high-level waste, and pilot facility						
198	WAhlw_Q_i	Gas generation rate at time index i	q_i		kg/s/m^3	V
		i=1: t = 0.0 s		0		
		i=2: t = 1.0 s		1.40E-09		
		i=3: t = 6.31152E+12 s		1.40E-09		
		i=4: t = 6.31153E+12 s		0		
Dirichlet Boundary Conditions						
199	bMALM_P	Pressure in Malm aquifer	P_{Malm}	4.5	MPa	V
200	bMUSC_P	Pressure in Muschelkalk aquifer	P_{Musc}	8.03	MPa	V
201	uWEDE_P	Upstream pressure Wedelsandstein aquifer	$P_{Wede,u}$	4.9331	MPa	V
202	dWEDE_P	Downstream pressure Wedelsandstein aquifer	$P_{Wede,d}$	4.5648	MPa	V
203	uSAND_P	Upstream pressure Sandsteinkeuper aquifer	$P_{Sand,u}$	8.2499	MPa	V
204	dSAND_P	Downstream pressure Sandsteinkeuper aquifer	$P_{Sand,d}$	6.8986	MPa	V
Potential# Fault						
205	FAULT_POR	porosity	Φ	n/a%	-	V
206	FAULT_PERX	absolute permeability in x	k_x	n/a	m^2	V
207	FAULT_PERY	absolute permeability in y	k_y	n/a	m^2	V
208	FAULT_PERZ	absolute permeability in z	k_z	n/a	m^2	V
209	FAULT_COM	pore compressibility	c_Φ	n/a	1/Pa	V
210	FAULT_TORTX	tortuosity factor for binary diffusion	τ	n/a	-	V
211	FAULT_GK	Klinkenberg parameter	b	n/a	1/Pa	V
212	FAULT_RP_Slrk	residual liquid saturation for relative permeability functions	S_{lrk}	n/a	-	V

Provide fault properties to invoke vertical high-transmissivity zone.

% Not applicable; in the base-case model, the vertical high-transmissivity zone (fault) does not exist, i.e., the properties of the elements within the potential fault zone are identical to those of the hydrostratigraphic units it intersects.

#	Parameter Designation	Description		Base-Case Value	Units	V/F/S @
213	FAULT_RP_Sgr	residual gas saturation	S_{gr}	n/a	-	V
214	FAULT_CP_Slrc	residual liquid saturation for capillary pressure function	S_{lrc}	n/a	-	V
215	FAULT_CP_n	van Genuchten parameter	n	n/a	-	V
216	FAULT_CP_1/a	van Genuchten parameter	$1/\alpha$	n/a	Pa	V
217	FAULT_CP_g	van Genuchten active fracture model parameter	γ	n/a	-	V
Simulation Time						
218	TMAX	Total simulation time	T	3.1536E+13	s	F

6 IFC-PICNIC Interface

The 3D flow fields calculated by iTOUGH2-IFC will be used as input to PICNIC-TD, which calculates radionuclide transport in a network of 1D stream tubes. Fluxes at selected cross sections will be extracted from the 3D flow fields and entered into the corresponding 1D stream tubes. The interface between IFC and PICNIC is defined by a list of quadrilateral cross sections. The average of liquid flow across this cross section, as well as porosity and liquid saturation, will be calculated at each time step, and written to three output files (one each for low rate, porosity, and saturation). These files will then be passed on to PICNIC-TD. The definition of cross sections is provided in the forward (i.e., TOUGH2) input file following the line with the keyword "PICNIC".

The procedure of mapping IFC results to PICNIC legs is a follows. iTOUGH2-IFC will loop through all TOUGH connections. If a connection (i.e., the line segment connecting two grid blocks) intersects the quadrilateral defining the cross section of a PICNIC (note that the quadrilateral can have any orientation in space, but should be planar), the flow rate along this connection (or, alternatively, the component of this flow rate normal to the quadrilateral PICNIC cross section) will be assigned to the corresponding PICNIC leg. Flow is considered positive if in the direction of the normal vector to the quadrilateral according to the right-hand rule. Multiple TOUGH connections can contribute to the total flow entering a PICNIC leg. The flow rate from each TOUGH connection intersecting the PICNIC leg is weighted by the relative contribution of its cross-sectional area to the cross-sectional area of the quadrilateral. It is recommended that the PICNIC leg is chosen such that the cross-sectional area of the quadrilateral and the sum of all intersecting TOUGH cross-sectional areas are identical or match closely. Porosity and liquid saturation for the PICNIC leg is calculated as the area-weighted sum of the porosities and saturations of the elements intersected by the quadrilateral.

7 Testing of Code Modifications

As outlined above, iTOUGH2-IFC is based on the TOUGH2 simulator and iTOUGH2 optimization software. Both codes are well established and have been extensively verified and validated. Specifically, TOUGH2 and iTOUGH2 have been verified for use within the Yucca Mountain project. The following subsections present simulation cases that were developed to test the correct implementation of code modifications needed to address the specific requirements of the IFC.

7.1 Replicating System States to Boundary Elements

To test the correct implementation of the replication capability, a one-dimensional model was set up, simulating water displacement due to constant-pressure gas injection. The system is represented using two approaches. In the reference case (Fig. 12a), water displacement is simulated in elements of equal size; in the test case (Fig. 12b), the first element is replaced with a smaller element (mimicking a representative waste emplacement tunnel); its volume *V* and cross-sectional area *A* are only one-tenth of the respective values in the reference case. The dynamic system state of this representative element is then copied to a boundary element that is connected to the second element. The TOUGH2 input files for the reference and test model is shown in Fig. 13. The input file for the test case (Fig. 14) contains the new input block COPY. The system state calculated for element A11 1 is copied after completion of each time step to the dummy boundary element DUM 1. The two systems are expected to yield consistent simulation results. Slight differences between the model results are anticipated, because the system state in the boundary element lags behind by one time step. As demonstrated in Fig. 15, this error is insignificant, even for a highly transient simulation with fast changes in flow rates and saturations. The correct implementation of the system state replication feature into iTOUGH2-IFC is thus considered verified.

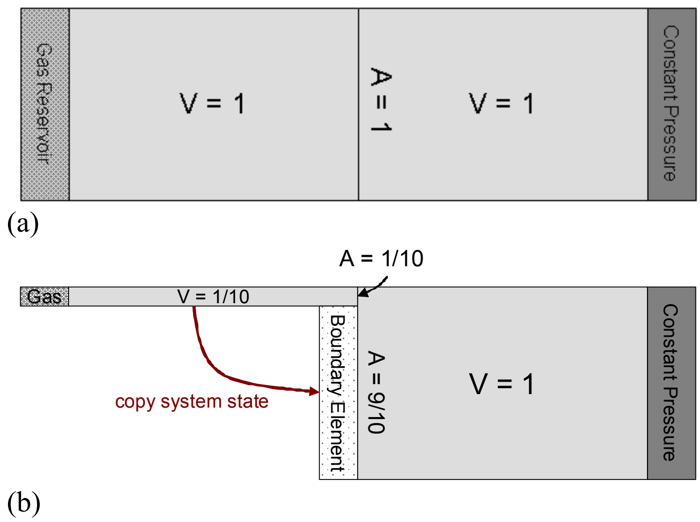

Fig. 12: Set-up of test case to verify implementation of replication feature; (a) reference case; (b) test case.

```
TOUGH2-IFC input file for testing replication feature; reference model
ROCKS----1----*----2----*----3----*----4----*----5----*----6----*----7----*---
-8
OPALI    0     2650.     .3500 1.000E-13                           2.51
920.
bOPAL    0     2650.     .9900 1.000E-13                           2.51
100000.

RPCAP----1----*----2----*----3----*----4----*----5----*----6----*----7----*---
-8
    3      0.200E+00 0.050E+00
    1      0.000E+00 0.000E+00 1.000E+00
PARAM----1----*----2----*----3----*----4----*----5----*----6----*----7----*---
-8
   22500      101000009000000004000006000
 0.000E+00 6.000E+03 0.100E+00 1.000E+00
    1.0E-7
 100000.000000000000    0.00000000000000  20.000000000000000
MULTI----1----*----2----*----3----*----4----*----5----*----6----*----7----*---
-8
    2    2    2    6
ELEME----1----*----2----*----3----*----4----*----5----*----6----*----7----*---
-8
A11 1          OPALI .1000E-03
A11 2          OPALI .1000E-03
IN             bOPAL
OUT            bOPAL

CONNE----1----*----2----*----3----*----4----*----5----*----6----*----7----*---
-8
IN   A11 1                   1 .1000E-10 .5000E-02 .1000E-01
A11 1A11 2                   1 .5000E-02 .5000E-02 .1000E-01
A11 2OUT                     1 .5000E-02 .1000E-10 .1000E-01

START----1----*----2----*----3----*----4----*----5----*----6----*----7----*---
-8
INCON----1----*----2----*----3----*----4----*----5----*----6----*----7----*---
-8
IN
 120000.000000000000  1.0000000000000000  20.000000000000000
OUT 0
 100000.000000000000 10.5000000000000000  20.000000000000000

ENDCY----1----*----2----*----3----*----4----*----5----*----6----*----7----*---
-8
```

Fig. 13: TOUGH2-IFC input file for testing the replication feature; reference case.

```
TOUGH2-IFC input file for testing replication feature; test case (includes
COPY)
ROCKS----1----*----2----*----3----*----4----*----5----*----6----*----7----*---
-8
OPALI    0     2650.     .3500 1.000E-13                          2.51
920.
bOPAL    0     2650.     .9900 1.000E-13                          2.51
100000.

RPCAP----1----*----2----*----3----*----4----*----5----*----6----*----7----*---
-8
    3      0.200E+00 0.050E+00
    1      0.000E+00 0.000E+00 1.000E+00
PARAM----1----*----2----*----3----*----4----*----5----*----6----*----7----*---
-8
   22500     1001000009000000004000006000
 0.000E+00 6.000E+03 0.100E+00 1.000E+00
    1.0E-7
 100000.000000000000    0.00000000000000  20.000000000000000
MULTI----1----*----2----*----3----*----4----*----5----*----6----*----7----*---
-8
    2    2    2    6
ELEME----1----*----2----*----3----*----4----*----5----*----6----*----7----*---
-8
A11 1          OPALI .1000E-04
A11 2          OPALI .1000E-03
IN             bOPAL
OUT            bOPAL
DUM 1          bOPAL

CONNE----1----*----2----*----3----*----4----*----5----*----6----*----7----*---
-8
IN   A11 1                    1 .1000E-10 .5000E-02 .1000E-02
A11 1A11 2                    1 .5000E-02 .5000E-02 .1000E-02
A11 2OUT                      1 .5000E-02 .1000E-10 .1000E-01
DUM 1A11 2                    1 .5000E-02 .5000E-02 .9000E-02

COPY ----1----*----2----*----3----*----4----*----5----*----6----*----7----*---
-8
    1     A11 1
DUM 1

START----1----*----2----*----3----*----4----*----5----*----6----*----7----*---
-8
INCON----1----*----2----*----3----*----4----*----5----*----6----*----7----*---
-8
IN
 120000.000000000000  1.0000000000000000  20.000000000000000
OUT
 100000.000000000000 10.5000000000000000  20.000000000000000

ENDCY----1----*----2----*----3----*----4----*----5----*----6----*----7----*---
-8
```

Fig. 14: TOUGH2-IFC input file for testing the replication feature; test case.

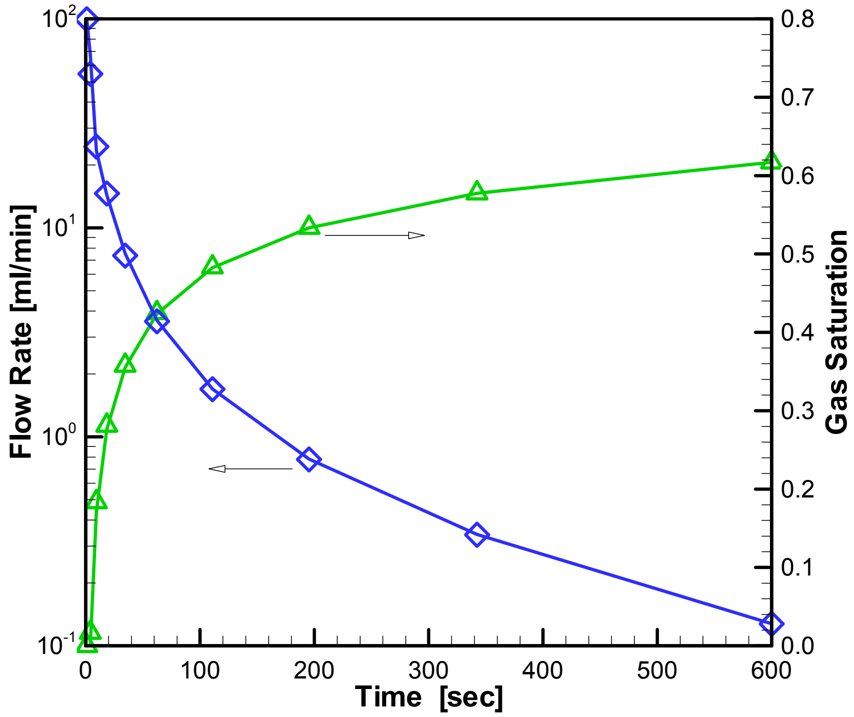

Fig. 15: Comparison between reference case (symbols) and test case (lines) for verification of replication feature.

7.2 Flowpath Dilation

If gas pressure exceeds a certain depth-dependent threshold pressure, pathway dilation leads to an anisotropic increase in absolute permeability and a reduction in capillary strength (see Section 4.3.3 for details). Verification of the correct implementation of this process is done by a simple inspection of the horizontal and vertical permeabilities and the van Genuchten $1/\alpha$ parameter in a gridblock (belonging to the material type `OPALI)` that exceeds the threshold pressure due to gas injection. The values calculated by TOUGH2-IFC are compared to a simple hand calculation of the pathway dilation model described by Eqs. (1)–(5).

The TOUGH2-IFC input file is shown in

Fig. 16. Gas is injected into a single element, which is at an elevation of -200 m.a.s.l. Initial horizontal and vertical permeabilities are 1×10^{-20} m^2 and 2×10^{-21} m^2, respectively; the initial capillary-strength parameter is 18 MPa. The parameters of the pathway dilation model are given in block `IFC.2` (and reproduced in the header of the output file); they include a lithostatic pressure gradient of 0.0025 MPa/m, an empirical parameter e of 2 MPa, and a surface elevation of 400 m.a.s.l.

Pathway dilation is initiated in an element if gas injection leads to an excess pressure that exceeds the threshold pressure p_d, Eq. (1)). For the input parameters of the test problem, the threshold pressure is:

$$p_d = 0.0025 \cdot (400 - (-200)) - 2.0 = 13 \text{ MPa}$$

Once this threshold pressure is exceeded (which occurs at the sixth time step), hydrogeologic properties are changed according to Eqs. (2)–(5). Specifically, the pressure in the test element after six time steps is 15,571,633 Pa, which is correctly reported as 2.571633 MPa above the threshold pressure. Vertical permeability is calculated using Eq. (2):

$$k_v = 2\times10^{-21} + 1\times10^{-21}\cdot(15.571633-13.0)^3 = 1.90\times10^{-20}\ \mathrm{m}^2$$

Given k_v, the horizontal permeability is calculated using Eqs. (3) and (4):

$$k_h = 1.90\times10^{-20}\cdot 5^{(2/19)^{0.25}} = 4.75\times10^{-20}\ \mathrm{m}^2$$

Finally, the capillary-strength parameter is calculated using Eq. (5):

$$\frac{1}{\alpha} = 1.8\times10^{6}\sqrt{\frac{1\times10^{-20}}{4.75\times10^{-20}}} = 8.26\times10^{6}\ \mathrm{Pa}$$

All these hand-calculated values are identical to those reported in the TOUGH2-IFC output file. The correct implementation of the pathway dilation model into iTOUGH2-IFC is thus considered verified.

```
Test for IFC implementation of pathway dilation
ROCKS----1----*----2----*----3----*----4----*----5----*----6----*----7----*---
-8
OPALI    2     2650.     .1200 1.000E-20 1.000E-20 2.000E-21
1000.

   11           0.50     0.003                          0.02
   11           1.67  18.0E+06    1.0E30
bOPAL    0     2650.     .1200 1.000E-20 1.000E-20 2.000E-21              -
1000.

PARAM----1----*----2----*----3----*----4----*----5----*----6----*----7----*---
-8
   1   6       6000000900000000400003000
 0.000E+00 2.000E+03 1.000E-00
    1.0E-5
 100000.000000000000   10.50000000000000  20.000000000000000
ELEME----1----*----2----*----3----*----4----*----5----*----6----*----7----*---
-8
s64 1          OPALI0.1125E+01                        470.25     44.75    -
200.00

CONNE----1----*----2----*----3----*----4----*----5----*----6----*----7----*---
-8

INCON----1----*----2----*----3----*----4----*----5----*----6----*----7----*---
-8
s64 1
 6000000.00000000000   0.000000000000000  20.000000000000000

GENER----1----*----2----*----3----*----4----*----5----*----6----*----7----*---
-8
s64 1SF  1                  0     COM2      0.001

IFC  ----1----*----2----*----3----*----4----*----5----*----6----*----7----*---
-8
    6    A         B         C         D         E         F          FEP
1.3.19
       3.0   1.0E-21      0.25     2.5E4     2.0E6     400.0
   -1                       EDZ self-sealing                        FEP
1.4.1
   -1                       LMA tunnel convergence                  FEP
1.4.3
   -1                       Uplift                                  FEP
1.4.7
   -1                       Geochemical sealing

ENDCY----1----*----2----*----3----*----4----*----5----*----6----*----7----*---
-8
```

Fig. 16: TOUGH2-IFC input file for testing pathway dilation.

7.3 EDZ Self-Sealing, Tunnel Convergence, and Uplift

With time, permeability and porosity of the EDZ are reduced as a result of geomechanical self-sealing, porosity is reduced in the ILW facility as a result of tunnel convergence, and permeability of the Opalinus Clay is increased as a result of uplift (see Section 4.3.4 for details). Verification of the correct implementation of these geomechanical processes is done by a simple inspection of the calculated permeabilities and porosities as a function of time. The values calculated by TOUGH2-IFC are compared to changes prescribed in look-up tables.

Fig. 17 shows the TOUGH2-IFC input file. It consists of three unconnected elements, each associated with a material type that triggers either EDZ self-sealing, tunnel convergence, or uplift.

The temporal variation of porosities and permeabilities is specified through look-up tables in the IFC block of the input file. The prescribed curves for permeability and porosity are shown as solid lines in Fig. 18 and Fig. 19, respectively. The symbols are the discrete values calculated by iTOUGH2-IFC for each time step taken by the simulator; they track the prescribed curves, confirming the correct implementation of these abstracted geomechanical FEPs.

As noted in Section 4.3.4, porosity at any given location does not only change due to the FEPs addressed here, but also in response to elastic deformation caused by pore-pressure changes. As a result, the porosity at any given time may not be identical to that prescribed in the look-up tables, but slightly higher or lower, depending on whether the element is, respectively, at a higher or lower pressure compared to its initial pressure. Similarly, the permeability of elements in the Opalinus Clay affected by pathway dilation are also influenced by uplift; the combined effect is calculated in iTOUGH2-IFC, i.e., the permeability in these elements may be different from those expected by uplift alone, should the dilation threshold pressure be exceeded.

Finally, porosity in fully saturated EDZ and ILW backfill elements may not be reduced at the externally prescribed rate. Porosity reduction is limited as to avoid excessive overpressures caused by the very low compressibility of water combined with the formation’s low permeability, which results in a significantly reduced consolidation rate.

```
Test for IFC implementation of mechanical FEPs
ROCKS----1----*----2----*----3----*----4----*----5----*----6----*----7----*---
-8
OPALI    0     2650.     .1200 1.000E-20 1.000E-20 2.000E-21
1000.
bOPAL    0     2650.     .1200 1.000E-20 1.000E-20 2.000E-21               -
1000.
EDZsf    0     2650.     .2000 1.000E-19 1.000E-19 1.000E-19
1000.
bEDZs    0     2650.     .2000 1.000E-19 1.000E-19 1.000E-19               -
1000.
ETlm1    0     2650.     .2500 1.000E-15 1.000E-15 1.000E-15
1000.
ETlm2    0     2650.     .2500 1.000E-15 1.000E-15 1.000E-15
1000.

RPCAP----1----*----2----*----3----*----4----*----5----*----6----*----7----*---
-8
   11           0.25     0.01                         0.02
   11           2.00  -0.1E+06    1.0E30
PARAM----1----*----2----*----3----*----4----*----5----*----6----*----7----*---
-8
   1  11       110000090000000040000300 0
 0.000E+00 1.100E+02 1.000E+00 1.000E+00
    1.0E-5
 100000.000000000000   10.5000000000000  20.0000000000000
ELEME----1----*----2----*----3----*----4----*----5----*----6----*----7----*---
-8
EDZ 1          EDZsf .1000E+01                                            -
200.00
LMA 1          ETlm1 .1000E+01                                            -
200.00
OPA 1          OPALI .1000E+01                                            -
200.00

CONNE----1----*----2----*----3----*----4----*----5----*----6----*----7----*---
-8

START----1----*----2----*----3----*----4----*----5----*----6----*----7----*---
-8
INCON----1----*----2----*----3----*----4----*----5----*----6----*----7----*---
-8

IFC  ----1----*----2----*----3----*----4----*----5----*----6----*----7----*---
-8
   -1                                                                 FEP
1.3.19
    1                        EDZ self-sealing                         FEP
1.4.1
    1                        Number of EDZ types
    2                        Number of materials in EDZ type
EDZsf
bEDZs
this                         File name containing permeability look-up table
    3                        Number of data points in permeability look-up
table
       1.0       1.0
       5.0       0.2
      10.0       0.1
this                         File name containing porosity look-up table
    3                        Number of data points in porosity look-up table
       1.0       1.0
       5.0      0.75
      10.0      0.60
```

```
    1                             LMA tunnel convergence                    FEP
1.4.3
    2                             Number of materials defining LMA backfill
material
ETlm1
ETlm2
this                              File name containing porosity look-up table
    3                             Number of data points in porosity look-up table
       1.0        1.0
       5.0        0.6
      10.0        0.5
    1                             Uplift                                    FEP
1.4.7
this                              File name containing permeability look-up table
    3                             Number of data points in permeability look-up
table
       1.0        1.0
       5.0       10.0
      10.0      100.0
   -1                             Geochemical FEPs

ENDCY----1----*----2----*----3----*----4----*----5----*----6----*----7----*---
-8
```

Fig. 17: TOUGH2-IFC input file for testing pathway dilation.

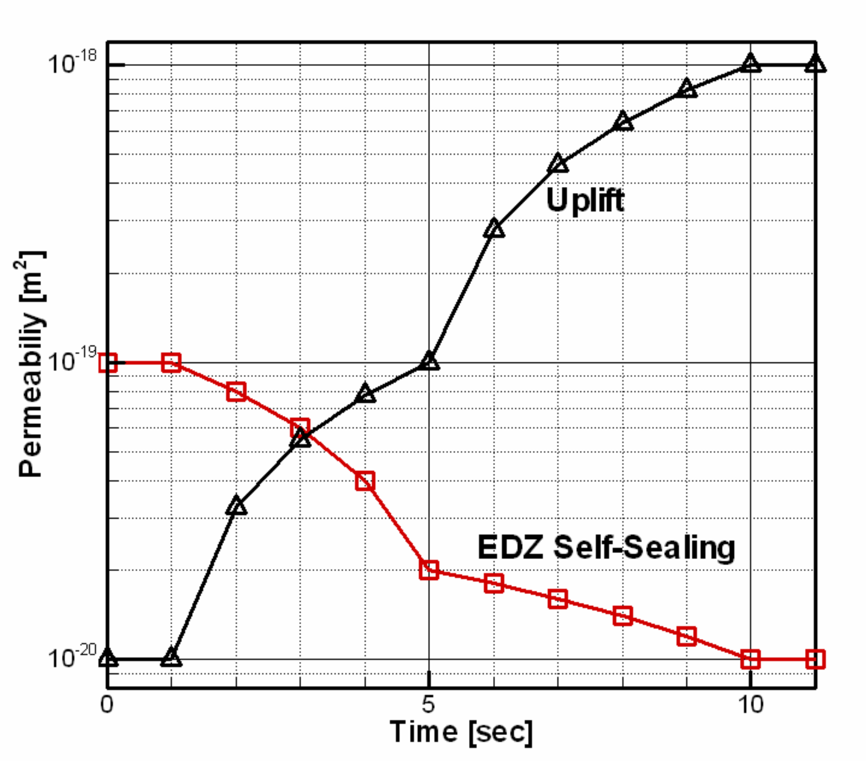

Fig. 18: Comparison between prescribed (lines) and calculated (symbols) permeabilities in elements subject to EDZ self-sealing and uplift.

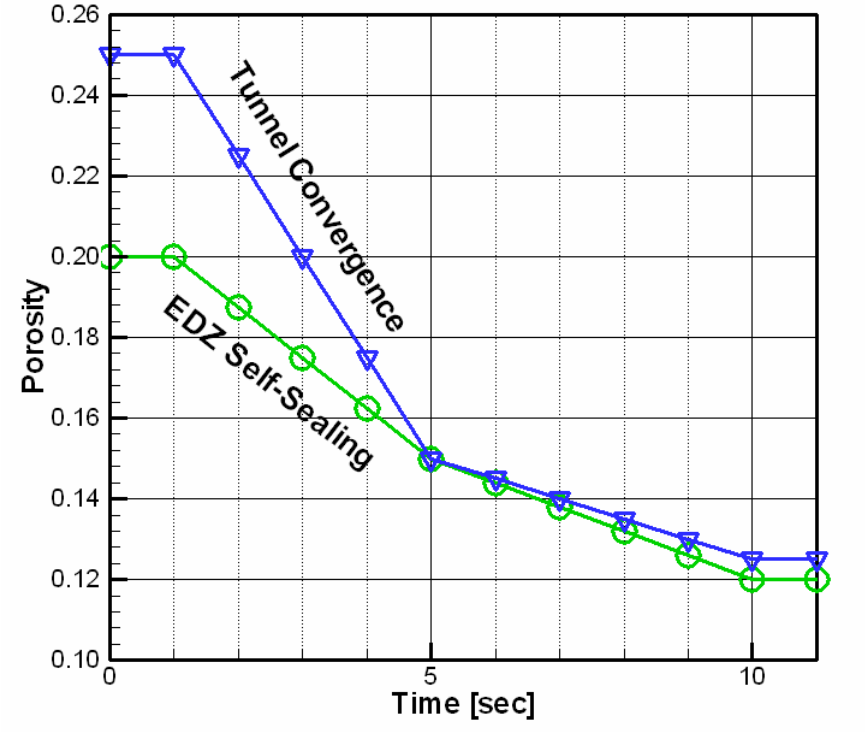

Fig. 19: Comparison between prescribed (lines) and calculated (symbols) porosities in elements subject to EDZ self-sealing and tunnel convergence.

7.4 Geochemical Sealing

With time, a thin layer of mineral precipitates develops at the interface between cementitious backfill material and the host rock, leading to a reduction in the permeability perpendicular to this interface (see Section 4.3.5 for details). Verification of the correct implementation of this geochemical sealing process is done by a comparison of fluxes across in interface with a sealing layer, and the corresponding hand calculation of serial flow through a layered system.

A model of a simple test cell is developed (see

Fig. 20 for the corresponding TOUGH2_IFC input file). It consists of two 0.1 m long elements, one representing backfill material (element `ET  1`), the other the EDZ (element `EDZ  2`). A constant pressure gradient of 0.2 bar per 0.2 m is imposed. The IFC block indicates that the clogging time is set to 100 years, the sealing layer has a thickness of 0.01 m, and the permeability is maximally reduced to 0.1 % of the undisturbed permeability (see Eq. (15)). The additional parameters (*l* and *m,* see Eq. (12)) determine the temporal evolution of the permeability reduction.

Darcy's law is used to calculate the expected flow rate Q [kg/s] in this heterogeneous system:

$$Q = A \cdot \bar{k} \cdot \frac{\rho}{\mu} \cdot \frac{\Delta P}{\Delta x} \tag{16}$$

Here, A [m^2] is the cross sectional area, $\bar{k}$ [m^2] is the effective permeability, ρ [kg m^{-3}] is water density, μ [Pa s] is dynamic viscosity, ΔP [Pa] is the imposed pressure difference, and Δx [m] is the flow distance. In the absence of geochemical sealing, the system considered consists of flow in series through two 0.1-m long layers with permeabilities of 10^{-17} and 10^{-19} m^2, respectively. The effective permeability for flow in series is calculated by the harmonic mean:

$$\bar{k}_0 = \frac{\Delta x}{\frac{b_1}{k_1} + \frac{b_2}{k_2}} = \frac{0.2}{\frac{0.1}{10^{-17}} + \frac{0.1}{10^{-19}}} = 1.98 \times 10^{-19} \text{ m}^2$$

With density and viscosity for water at 1 atm and 30°C, the flow rate is:

$$Q_0 = 1.0 \cdot 1.98 \times 10^{-19} \cdot \frac{995.75}{7.97 \times 10^{-4}} \cdot \frac{0.2 \times 10^5}{0.2} = 2.47 \times 10^{-8} \text{ kg s}^{-1}$$

Inserting a sealing layer of 0.01 m thickness and a permeability that is 0.1 % of the unclogged permeability yields an effective permeability after maximum clogging of

$$\bar{k}_s = \frac{0.2}{\frac{0.19}{1.98 \times 10^{-19}} + \frac{0.01}{1.98 \times 10^{-22}}} = 3.96 \times 10^{-21} \text{ m}^2$$

and a steady-state flow rate of

$$Q_0 = 1.0 \cdot 3.96 \times 10^{-21} \cdot \frac{995.75}{7.97 \times 10^{-4}} \cdot \frac{0.2 \times 10^5}{0.2} = 4.95 \times 10^{-10} \text{ kg s}^{-1}$$

As shown in Fig. 21, the flow rate calculated by TOUGH2-IFC transitions from the theoretical value for the unclogged system to that of the maximally clogged system within the specified clogging time of 100 years. The correct implementation of geochemical sealing under fully saturated conditions is thus considered verified. Recall, that the clogging time is dynamically adjusted to account for partial clogging under unsaturated conditions, yielding a smaller permeability reduction in the presence of gas.

```
Test for IFC implementation of geochemical sealing
ROCKS----1----*----2----*----3----*----4----*----5----*----6----*----7----*---
-8
OPALI    0     2650.     .1200 1.000E-20 1.000E-20 2.000E-21
1000.
bOPAL    0     2650.     .1200 1.000E-20 1.000E-20 2.000E-21              -
1000.
ETsf     0     2650.     .2500 1.000E-17 1.000E-17 1.000E-17
1000.
bETsf    0     2650.     .2500 1.000E-17 1.000E-17 1.000E-17              -
1000.
EDZsf    0     2650.     .2000 1.000E-19 1.000E-19 1.000E-19
1000.
bEDZs    0     2650.     .2000 1.000E-19 1.000E-19 1.000E-19              -
1000.

RPCAP----1----*----2----*----3----*----4----*----5----*----6----*----7----*---
-8
   11           0.01      0.01                          0.02
   11           2.00  -0.1E+06    1.0E30
PARAM----1----*----2----*----3----*----4----*----5----*----6----*----7----*---
-8
   2 300       1100000900020000400003000
 0.000E+006.3115E+09 1.000E+05
    1.0E-7
 100000.000000000000    0.00000000000000  30.000000000000000
MOMOP----1----*----2----*----3----*----4----*----5----*----6----*----7----*---
-8
2
ELEME----1----*----2----*----3----*----4----*----5----*----6----*----7----*---
-8
ET  1          ETsf 0.1000E+00                       1346.00    439.50   -
196.40
EDZ 2          EDZsf0.1000E+00                       1347.00    439.50   -
196.40
IN  0          bETsf0.0000E+00
OUT 3          bEDZs0.0000E+00

CONNE----1----*----2----*----3----*----4----*----5----*----6----*----7----*---
-8
IN  0ET  1                    10.1000E-100.5000E-010.1000E+01
ET  1EDZ 2                    10.5000E-010.5000E-010.1000E+01
EDZ 2OUT 3                    10.5000E-010.1000E-100.1000E+01

START----1----*----2----*----3----*----4----*----5----*----6----*----7----*---
-8
INCON----1----*----2----*----3----*----4----*----5----*----6----*----7----*---
-8
IN  0
 120000.000000000000   0.000000000000000  30.000000000000000
OUT 3
 100000.000000000000   0.000000000000000  30.000000000000000

IFC  ----1----*----2----*----3----*----4----*----5----*----6----*----7----*---
-8
   -1                         Pathway dilation                         FEP
1.3.19
   -1                         EDZ self-sealing                         FEP
1.4.1
   -1                         LMA tunnel convergence                   FEP
1.4.3
   -1                         Uplift                                   FEP
1.4.7
    1                         Geochemical sealing
```

```
    1                           Number of geochemical interface types
    1                           Number of material pairs for 1st interface type
ETsf      EDZsf                 Materials defining interface with geochemical
sealing
 3.15576E9                      Clogging time
 1.0                            Parameter l
 0.4                            Parameter m
 0.001                          Parameter kappa
 0.01                           Sealing layer thickness

ENDCY----1----*----2----*----3----*----4----*----5----*----6----*----7----*---
-8
```

Fig. 20: TOUGH2-IFC input file for testing geochemical sealing.

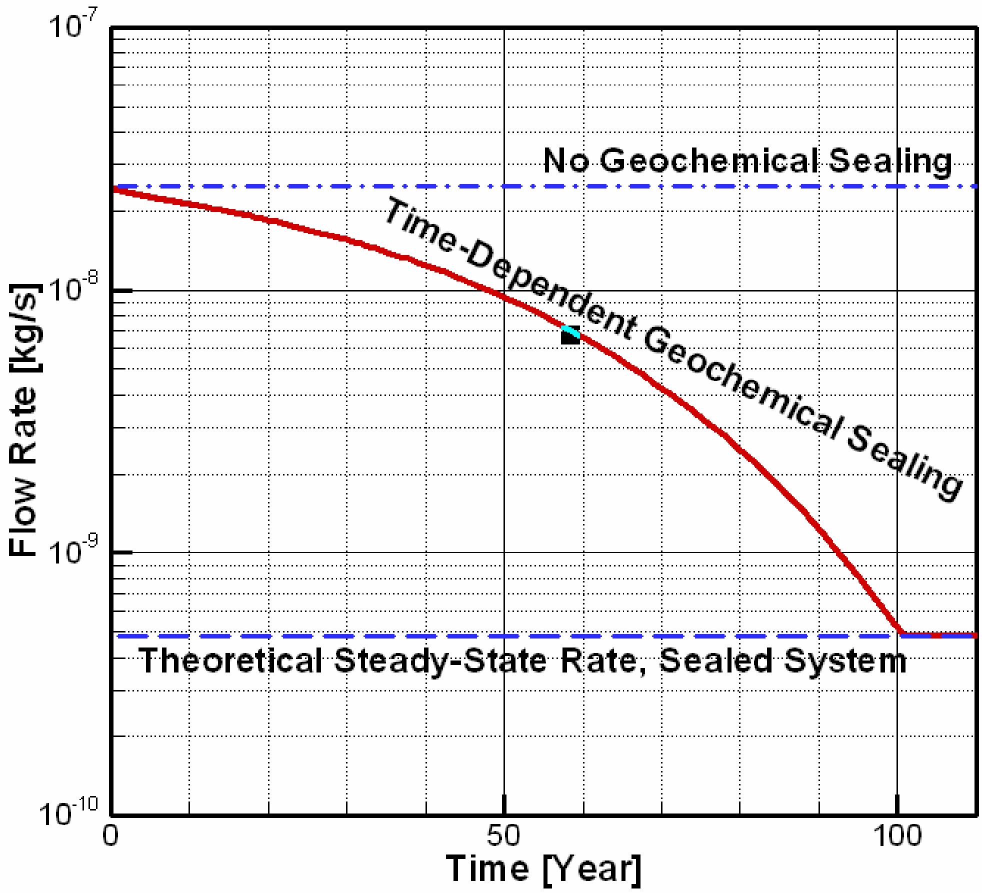

Fig. 21: Flow rate through test cell with and without time-dependent geochemical sealing.

8 Test Simulation

A test simulation was performed using the iTOUGH2-IFC code and IFC model with the base-case parameter set as described in Section 5. The purpose of this test run is to examine whether the simulation proceeds to the end time of 1 million years, and to get an indication of CPU time requirements. The simulation results are not discussed here.

A second simulation was conducted without inclusion of the FEPs described in Sections 4.3.3 - 4.3.5, i.e., without pathway dilation, EDZ self-sealing, tunnel convergence, uplift, and geochemical sealing.

The simulation was performed on a Dell laptop, Latitude D620, with an Intel© Corel™ 2 CPU T7600 @ 2.33 GHz and 2.00 GB of RAM, running under Microsoft Windows XP, Professional, Version 2002, Service Pack 3. The Fortran source code was compiled using the Intel® Visual Fortran Compiler 9.1.

The test simulation included three runs, where the first two generate the steady-state field that is used as the initial condition for the transient simulation in response to gas generation and imposed property changes (i.e., EDZ self-sealing, tunnel convergence, uplift, and geochemical alterations. The steady-state runs are not further described here.

Fig. 22 shows the CPU time as a function of simulation time. Simulating the strong changes at early times with the initial expansion of the two-phase zone consumes a considerable fraction of the total CPU time. The difference in the computational demands for the simulations with and without the geomechanical and geochemical FEPs attests to the difficulties in resolving the nonlinearities and counteracting effects (specifically the early-time pressure increase due to high gas generation in the ILW facility combined with tunnel convergence, and the late-time transient effects imposed to account for uplift).

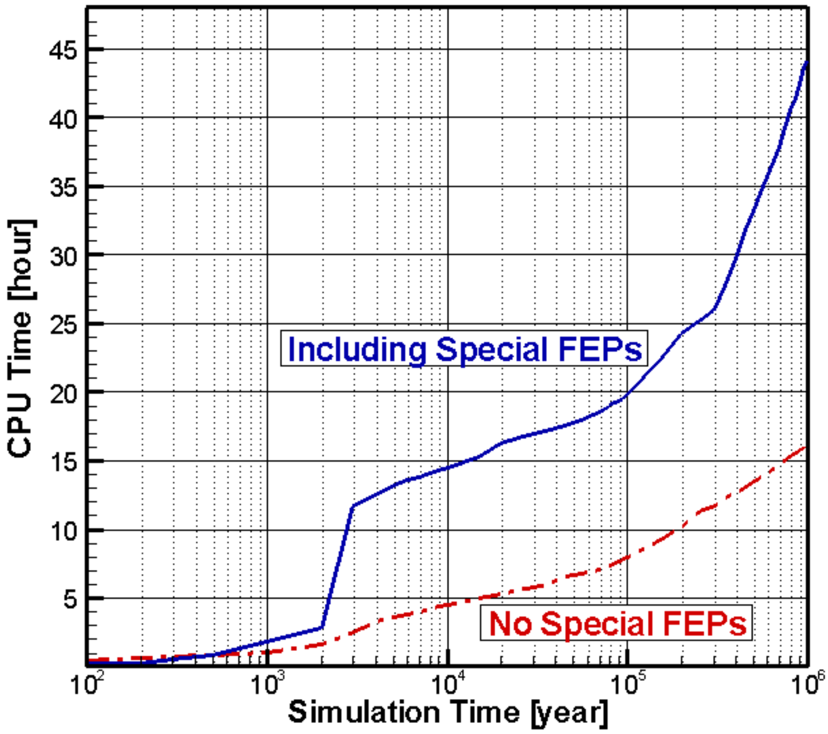

Fig. 22: CPU time as a function of simulation time for a simulation with and without the inclusion of geomechanical and geochemical FEPs.

In the main iTOUGH2-IFC output file after extensive header information, a list of element-related output variables is printed, including:

- Pressure [Pa]
- Gas saturation [m^3/m^3]
- Hydrogen mass fraction in the liquid phase [kg/kg]
- Capillary pressure [Pa]
- Gas density [kg/m^3]
- Horizontal and vertical absolute permeability [m^2]
- Capillary-strength parameter [Pa]
- Porosity [m^3/m^3]

In a second block, all connection-related output variables are printed, including:

- Total fluid mass flow rate [kg/s]
- Gas mass flow rate [kg/s]
- Liquid mass flow rate [kg/s]
- Gas phase velocity [m/s]
- Liquid phase velocity [m/s]
- Liquid relative permeability [-]

- Gas relative permeability [-]
- Permeability reduction fraction due to geochemical sealing [-]

The third block lists the specified gas generation rates, and the fourth block contains global mass and volume balances. Some information about the behavior of the geomechanical and geochemical FEPs is printed as needed.

9 Summary and Concluding Remarks

The developed iTOUGH2-IFC code and the related IFC model is intended to capture safety-relevant features and processes for simulating flow of liquid and gas in a SF/HLW/ILW repository in Opalinus Clay. The computational approach combines a site- and process-specific conceptual model with numerical simulation of two-phase, two-component flow, and is based on a module of the TOUGH simulator (Pruess et al., 1999) as implemented in iTOUGH2 (Finsterle, 2007abc). The implemented approach captures these features and processes explicitly in an appropriately simplified process model.

To achieve computational efficiency, the repository system and its elements as well as the geosphere are represented in a simplified manner. Specifically, advantage is taken from approximate symmetries encountered in the system, and from expected flow patterns. Following this approach, less only 2.5 % of the emplacement tunnels of the SF/HLW facility need to be modeled. The remainder of the tunnel system, however, is represented in full.

While the main features and processes are simulated using the built-in modeling capabilities of TOUGH2, a limited number of FEPs (i.e., pathway dilation, mechanical and chemical alterations of backfill materials, the EDZ, and the host rock) are represented by abstraction models. According to Order 690.09 (p. 2, bullet 2), the basis and justification for these representations can be taken from previous Nagra reports, specifically Nagra (2002b, NTB 02-05; NTB 02-05, 2004); consequently, the details of these submodels or their abstraction are not discussed in this report. In their implementation within the IFC, these submodels can be provided either as parameterized functions or as look-up tables.

The correct implementation of new features built into the iTOUGH2 code has been tested (see Section 7). The mesh was generated using an automatic procedure that reduces the risk of introducing discretization errors (see Section 5.3), and property values were carefully selected (see Section 5.4). Nevertheless, the code and model should undergo additional testing for correctness, robustness, and efficiency. Specifically, the continuity of the tunnel system and its connection to the geosphere should be further inspected. The efficiency of the simulation may be improved by adjusting certain property values, computational parameters, program options, and mesh resolution. Property adjustments and mesh coarsening need to be justified through sensitivity analyses.

The iTOUGH2-IFC code and the numerical repository model have been designed and built such that they can be modified and enhanced to accommodate new insights, computation resources, and other needs of Nagra's probabilistic safety assessment of a repository for spent fuel, high-level waste, and long-lived intermediate-level wastes in Switzerland.

10 Comments and Recommendations

This section summarizes some observations and makes suggestions regarding alternative implementations, supporting studies, and future developments. Section 10.1 contains recommendations regarding investigations that could be performed to justify certain simplifying assumptions made in the IFC, and to analyze their impacts on model predictions. Section 10.2 lists iTOUGH2-IFC capabilities that are currently not used, but could be invoked to refine the IFC. Section 10.3 discusses miscellaneous issues.

10.1 Testing of Assumptions

10.1.1 Resaturation and Multi-Component Gas Generation

The IFC only considers a single gas component (hydrogen). However, some of the pore space may be initially filled with air (as a result of dry-out during the construction phase). Moreover, the gas generated by corrosion and waste degradation consists of multiple components (hydrogen being the dominant molecule). Representing the gas mixture as a single-component gas (hydrogen) is a simplifying assumption. It is recommended that the impact of this simplification on compressibility, solubility, and other performance-relevant processes and parameters be examined in a separate study using a multi-component module of the TOUGH suite of simulators.

10.1.2 Gas Migration within Waste Emplacement Tunnels

It is recommended that gas generation and gas flow within a backfilled emplacement tunnel segment of the length of a waste canister (including canister spacing) be studied in detail to confirm the appropriateness of the line-source assumption, and to justify the discretization and effective parameters used for simulating gas flow along the emplacement tunnel.

10.1.3 Appropriateness of Representative Emplacement Tunnel Approach

To significantly increase computational efficiency, the array of waste emplacement tunnels is not fully discretized, but replaced by a single representative tunnel, which is then replicated (see Sections 5.2.2 and 2). This approach is based on symmetry assumptions that are a simplification of the real system and its expected behavior. Specifically, the symmetry assumption is violated near the edges of the tunnel array. Moreover, the pressure and saturation conditions in the construction and operation tunnels, to which the waste emplacement tunnels are connected, are non-uniform, leading to non-symmetric flow conditions. Finally, the regional-scale hydrologic conditions and non-symmetry of the entire repository system have a non-symmetric impact on the near-field conditions. It is recommended that the simplification inherent in the representative emplacement tunnel approach be tested using a separate, comprehensive model of the facility.

10.1.4 Coupled Hydrologic-Mechanical Effects under Two-phase Conditions

Tunnel convergence is simulated by externally specifying a time-dependent porosity reduction (see Section 4.3.4). This approach does not consider coupled hydro-mechanical effects. For example, it is unlikely that materials consolidate under imposed stress changes at a rate that is independent of whether the pore space is gas filled or fully liquid saturated. Prescribing a porosity reduction in a fully water saturated, tight formation may lead to abrupt and excessive pressure increases due to the small water compressibility. The consolidation behavior under two-phase conditions could be examined theoretically, analytically, and numerically, to gain confidence in the simplified representation of tunnel convergence in the IFC model, or to provide a basis for an alternative abstraction.

10.2 Simulation Capabilities not Invoked by Current Base-Case Model

10.2.1 Water Consumption

FEP 1.3.13, i.e., the consumption of water due to corrosion reactions, is not considered a relevant process and is thus not included in the base-case model. However, the iTOUGH2-IFC code is capable of handling a phase-specific water withdrawal rate, which could be made proportional to the time-dependent gas generation rate. Sensitivity analyses on the effects of water consumption could be performed.

10.2.2 Gas Production Limited by Water Availability

Corrosion and gas generation rates depend on the availability of water, which may be limited near the waste packages due to reduced liquid saturation combined with low permeability of the surrounding material. The coupled effect of gas generation, fluid displacement and water availability, which potentially limits further gas generation, could be examined using appropriate coupled process models that account for two-phase flow and reactive transport.

10.2.3 Consistency in Treatment of Property Changes

Certain coupled geomechanical and geochemical processes are accounted for in a simplified manner by externally imposing changes in hydrogeologic properties, i.e., porosity, permeability, and the capillary-strength parameter of the van Genuchten capillary pressure curve. All the processes described in Section 4.3 essentially lead to an increase or reduction in porosity. However, the inherent correlations among porosity, permeability, and capillary strength are not accounted for in a consistent manner. Specifically, pathway dilation is implemented as a change in permeability and capillary strength, while porosity remains unchanged; EDZ self-sealing processes are implemented as a change in permeability and porosity, while capillary strength remains unchanged; tunnel convergence is implemented as a change in porosity, while permeability and capillary strength remain unchanged; and finally, uplift and geochemical processes are implemented as a change in permeability, while porosity and capillary strength remain unchanged. The justification for this variable treatment of changes in potentially correlated parameters is not obvious. A consistent implementation of property changes would be straightforward.

10.2.4 Representation of Uplift

Several effects resulting from uplift are neglected in the simplified treatment discussed in Section 4.3.4, but could be implemented. Changes in two-phase flow parameters (e.g., reduction in capillary strength) could be implemented analogous to Section 4.3.3. Uplift and erosion changes the depth of the host rock and thus the depth-dependent pathway-dilation effects. Changes in vertical effective stress due to uplift could be implemented by specifying a time-dependent surface elevation in Eq. (1). Most important, the pressure at the top boundary of the model is also affected by uplift and erosion; the corresponding time-dependent Dirichlet boundary condition could be provided as a function of the erosion rate using standard iTOUGH2-IFC features.

10.2.5 Representation of Fractures

Fractures and discontinuities (FEPs 1.3.1 and 1.3.2) on a relatively small scale could be included using the double-porosity, dual-permeability, or multiple interacting continua (MINC) approaches (Pruess and Narasimhan, 1985), or using an effective continuum model for relative permeability and capillary pressure (Doughty, 1999); all these approaches are available in iTOUGH2-IFC. (Note that in Opalinus Clay, fractures appear to be hydraulically active only if the overburden is reduced to less than 200 m due to uplift or erosion (FEP-Screening report M.2.2.E.2)

10.2.6 Representation of Gas Channeling Effects

The displacement of water by (low-viscosity) gas in a heterogeneous porous medium may lead to flow channeling effects. In Nagra (FEP-Screening report M.2.2.E.2), such effects are mentioned as potentially relevant for gas flow in transmissive discontinuities (R9; FEP 1.3.2) and the EDZ (R10; FEP 1.3.4). These small-scale features (compared to the size of a computational element) can be approximately accounted for in a continuum model by the Active Fracture Model (AFM; Liu et al., 1998), which is implemented in iTOUGH2-IFC (Finsterle, 2007b, Appendix A7). The AFM accounts for flow channeling effects within a fracture network and individual fractures. It is based on the van Genuchten model, requiring one additional parameter. The impact of this parameter on repository performance should be evaluated by sensitivity analyses.

10.3 Miscellaneous Comments

10.3.1 Initial Conditions

As discussed in Section 5.6, the system is initially (i.e., prior to gas generation) assumed to be at steady state, that is, in equilibrium with the imposed boundary pressures, which results in fully saturated conditions throughout the model domain. Perturbations induced by, for example, repository construction (affecting pressure and saturation distribution in the vicinity of waste emplacement tunnels), heat output during the early post-closure stage (affecting temperature, pressure, and saturation distribution), or other short- or long-term transient effects not explicitly represented in the model, will lead to a deviation from this idealized initial state.

A starting time for IFC simulations that evaluate the long-term performance of the repository system has to be selected. The choice of this starting time affects computational demands, specifically because the early-time perturbations lead to strong transients that are computationally expensive because time steps are relatively small. Moreover, it determines which effects (e.g., resaturation, thermal output) have to be included in the simulation model or, if omitted, which simplifications need to be justified. Finally, the starting time determines the initial conditions and the difficulty with which they are to be obtained. These three aspects regarding the choice of the starting time need to be balanced. In the current base-case model, the starting time was chosen to be the time gas generation is initiated. However, the initial conditions (while simple and efficient to calculate) do not properly reflect the perturbation induced by repository construction, which leads to a pressure drop, pre-closure dry-out effects, and unsaturated conditions in and near the tunnels, nor does it account for early-time post-closure effects, such as the release of decay heat. Most of the calculation time is spent to resolve the initial period with high gas generation rates in the intermediate-level waste facility. Justifying this particular choice of the starting time and initial conditions in the current base-case model is beyond the scope of this report on the development of the iTOUGH2-IFC code and IFC model.

There are essentially two ways to obtain initial conditions:

1. The initial distribution of pressure, saturation or hydrogen mass fraction (which are the primary variables solved by the numerical model) are calculated by iTOUGH2-IFC prior to or as part of the PSA simulation. Depending on the processes to be included in the initial condition field, this simulation may be a simple steady-state calculation (as described in Section 5.6), or a complex sequence of steady-state and transient simulations with time-dependent boundary conditions (e.g., to represent repository construction).
2. Initial conditions are pre-calculated externally using numerical simulations or simplified abstractions or scenarios, and provided to the iTOUGH2-IFC simulator at run time during a PSA analysis.

The first approach has the advantage that the initial conditions are automatically available in the required format, and that no residual transients have to be resolved at early time due to errors induced by mapping, non-equilibrium conditions, and other effects that are likely to be introduced at the interface between the externally provided information and the iTOUGH2-IFC initial condition file. A disadvantage of the first approach is that it may be computationally demanding.

A new set of initial conditions needs to be provided or calculated each time a parameter is adjusted during the PSA sampling, if this parameter affects the initial conditions. This could be accomplished in a more natural and more accurate way if the first approach is used.

10.3.2 Performance-Affecting Parameters and Options

The computational efficiency of the IFC depends on the sampled parameter set, which leads to potentially significantly different flow behavior, which in turn affects time-step size and convergence rates of the simulator. The iTOUGH2-IFC code and IFC model must be able to handle a large variety of parameter combinations in a robust manner. Computational efficiency is also affected by certain parameters that are not part of the parameter set to be varied within PSA (see Tab. 22). Moreover, adjustments of these parameters are not expected to significantly affect the simulated system behavior, i.e., they are not safety-relevant. Finally, the values of some of these parameters are unknown, unmeasured, or highly uncertain, i.e., no preference to a specific value can be reasonably justified. Provided that uncertainty in these parameters is not subject to evaluation in the probabilistic analysis, and that they have a significant impact on the numerical stability and performance of the simulation, a study could be performed to investigate which value should be picked to aid computational efficiency. The following is a list of potential candidate parameters for such an analysis, which includes (1) compiler options, (2) computational parameters, (3) hydrogeological parameters, and (4) changes in model conceptualization:

- Compiler options for code optimization, including parallelization
- Choice of linear equation solver (TOUGH2 variable MOP(21))
- Choice of preconditioner (TOUGH2 variables ZPROC and OPROC)
- Linear equation solver parameters (TOUGH2 variables RITMAX and CLOSUR)

- Convergence criteria for Newton-Raphson iterations (TOUGH2 variables RE1, RE2, MOP2(1), and WNR)
- Increment factor for numerically computing derivatives (TOUGH2 variable DFAC)
- Weighting scheme for mobility and permeability at interfaces (TOUGH2 variable MOP(11))
- Parameters affecting automatic time step control (TOUGH2 variables MOP(16), NOITE, DELTMX, and REDLT)
- Residual gas saturation (TOUGH2 variable RP(2))
- Linearization of liquid relative permeability near saturation (TOUGH2 variable RP(5))
- Linearization of capillary pressure near residual liquid saturation (TOUGH2 variable CP(3))
- Different residual saturations for capillary pressure and relative permeability curves (TOUGH2 variable CP(7))
- Initial gas saturation after phase change (variable ZERO in subroutine EOS)
- Vapor pressure reduction at low liquid saturations (TOUGH2 variable MOP2(4))
- Gas diffusion (TOUGH2 variables TORTX, DIFF0, TEXP, and BE)

It is highly recommended to analyze model regions and processes (specifically phase appearances and disappearances) causing convergence difficulties and associated time-step reductions. Justifiable adjustment in those regions and in parameters controlling the problematic process should be investigated.

As demonstrated in Fig. 22, the inclusion of geomechanical and geochemical FEPs significantly affects the efficiency of the simulation. It is recommended that the impact of each of these FEPs on the simulation results be evaluated and put in context with prediction uncertainties due to parameter variability, other conceptual simplifications, and computational errors. Insignificant processes may be omitted, enhancing computational efficiency.

References

Doughty, C., Investigation of conceptual and numerical approaches for evaluating moisture, gas, chemical, and heat transport in fractured unsaturated rock, *J. Contam. Hydrol.*, *38*, 69–106, 1999.

Finsterle, S., *Parallelization of iTOUGH2 Using PVM,* Report LBNL-42261, Lawrence Berkeley Natl. Lab., Berkeley, California, 1998.

Finsterle, S., *iTOUGH2 User's Guide,* Report LBNL-40040 (revised), Lawrence Berkeley Natl. Lab., Berkeley, California, 2007a.

Finsterle, S., *iTOUGH2 Command Reference,* Report LBNL-40041 (revised), Lawrence Berkeley Natl. Lab., Berkeley, California, 2007b.

Finsterle, S., *iTOUGH2 Sample Problems,* Report LBNL-40042 (revised), Lawrence Berkeley Natl. Lab., Berkeley, California, 2007c.

Finsterle, S., Multiphase inverse modeling: Review and iTOUGH2 applications, *Vadose Zone J.*, *3*, 747-762, 2004.

Finsterle, S., C. Doughty, M.B. Kowalsky, G.J. Moridis, L. Pan, T. Xu, Y. Zhang, and K. Pruess, Advanced vadose zone simulations using TOUGH, *Vadose Zone J.*, 7:601-609, doi:10.2136/vzj2007.0059, 2008.

Liu, H.H., C. Doughty, and G.S. Bodvarsson, An active fracture model for unsaturated flow and transport in fractured rocks, *Water Resour. Res*., *34*(10), 2633-2646, 1998.

Nagra, *Projekt Opalinuston: Konzept für die Anlage und den Betrieb eines geologischen Tiefenlagers, Entsorgungsnachweis für abgebrannte Brennelemente, verglaste hochaktive sowie langlebige mittelaktive Abfälle*, Nagra Technical Report NTB 02-02, Nagra, Wettingen, Switzerland, December 2002a.

Nagra, *Project Opalinus Clay: Safety Report, Demonstration of Disposal Feasibility for Spent Fuel, Vitrified High-Level Waste and Long-Lived Intermediate-Level Waste (Entsorgungsnachweis)*, Nagra Technical Report NTB 02-05, Nagra, Wettingen, Switzerland, December 2002b.

Nagra, *Project Opalinus Clay: Models, Codes and Data for Safety Assessment. Demonstration of Disposal Feasibility for Spent Fuel, Vitrified High-Level Waste and Long-Lived Intermediate Level Waste (Entsorgungsnachweis)*, Nagra Technical Report NTB 02-06, Nagra, Wettingen, Switzerland, December 2002c.

Nagra, *Effects of Post-Disposal Gas Generation in a Repository for Spent Fuel, Vitrified High-Level Waste and Long-Lived Intermediate-Level Waste Sited in Opalinus Clay*, Nagra Technical Report NTB 04-06, Nagra, Wettingen, Switzerland, July 2004.

Nagra, *Kostenschätzung 2006 KS 06, Bauliche Anlagen eines geologischen Tiefenlagers HAA im Opalinuston der Nordschweiz*, Nagra Internal Report, 2006, Nagra, Wettingen, Switzerland, August, 2006.

Nagra, FEP-Screening report M.2.2.E.2*: Agreed List of Safety-Relevant Phenomena as of 21.02.2007 (final version)*, Nagra, Wettingen, Switzerland, March 8, 2007a.

Nagra, Effects of Post-Disposal Gas Generation in a Repository for Low- and Intermediate-Level Waste Sited in the Opalinus Clay of Northern Switzerland, Nagra Technical Report NTB 08-07, Nagra, Wettingen, Switzerland, October, 2008a.

Nagra, STMAN 5.7, Nagra Arbeitsbericht NAB 08-46, Nagra, Wettingen, Switzerland, 2008.

Nagra, *Probabilistic Safety Assessment (PSA): Design Proposal for an Integrated Flow Code (IFC)*, Order 960.09, Nagra, Wettingen, Switzerland, May 16, 2007b.

Pruess, K., The TOUGH codes – a family of simulation tools for multiphase flow and transport processes in permeable media, *Vadose Zone J.*, *3*, 738-746, 2004.

Pruess, K., and T.N. Narasimhan, A practical method for modeling fluid and heat flow in fractured porous media, *Society of Petroleum Engineers Journal*, *25*,14-26, 1985.

Pruess, K., C. Oldenburg, and G. Moridis, *TOUGH2 User's Guide, Version 2.0,* Report LBNL-43134, Lawrence Berkeley Natl. Lab., Berkeley, California, 1999.

Robinson, R., and P. Suckling, PICNID TD User Guide for Version 1.2, unpublished Nagra Internal Report, Wettingen, Switzerland, 2009.

Schneider, J., and C. Sprecher, *Introduction to Nagra's PSA Concept*, presentation given at meeting, Wettingen, Switzerland, May 4, 2007.

Wu, Y.S., K. Zhang, C. Ding, K. Pruess, E. Elmroth, and G.S. Bodvarsson, An efficient parallel-computing method for modeling nonisothermal multiphase flow and multi-component transport in porous and fractured media, *Adv. Wat. Resour.*, *25*, 243-261, 2002.

Zhang, K., Y.S. Wu, and G.S. Bodvarsson, Massively parallel computing simulation of fluid flow in the unsaturated zone of Yucca Mountain, Nevada, *J. of Contam. Hydrol., 62-63*, 381-399, 2003.

Zhang, Y., C.M. Oldenburg, S. Finsterle, and G.S. Bodvarsson, System-level modeling for economic evaluation of geological CO_2 storage in gas reservoirs, *Energy Conservation and Management*, *48* (6), 1827-1833, 2007.

Appendix 1: Network for the IRRC

A1 Introduction

This note sets out a transport network for use in development of the IRRC (Integrated Radionuclide Release Code). The network will also be used initially to confirm the linkage between the IFC and PICNIC-TD is functioning correctly. The network design follows the approach used in NTB 02-06 (Figure 3.6-5) with the current repository layout as specified for the IFC (Integrated Flow Code) in AN 08-327.

The major change in layout between NTB 02-06 and now is the location of the shaft. This is now near the ramp and operations area rather than being at the other end of the repository. The SF and HLW are now treated separately.

The note is structured as follows:

- Section A2 describes the PICNIC-TD network;
- Section A3 gives the properties of each leg;
- Section A4 shows some images that confirm the locations of the interfaces for the IFC.

A2 The Network

The network for PICNIC-TD consists of a set of nodes (or junctions) and legs between these. For some nodes, radionuclide releases will be provided from STMAN calculations.

The current network does not consider the scenario where a transmissive fracture intersects the system.

The approach taken to developing the network is that all potential transport paths are included – how significant each of these is will be determined by the particular flow rates in a realisation. In practice, this means that the network consists of two distinct components.

First there is a representation of the repository horizon, including emplacement tunnels or vaults for each waste type and the various tunnels that connect these. The shaft and ramp link into the tunnel system within this horizon.

Second, is a representation of the vertical flows through the host rock (up or down), leading ultimately to discharge points where any release is considered to be in the biosphere.

To help anchor the network, the nodes and legs have been superimposed on the repository and geosphere diagrams

Fig. A-1 shows the repository horizon and Fig. A-2 shows the vertical cross section.

In these figures the following conventions are used.

- Nodes (junctions) are shown as black ellipses. The size of the ellipse is intended to indicate the extent of the region over which the node extends (in which a homogeneous concentration is assumed).
- Nodes are named as N_xxx, except for the final (discharge) nodes, which are named Bio_xxx.
- STMAN inputs are shown in the blue boxes.
- Legs are shown as arrows. The arrow gives a direction to the leg although this does not restrict transport to be in that direction (it merely provided a sign convention).
- Legs will be named according to their end nodes and what type they are, e.g. LT_T1_T2 is a tunnel leg, LR, LS and LG are used for ramp, shaft and geosphere legs, with LA for the shaft access leg. This is not shown on the figures for clarity.
- Legs are colour coded according to the type of feature they represent:
  - Red legs are for the (non-emplacement) tunnels, with dotted versions in Fig. A-2 showing pathways without showing the full structure in the repository horizon;
  - Green legs are for access tunnels and the end of emplacement tunnels;
  - Orange legs are for the ramp;
  - Grey legs are for the shaft;
  - Blue legs are in the geosphere;
  - A Yellow leg is for the shaft access from the tunnels.

Note that the ramp and shaft at the Wedelsandstein level are assumed to be in direct contact with the aquifer water, enabling mixing to occur. This is because the time at which any radionuclides reach this point will be long enough for any lining to have failed, and because the EDZ surrounding these features may in any case be the dominant path.

In general, all the tunnel legs are taken to represent the tunnel section along with any associated EDZ which in many cases may be the dominant transport feature.

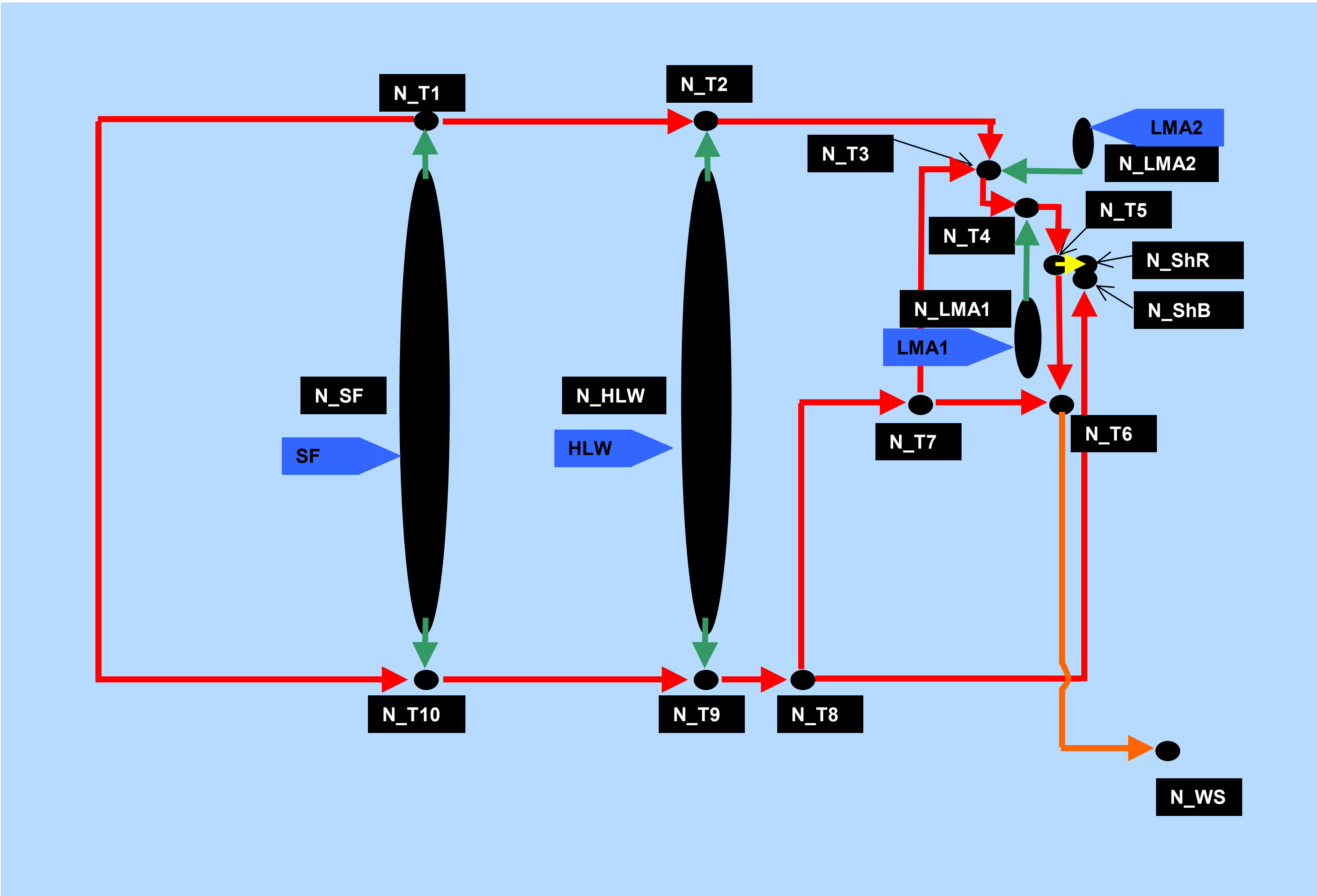

Fig. A-1: Network in the Repository Horizon.

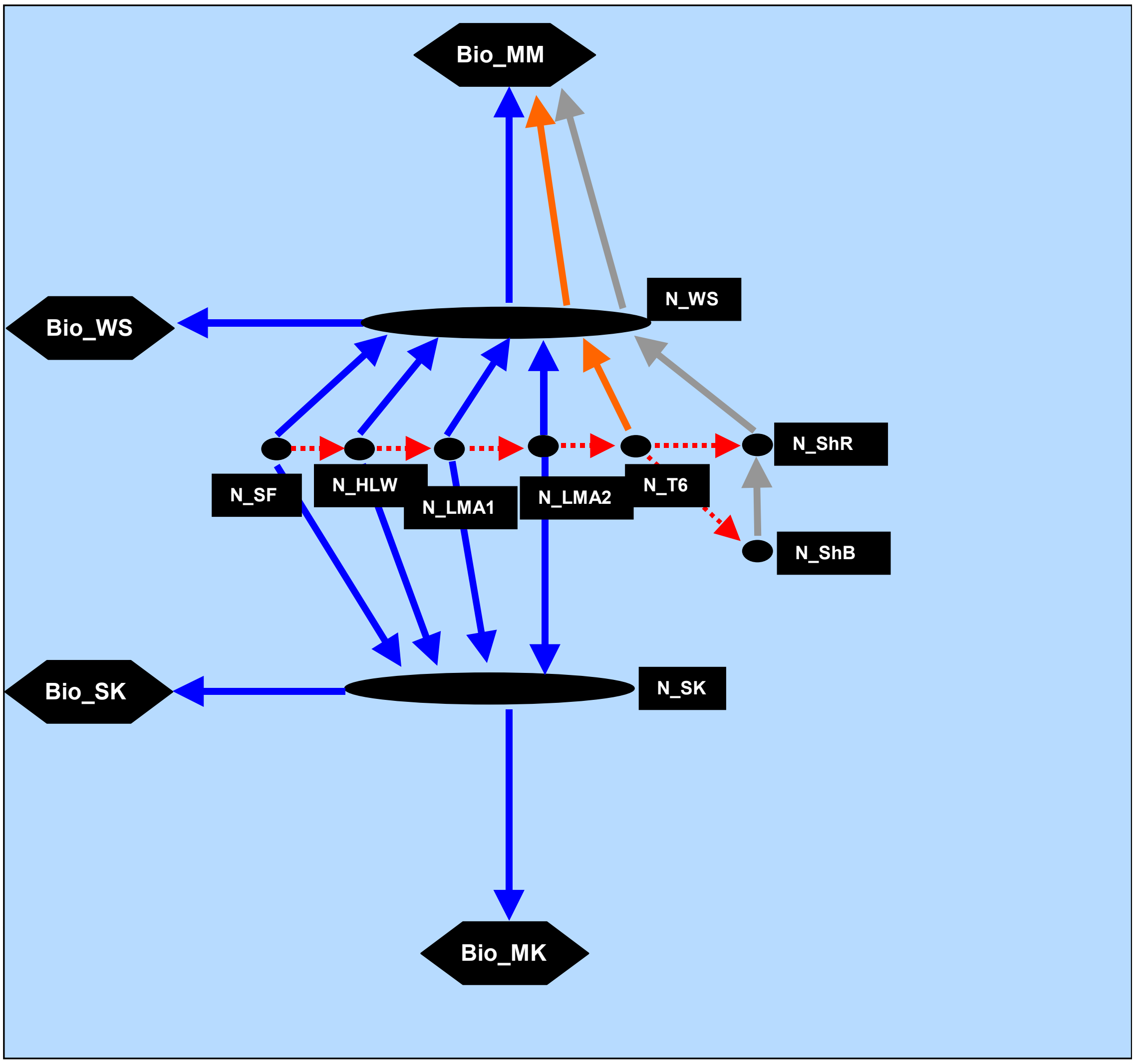

Fig. A-2: Network in a Vertical Cross Section.

A3 Leg Properties

Each leg will get flow information from the IFC. This will be obtained at two points for each leg – once near the start and one near the end (according to the arrow direction). The precise positions are specified for each leg – with the aim of avoiding being direct adjacent to discontinuities that may make the reported flow unreliable. The area across which the flow is required is also dependent on the leg. In the tunnels, the tunnel cross-section plus associated EDZ is used. In the geosphere, the footprint of the relevant feature is generally used.

Leg lengths are determined from the geometry. Other leg properties depend on the material through which transport predominantly occurs. For tunnels, ramps and shafts the potential for diffusive interchange with surrounding material should be included. The same applies for the aquifers. Any of these could conservatively be ignored.

A4 Visualisation for IFC

In order to verify the location of the flow planes for the IFC, graphical data (see Fig. A-3 to Fig. A-9) as well as the PICNIC-TD related input of the IFC model is generated by a script which requires a minimum of input and can be easily changed:

- Coordinates of the PICNIC-nodes;
- Start- and end-nodes of each leg;
- Extension (i.e. width, height) of the cross-section for each leg.

This figures allow each aspect of the PICNIC-TD network to be checked.

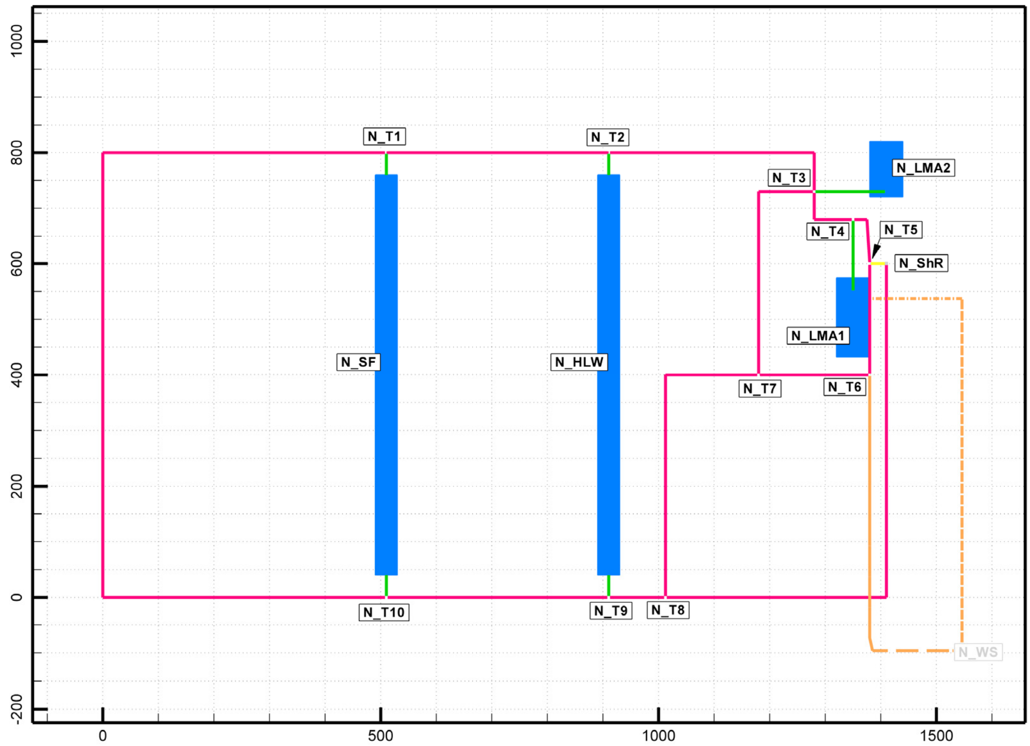

Fig. A-3: PICNIC representation of repository structures (horizontal cross-section at repository level).

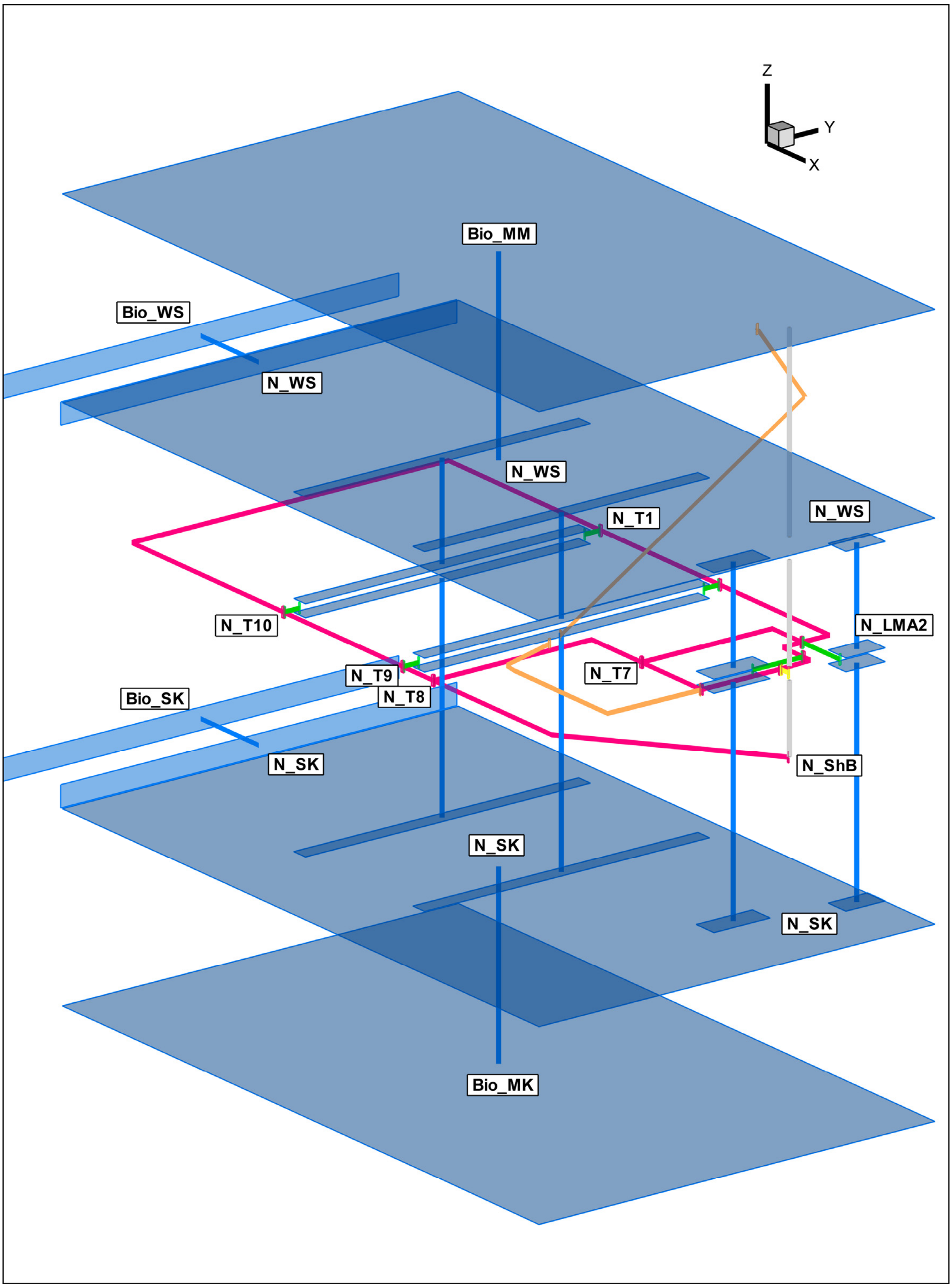

Fig. A-4: Overall view of network and interface cross-sections (vertically exaggerated).

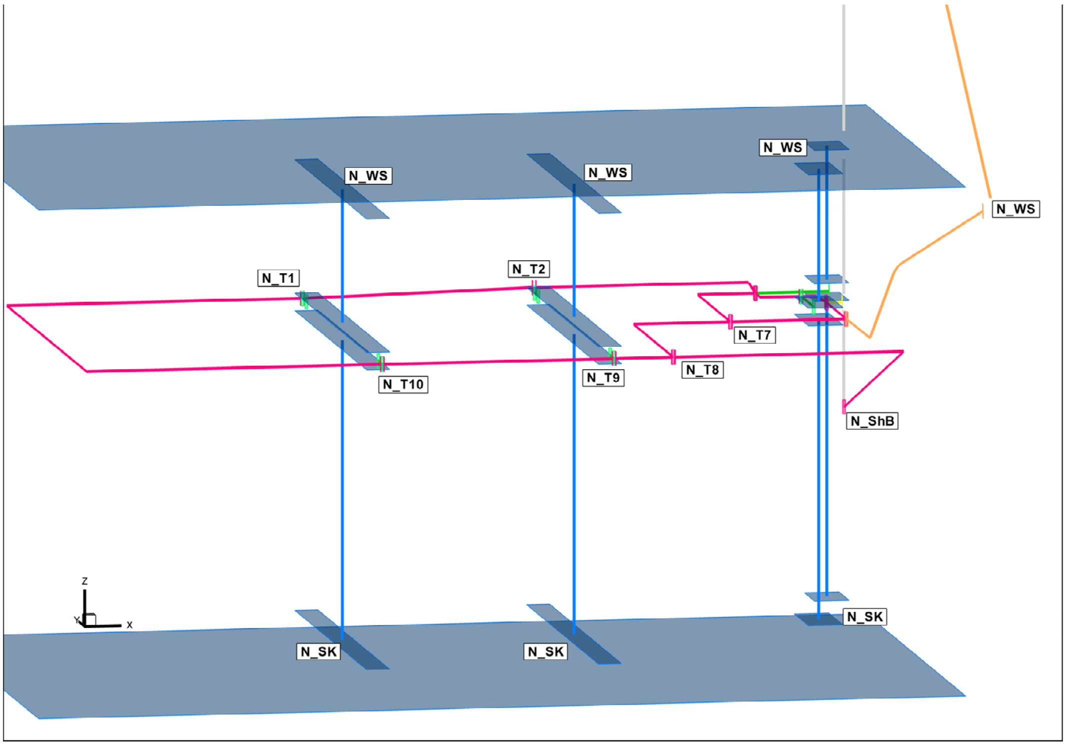

Fig. A-5: Network and interfaces: repository and aquifers WS, SK (vertically exaggerated).

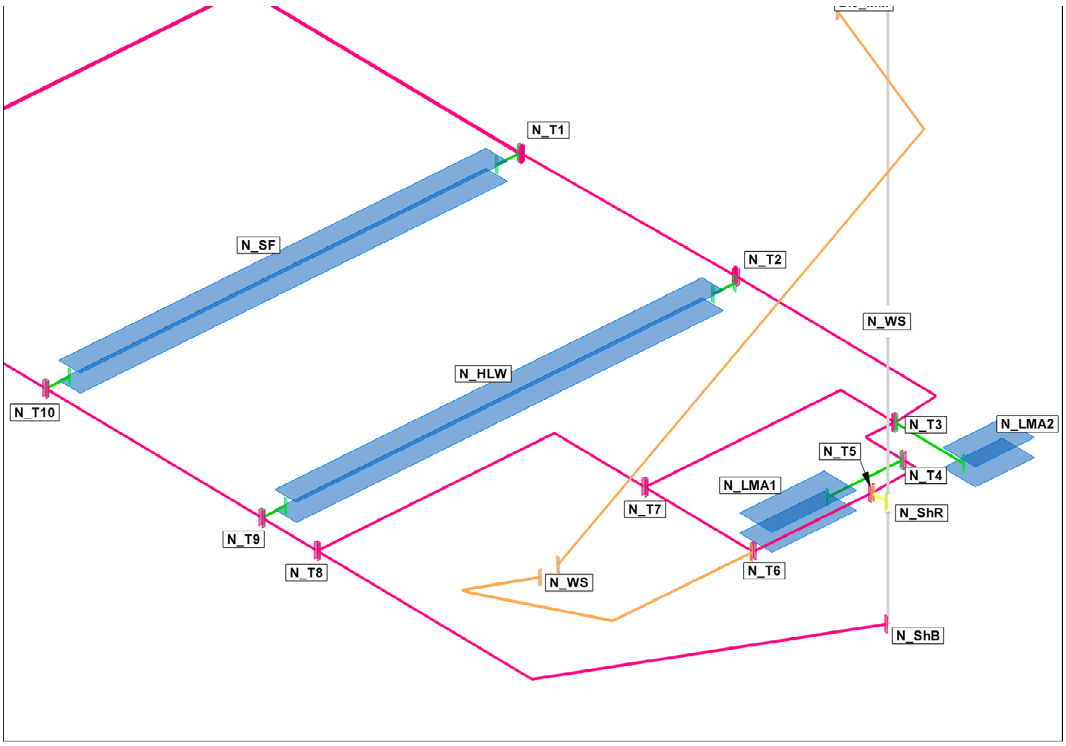

Fig. A-6: Network and interfaces of repository structures (view from SE, vertically exaggerated).

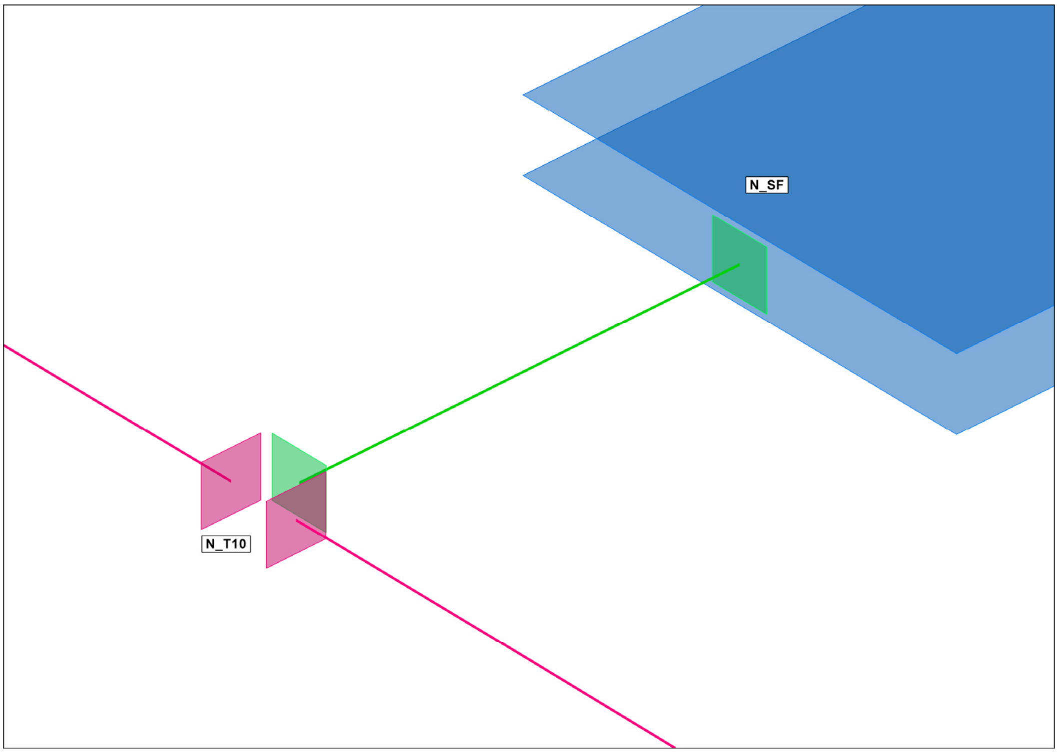

Fig. A-7: Network detail: connection between SF emplacement tunnel and construction tunnel.

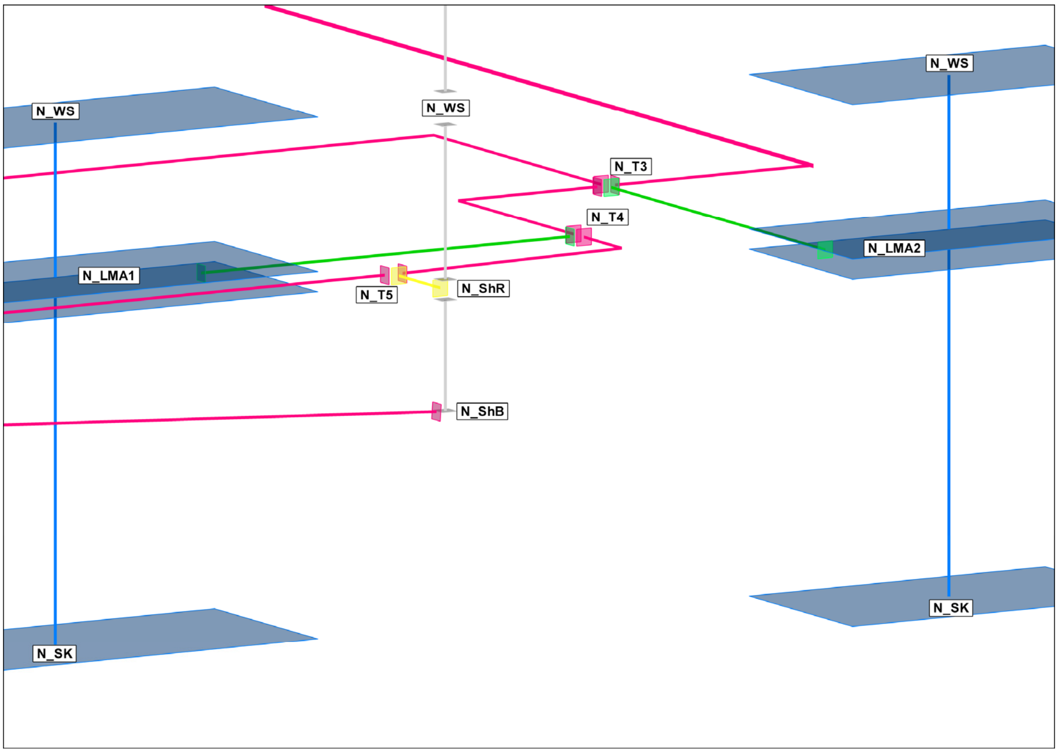

Fig. A-8: Network detail: LMA emplacement tunnels, ventilation shaft (vertically exaggerated).

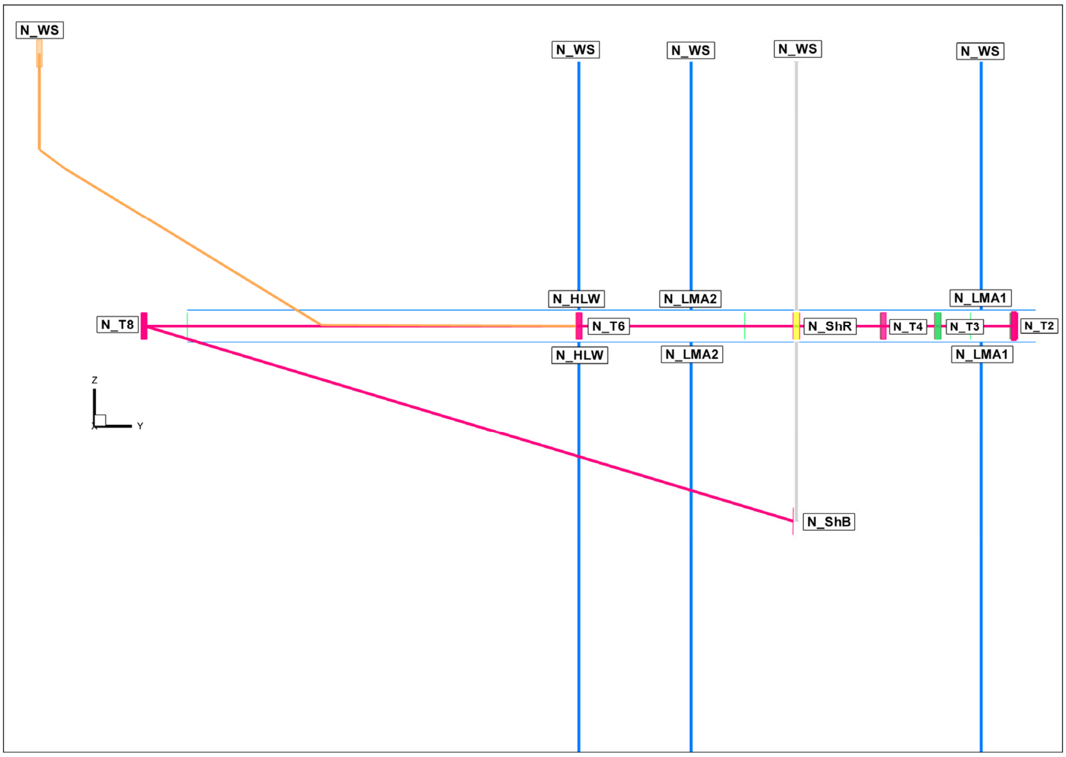

Fig. A-9: Repository and connection to aquifers (vertical cross-section, view from E, exaggerated).